EFFECTS OF POLYMERS ON THE IMPINGEMENT OF COLLOIDAL PARTICLES ONTO FLAT SURFACES

A Thesis

by

Suzanne Varennes, B.Sc., Université du Québec à Montréal
Montreal, Canada

Submitted to the Faculty of Graduate Studies
and Research of McGill University in partial
fulfillment of the requirements for the
degree of Doctor of Philosophy

Department of Chemistry
McGill University
Montreal, Quebec, Canada

September 1987

ISBN 0-315-45945-X

ABSTRACT

A recently developed method was employed to study the deposition of colloidal particles under well-controlled hydrodynamic conditions. With this technique we studied the effects of polymers on the impingement of colloidal particles onto flat surfaces. In the deposition-detachment studies of bare latex particles, anomalous deposition rates and surface motions were observed. These types of behavior can be qualitatively explained by surface protrusions on the latex surface. Bare particles were dislodged from the surface by hydrodynamic forces exerted on them and by surface collisions between freely suspended and deposited particles. By coating the particles with neutral polymer, we found a decrease in the deposition rate but an increase in adhesion. The presence of free polymer in the jet increases the probability of escape. The detachment rate can be explained by an exchange between polymer segments bridging the particles to the surface and those freely dissolved in the jet. The presence of cationic polyelectrolyte promotes deposition and prevents the release of the particles.

Résumé

Une méthode développée récemment, a été utilisé pour étudier la déposition des particules colloidales avec des conditions hydrodynamiques bien controllées. Par cette technique, nous avons étudié les effets des polymères sur les particules colloidales entrant en collision avec une surface plane. Dans les études de déposition et de détachement des particules de latex vierges, nous avons observé des taux anormaux de déposition et des oscillations en surface. Ces deux comportements peuvent être expliqué qualitativement par des protubérances à la surface du latex. Les particules vierges sont détachées de la surface par des forces hydrodynamiques agissant sur elles et par collisions entre des particules en suspension et d'autres déposées à la surface. En recouvrant ces particules de polymère neutre, nous avons trouvé une diminution du taux de déposition mais une augmentation de l'adhésion. Un flux constitué plutôt de polymère libre augmente la probabilitité de détachement. Le taux de détachement peut être expliqué par un échange entre des segments de polymère reliant des particules à la surface et d'autres dissous dans le flux. La présence de polyélectrolytes cationiques favorise la déposition et prévient le détachement des particules.

ACKNOWLEDGEMENTS

I wish to express my sincere thanks to

Dr. T.G.M. van de Ven

for his valuable guidance, encouragement and assistance as my Director of Research.

Grateful acknowledgement is also made to

Dr. T. Dabros

for performing numerical calculations of the flow field in Chapter 2 and to

Dr. Y. Boluk

for interesting and stimulating discussions.

Fonds F.C.A.C. pour l'aide et le soutien à la recherche

for an F.C.A.C. grant during 1983-84; to

The Pulp and Paper Research Institute of Canada

for a PPRIC studentship during 1984-85 and for a C.A. Winkler Fellowship during 1985-87, to

My fellow graduate students and postdoctoral fellows

of the Physical Chemistry Section, Pulp and Paper Research Institute of Canada, for their friendship, encouragement and readiness to discuss problems, to

G. Kopp and F. Kluck (Chemistry Department)

for their contributions to the design of the deposition cell; to

R.J. Rychel

for photography of the apparatus and drawing; to

A. McGuinness

for her patience and care in typing this thesis and, finally, to

my husband Denis

for his loving and emotional support during the period of this research.

TABLE OF CONTENTS

Page

CHAPTER 1

INTRODUCTION

CHAPTER 2

DEPOSITION AND DETACHMENT OF LATEX PARTICLES AT GLASS SURFACES EXPOSED TO FLOW

CHAPTER 3

EFFECTS OF NEUTRAL POLYMERS ON THE KINETICS OF PARTICLE DEPOSITION

CHAPTER 4

EFFECTS OF POLYMERS ON THE DETACHMENT OF POLYMER COATED LATEX PARTICLES FROM GLASS SURFACES

Page

CHAPTER 5

EFFECTS OF POLYELECTROLYTE ON THE DEPOSITION AND DETACHMENT OF COLLOIDAL PARTICLES SUBJECTED TO FLOW

CHAPTER 6

GENERAL CONCLUSIONS

Page

APPENDIX I

LIST OF FIGURES

Figure Page

CHAPTER 1

CHAPTER 2

---

* Numbers in brackets refer to negative numbers held in PPRIC Photography Department.

CHAPTER 3

CHAPTER 4

Figure Page

CHAPTER 5

APPENDIX I

LIST OF TABLES

Page

Table

CHAPTER 2

CHAPTER 4

CHAPTER 5

GUIDELINE CONCERNING THESIS PREPARATION

In accordance with the regulations concerning the submission of theses, we reproduce the following:

The Candidate has the option, subject to the approval of the Department of including as part of the thesis the text of an original paper, or papers, suitable for submission to learned journals for publication. In this case the thesis must still conform to all other requirements explained in Guidelines Concerning Thesis Preparation (available at the Thesis Office). Additional material (experimental and design data as well as descriptions of equipment) must be provided in sufficient detail to allow a clear and precise judgement to be made of the importance and originality of the research reported. Abstract, full introduction and conclusion must be included, and where more than one manuscript appears, connecting texts and common abstracts, introduction and conclusions are required. A mere collection of manuscripts is not acceptable, nor can reprints of published papers be accepted.

While the inclusion of manuscripts co-authored by the Candidate and others is not prohibited by McGill, the Candidate is warned to make an explicit statement on who contributed to such work and to what extent, and Supervisors and others will have to bear witness to the accuracy of such claims before the Oral Committee. It should also be noted that the task of the External Examiner is made much more difficult in such cases, and it is in the Candidate's interest to make authorship responsibilities perfectly clear.

CHAPTER 1

INTRODUCTION

I. GENERAL REMARKS

The deposition and detachment of colloidal particles onto and from solid surfaces is, besides the large relevance to many industrial applications, also of intrinsic interest to the field of colloid chemistry. However, our knowledge of colloidal deposition and detachment is far from complete. Most studies performed so far have been on the deposition and detachment of model colloids on well-defined surfaces. An important mechanism by which particles can stick to surfaces is polymer bridging. Little is known of how the presence of polymers affects the deposition and detachment processes, or how strong polymer bonds are between a particle and a surface. To answer these questions, Dabros and van de Ven [1] designed a special deposition cell used in combination with a microscope and video equipment. The flow in the cell is a well-defined stagnation point flow and can vary from laminar to unstable flow. Such a flow field is very smilar to the flow near a rotating disk, but has the advantage of a stationary surface, thus making it relatively easy to observe the collector surface while particle deposition or detachment takes place. Hence this technique allows us to study both particle deposition and detachment at the same time. The great advantage of this method is the possibility of direct observation of particle deposition and detachment. This method allows us to observe the dynamic nature of the processes connected with the escape of deposited particles from the collector surface, the distribution of particles on the surface and the behavior of particles in the vicinity of the collector. In other experimental methods [2,3] the collector surface, after exposure to deposition for a given time, is rinsed and dried while it is being prepared for microscopic observations. In some cases these preparations have to be made very carefully to avoid changes in the coating density. Because of the possiblity of damaging the coating by rinsing and drying, the most reliable results can be obtained by observing the coating in situ in the original flow field.

Some papers have been published on the stagnation point flow method [4,5], containing experimental work dealing with barrierless deposition rates as a function of particle dimension and flow intensity.

Published data are available on the adsorption characteristics of polymer onto solid surfaces in aqueous media [6-9]. However, only a relatively few studies have considered the strengths of the bonds formed during flocculation [10-15]. Those bonds are critical to the survival of flocs in shear flow [10] and the retention of fine particles during paper manufacture [15]. Pelton [14,16] and Hubbe [15] studied the strength of bonds formed between particles and a solid surface in the presence of polyelectrolytes. Pelton [16] found that the strength of polystyrene-polyethyleneimine (PEI)-glass bonds increased with increasing molecular weight of PEI and pH.

The research described in this thesis consists of deposition/ detachment experiments, together with a theoretical analysis for a variety of systems, using neutral polymers of low molecular weight and high molecular weight polyelectrolytes. These polymers were chosen as they represent the most extreme examples, one being short and linear while the other is large and branched. Other macromolecules are expected to show behavior intermediate between these two extremes.

When theories of specific and hydrodynamic interactions are incomplete, experimental results obtained from a direct observation of the deposition/detachment process are of great importance.

II. HISTORICAL BACKGROUND

Classical DLVO-theory

Derjaguin and Laudau [17] and Verwey and Overbeek [18] have independently developed a quantitative theory in which the stability of lyophobic colloids is treated in terms of the energy changes which take place when particles approach one another. They combined the energy of attraction (London-van der Waals forces) with the energy of repulsion (overlapping of electric double layers) to explain the stability of colloidal dispersions. The theory that describes this competition between electrostatic repulsion and van der Waals attraction is called the DLVO-theory.

For the case of two spherical particles, at short separations, the total free energy of interaction V_{int} is the sum of repulsion and attraction contributions:

$$V_{int} = -\frac{Aa}{12h} + C\,e^{-\kappa h} \qquad (1)$$

where the first term on the right hand side corresponds to the van der Waals attractive forces, a being the particle radius, h the gap between the spheres, and A the Hamaker constant. The second term is the double layer repulsive interaction, C being a constant and κ a characteristic parameter given by the Debye length κ^{-1} (double layer thickness). Above we have given the interaction energy in its simplest form. For more details on more sophisticated expressions or numerical results for the dispersion and electrostatic interactions, several textbooks on colloid science are available [19].

Schematically, the energy of interaction is shown in Fig. 1. Depending on the relative strength of repulsive and attractive forces, the energy of interaction can exhibit both a maximum and a minimum. Including the Born repulsion results in two minima. The Born repulsion is noticeable at very short separations and prevents the particles from interpenetration. As can be seen from Fig. 1, neglecting the Born repulsion, at short and large distances, the van der Waals force dominates and the energy of interaction is negative (attractive). At intermediate distances the forces are repulsive, provided the electrostatic repulsion is sufficiently large. The height of the energy maximum determines the stability of the suspension. When the barrier is high ($V_{max} \gtrsim 10$ kT), few particles can move over it and no coagulation occurs (in the absence of external force fields). The height of the barrier can be varied by varying either the surface potential ψ_o or the ionic strength which affects the double layer thickness κ^{-1}. At low potentials or high ionic strength the barrier disappears.

Fig. 1 Schematic representation of the energy of interaction between two electrically charged colloidal particles as a function of the distance between them.

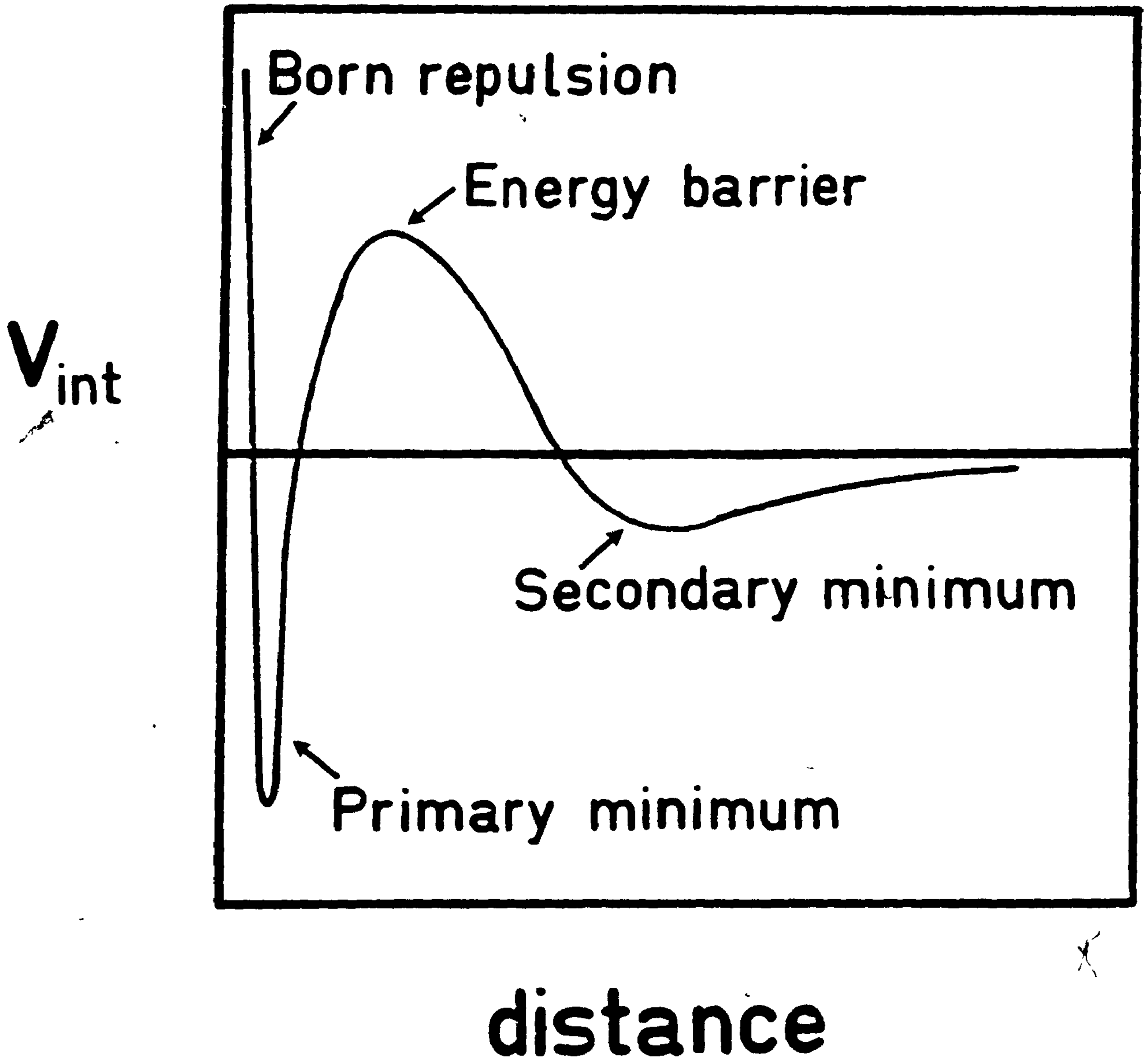
Born repulsion
Energy barrier
V_{int}
Secondary minimum
Primary minimum
distance

Forces between colloidal particles in the presence of polymer

General remarks

One of the ways in which the stability of colloids can be influenced is by the addition of polymers. Depending on the circumstances, polymers can give rise to attractive or repulsive forces between the particles. Polymers may adsorb onto the colloidal particles. This could lead to a repulsive force when two such particles approach one another (steric repulsion). This is called steric stabilization. When the particles are only partly covered with polymer, the adsorbed polymer can form a macromolecular bridge by adsorbing on two particles simultaneously. This attractive force results in bridging flocculation. Polymers may have no affinity to the surface of colloidal particles and remain free in solution. In this case when two particles approach there is repulsion at large distances due to the fact that free polymer must be squeezed out of the gap (depletion stabilization), but there is attraction at small distances due to an osmotic pressure difference between the gap and the solution. This attraction can result in depletion flocculation. The existence of depletion stability has recently been questioned (E. Evans, private communication).

Particles with adsorbed polymer

The main difference between polymer adsorbed or anchored onto a colloidal particle and polymer free in solution is a change in their configurations. When in contact with a solid, the number of configurations is severely restricted. The process of polymer adsorption is relatively complicated. One of the principal problems of polymer adsorption to be resolved is the configuration of the polymer on the surface or, stated differently, its segment distribution.

Several attempts have been made to develop adequate theories for the complicated phenomena occurring in polymer adsorption. Two main lines of approach have been adopted. The first quantitative equilibrium theory of polymer adsorption was derived by Frisch, Simha and Eirich [20-24]. They used a statistical approach to the problem based on the random walk concept with a reflecting barrier. They were then able to calculate thermodynamic properties of the adsorbed layer, and hence deduce an adsorption isotherm. Other workers have used related approaches [25-27]. The original Frisch-Simha-Eirich approach has been criticized, for example, by Silberberg [28] and DiMarzio [29]. One of the objections is that the total number of distinguishable conformations is overestimated. The second main approach, originated by Silberberg [28,30] makes use of the Jenckel and Rumbach concept [31] that polymer segments exist in two (energy) states at an interface: (a) sequences of segments lying in the layer immediately adjacent to the surface (trains), (b) sequences of segments extending into the bulk solution (loops or tails). The approach is to calculate the most probable configuration of the polymer molecule at the interface, to set-up a partition function for the system, and so calculate the required thermodynamic functions by this route. Silberberg [28,30] originally assumed that the loop size was uniform for a given adsorbed molecule, but Hoeve et al. [32] later introduced loop size distributions. Other authors have extended the partition function approach [33-39].

Most of this earlier work was restricted to the consideration of isolated polymer molecules adsorbed at an interface, i.e. under conditions of low coverage, and these theories are valid for very good solvents and in systems so dilute that the interaction of segments with each other and with solvent molecules can be neglected. Recent papers have extended the theory to account for lateral interactions on the surface, i.e. at high coverage, polymer-polymer interactions take on increased significance [38,40,41]. The interaction between the segments will then drastically influence the distribution of segments in trains, loops and tails. Since this interaction depends on the segment concentration profile in the adsorbed layer (which is a priori unknown), the solution of the problem presents considerable mathematical difficulties. Previous treatments [illegible] all therefore made simplifying approximations, the most important of which are: (i) neglect of end effects, considering only trains and loops but no tails, (ii) an a priori assumption about the segment concentration profile.

Recently it has become possible to make predictions of the segment density profile either by generating polymer configurations using Monte Carlo methods [42], or by considering various lattice models in which each site is either occupied by a solvent molecule or a polymer segment [43-45].

Two interacting polymer coated surfaces

When two particles coated with polymer approach one another, the segment density distribution and segment configurations will change. This will lead to a change in the entropy of the system. Also, the concentration of polymer will be higher in the gap than in solution, resulting in an osmotic pressure difference between the gap and the bulk. So the enthalpy of the system will change too. In general we can write the

Gibbs free energy ΔG of the system as;

$$\Delta G = \Delta H - T\Delta S \ , \qquad (2)$$

where H is the enthalpy, T the absolute temperature and S the entropy. The force between the particles can be found from

$$F = -\frac{d\Delta G}{dx} \ . \qquad (3)$$

Several theories exist to calculate ΔH and ΔS. For an excellent summary the reader is referred to a book by Napper [42].

Napper [42] proposed an equation that is used to derive the mixing contribution between two polymer coated particles

$$\Delta G^{M} = kT\,(V_s^2/V_1)\,(1/2 - \chi_1)\left[\int_V \rho_s^2(d)\,dV - \int_V \rho_s^2(\infty)\,dV\right] , \qquad (4)$$

where V_s is the volume of a segment, V_1 the volume of a molecule of the dispersion medium, χ the Flory-Huggins interaction parameter, and ρ_s the number of segments per unit volume. Eq. (4), together with Eq. (3), describe the forces between two polymer coated particles.

In the interpenetrational-plus-compressional domain, the mixing free energy calculated as described above must be supplemented by the elastic free energy, given by Napper [42].

$$\Delta G^{EL} = -T\Delta S^{EL} = -2\nu kT\,\frac{\ln\Omega(d)}{\Omega(\infty)} \ , \qquad (5)$$

where ν is the number of polymer chains per unit area of surface and Ω(d) the configurational thermodynamic probability at a particle separation d. Note that the factor of 2 allows for the two surfaces.

To calculate the forces between two particles suspended in a polymer solution, in the absence of polymer adsorption, we have to calculate the change in entropy and enthalpy occurring when the free polymer is squeezed out of the gap (depletion stabilization), but there is attraction at small distances due to an osmotic presure difference between the gap and the solution (depletion flocculation). If the segment density distribution is known we can calculate the change in free energy.

Fig. ? shows schematic examples of interaction curves as a function of distance. Curve 1 represents colloidal particles sterically stabilized by polymer. Curve 2 is for conditions where there is attraction at large separations due to bridging, but repulsion at short distance (steric repulsion) or, alternatively, it can represent the repulsive elastic contribution to the interaction energy at short separations, while the deep minimum is due to the mutual attraction of adsorbed polymer segments in a worse than θ-solvent. Curve 3 represents, in the absence of polymer adsorption, depletion flocculation where we have only attraction at all distances of separation or for adsorbing polymers, bridging flocculation is observed and attraction is found at all distances of separation.

Interaction of polymer chains attached to macroscopic objects

Probably the most direct method for determining the distance dependence of steric interactions is the compression of polymer chains

Fig. 2 Schematic representation of some of the ways that polymer chains can affect colloid stability. Plots of interaction energy as a function of the distance between two colloidal particles for adsorbing or non-adsorbing polymers. Curve 1 steric stabilization. Curve 2 van der Waals attraction plus steric repulsion or attraction in a worse than θ-solvent plus elastic repulsion. Curve 3 bridging or depletion flocculation.

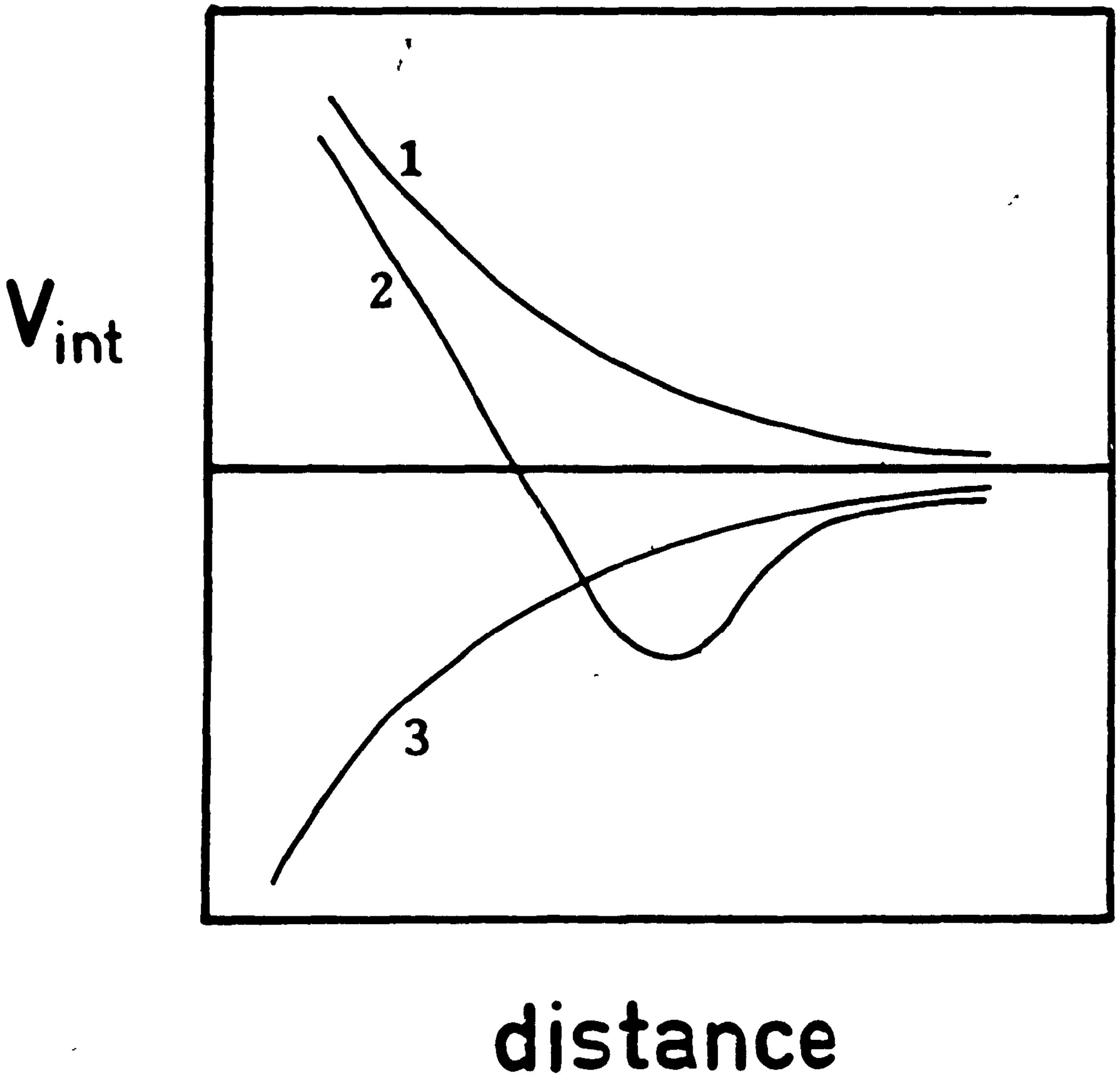
1
2
3
V_{int}
distance

attached to macroscopic objects as they undergo close approach. The method has been the crossed mica cylinders technique. This technique was originated by Tabor and coworkers [46,47] and improved by Israelachvili and Adams [48,49]. In the hands of Pashley and Israelachvili [50], it was successfully used to test the predictions of the DLVO-theory of electrostatic stabilization. The force as a function of distance between the mica surface in aqueous KCl solutions was measured, with particular attention given to the forces at separations below 2 nm. As previously reported, the forces in dilute electrolyte solutions are well described by the DLVO theory, (i.e. repulsive double-layer forces and attractive van der Waals forces), but above a certain electrolyte concentration an additional short range repulsive hydration force arises as hydrated cations adsorb onto the mica surfaces. They [51] found that the repulsive hydration force is not purely monotonic, but has an oscillatory component superimposed on it which is particularly pronounced at separations below 1 nm. The attractive force law between two hydrophobic (hydrocarbon) surfaces in aqueous solutions has been derived [52] from total force measurements on monolayer coated mica surfaces. This 'hydrophobic interaction' is much stronger than the expected van der Waals interaction at a distance below 8 nm and decays exponentially with distance.

In this thesis we measure the effect of polymers on particles of colloidal size rather than on macroscopic surfaces. Hopefully the information gained from such studies is complementary to the macroscopic studies. The main advantage of our approach is that we can measure dynamic effects, while the macroscopic measurements are all done under thermodynamic equilibrium conditions.

We can summarize that for adsorbing polymers, the free energy of interaction is a compromise between an attractive term due to polymer bridging and a repulsion caused by segmental overlap and conformational entropy losses. And for non-adsorbing polymers there is an overlap of depletion zones. In dilute solutions this overlap leads to a smaller depleted amount and hence to an attractive force. In concentrated systems (in polymer) a repulsive force may exist at large distances while an attraction exists at short distances (due to osmotic pressure differences).

Discussion of literature on deposition and detachment

Deposition

The first experimental data on deposition on a collector with a well-defined geometry under well-defined hydrodynamic conditions have been reported by Marshall and Kitchener [2] and Hull and Kitchener [3]. In their study of the deposition process they used the rotating disk technique. In ref. [2] the deposition of carbon black particles from dilute aqueous suspensions on various collectors such as glass, polystyrene, polyvinyl formaldehyde, polyvinyl pyridine and cellulose was studied with various concentrations of anionic or cationic surfactants and addition of electrolyte (KCl). It was found, in the absence of energy barriers and when the ζ-potentials of the particles and the collector were of opposite sign, that the value of the flux to the collector surface was one order of magnitude smaller than expected theoretically. This discrepancy was explained quantitatively by the instability of the colloidal dispersion. A much better quantitative agreement with the Levich theory of diffusion-controlled transport to a rotating disk was reached in ref. [3] with the deposition of polystyrene latex particles carrying a negative double-laver charge on positively charged plastic films. In contrast to the deposition of negative particles onto positive surfaces, the deposition of negative particles onto surfaces negative was, firstly, not linear with time and, secondly, not proportional to the sol concentration. Some tentative deductions were made from the available results. Surface roughness, the approximate nature of formulae for van der Waals and double laver interactions used in the calculations, colloid stability and, finally, heterogeneity of the collector and particle surfaces were found to provide the best explanation of the observed discrepancies.

Other methods are based on the use of radioactive tracers. Bowen and Epstein [53] studied the deposition of uniform spherical silica particles in a parallel-plate channel. When the channel wall was charged positively and the particles negatively, the theory and experiments yielded very close results, especially at intermediate counterion concentrations, assuming that the process was mass-transfer controlled. However, for negative particles and negative channel walls, the measured deposition rates were always much greater than those predicted theoretically. They explained this discrepancy by surface heterogeneity, which could result in preferential deposition onto areas of locally favorable potential or geometry.

In summary, the particle deposition rate will depend on a large number of experimental parameters, but it is by now clear that the number of parameters presently used is insufficient to fully describe the deposition phenomena, certainly when electrical double-layer interactions are repulsive. Especially in this case, it is essential to know the energy of interaction at small particle-collector separations. Until now theories have been based on continuum concepts. Deposition experiments can provide essential information needed to formulate a more powerful theory of the interactions in the vicinity of a wall.

Detachment

The force of adhesion between solid particles and a flat substrate can be determined by applying external forces such as centrifugation [54] or hydrodynamic shear [55,60]. Visser [55] had used hydrodynamic techniques, i.e, rotating cylinders, to study the removal of submicron particles from various substrates. He developed empirical relationships which relate the force of adhesion to the viscous drag experienced by the particle, which is assumed to be embedded in a steady, viscous sublayer. Visser proposed that an attached particle is dislodged by a component of hydrodynamic force acting parallel to a flat substrate in shear flow. Cleaver and Yates [57] objected that such a mechanism did not account for the possibility of motion away from the wall surface. They proposed a model in which a lifting force [61] arises due to stagnation point flow in the viscous sublayer of turbulent shear. An expression derived by Dahneke [58,59] for the rate of escape of Brownian particles from deep minima of potential energy can be used to predict detachment in the presence of flow.

The greatest diversity between the alternative approaches lies in the choice of flow regime used to promote the release of particles. Pelton et al. [13,14] employed Poiseuille flow in the case of polystyrene particles attached to the inner wall in a capillary. Hubbe [62] used the coaxial shearing method to detach TiO_2 particles from cellulose and glass. Turbulent shear flow has been found to be an effective agent for the detachment of very small solid particles from solid walls [55-57,66]. Visser [55,56] showed that the hydrodynamic shear stress required to detach carbon black and polystyrene spheres from cellulose was a function of pH and ionic strength. Matijevic and coworkers [63-65] showed that the release of uniform spherical particles of hematite from packed columns of glass and steel beads was a function of pH, ionic strength and specifically adsorbed ions. Hubbe [66] found that the detachment of TiO_2 particles from cellulose and glass substrates depends on the applied shear stress, the size of the particles, pH and the time of shearing.

III. SCOPE OF THIS THESIS

The present work describes theoretical and experimental studies of the effects of polymer on the impingement of colloidal particles onto glass surfaces. The layout of this thesis is as follows

In Chapter 2, the fluid flow field and kinetics of mass transfer are described and the experimental technique and conditions are specified. Results of deposition-detachment experiments of the latex particles on and from glass surfaces are presented and discussed. It turned out that the behavior of model latexes is much more complex than envisaged. It was shown that surface collisions can play an important role in the detachment process.

In Chapter 3 we investigate the effects of polymer, either adsorbed on latex particles or free in solution, on the deposition process. We compare the deposition of polymer coated latexes with bare ones. From observations of the deposition of a polystyrene latex suspension in the presence of non-ionic polymer and electrolyte, we can derive quantitative information concerning the influence of the polymer on the interaction between particles and the solid surface.

In Chapter 4 we investigate the adhesive strength of polystyrene latex particles bonded to glass with polymer. As a polymer we used polyethylene oxide, a neutral linear polymer. It will be shown that the presence of polymers dissolved in the jet significantly affects the particle detachment process. The molecular weight and polymer concentration in the solution were varied, as well as the Reynolds number (flow rate).

In Chapter 5 we studied the effects of polyelectrolytes on the deposition and detachment of colloidal particles subjected to flow. The aim of this work is to check whether, under such conditions, experimental results are in agreement with mass-transfer theory, and whether polyelectrolyte increases the bond strength between a particle and the collector surface.

In Chapter 6, General Conclusions, claims for original research and suggestions for further work are described.

Finally, in Appendix 1, further details of the main experimental technique are described.

The work described in Chapters 2, 3, 4 and 5 have been written in a manner suitable for regular publication with little or no further modifications. Thus each Chapter is complete in itself, having its own abstract and references. Actually Chapters 2, 3, 4 and 5 have already been accepted by or are being submitted to the following journals:

Chapter 2 - Varennes, S., and van de Ven, T.G.M., Physico Chemical Hydrodynamics (in press).

Chapter 3 - Varennes, S., and van de Ven, T.G.M., (submitted to Physico Chemical Hydrodynamics).

Chapter 4 - Varennes, S., and van de Ven, T.G.M., (submitted to Physico Chemical Hydrodynamics).

Chapter 5 - Varennes, S., and van de Ven, T.G.M., (submitted to the J. Colloids and Surfaces).

These entities have their own symbols which, as far as possible, are used consistently throughout the thesis.

REFERENCES

1. Dabros, T., and van de Ven, T.G.M., Colloid Polym. Sci., 261, 694 (1983).

2. Marshall, J.K., and Kitchener, J.A., J. Colloid Interface Sci., 22, 342 (1966).

3. Hull, M., and Kitchener, J.A., Trans. Faraday Soc., 65, 3093 (1969).

4. Adamczyk, Z., Zembala, M., Siwek, B., and Czarnecki, J., J. Colloid Interface Sci., 110, 188 (1986).

5. Dabros, T., and van de Ven, T.G.M., Physico Chemical Hydrodynamics, 8, 161 (1987).

6. Kitchener, J.A., Br. Polymer J., 4, 217 (1972).

7. Fleer, G.J., and Lyklema, J., J. Colloid Interface Sci., 46, 1 (1974).

8. Gregory, J., J. Colloid Interface Sci., 55, 35 (1976).

9. La Mer, V.K., and Healy, T.W., Rev. Pure Appl. Chem., 13, 112 (1963).

10. Smith, D.K.W., and Kitchener, J.A., Chem. Eng. Sci., 33, 1631 (1978).

11. van Voorst Vader, F., and Dekker, H., J. Colloid Interface Sci., 83, 377 (1981).

12. Mühle, K., Colloid Polymer Sci., 263, 660 (1985).

13. Pelton, R.H., Nugent, H., and Allen L.H., Colloids Surfaces, 4, 397 (1982).

14. Pelton, R.H., Allen, L.H., J. Colloid Interface Sci., 99, 387 (1984).

15. Hubbe, M.A., Preprints to Tappi Papermakers Conf., Atlanta, 2-4 April 1984, Tappi Press, Atlanta, GA, 22-30.

16. Pelton, R.H., Tappi J., 67, 116 (1984).

17. Derjaguin, B.V., and Landau, L., Acta Phys. Chem. URSS, 14, 633 (1941).

18. Verwey, E.J.W., and Overbeek, J.Th.G., Theory of the stability of lyophobic colloids, Elsevier (1948).

19. Hiemenz, P.C., Principles of colloid and surface chemistry, M. Dekker, N.Y., (1977).

20. Frisch, H.L., Simha, R., and Eirich, F.R., J. Chem. Phys., 21, 365 (1953).

21. Simha, R., and Eirich, F.R., J. Phys. Chem., 57, 584 (1953).

22. Frisch, H.L., and Simha, R., J. Phys. Chem., 58, 507 (1954).

23. Frisch, H.L., J. Phys. Chem., 59, 633 (1955).

24. Frisch, H.L., and Simha, R., J. Chem. Phys., 27, 702 (1957).

25. Forsman, W.C., and Hughes, R., J. Chem. Phys., 38, 2130 (1963).

26. Hoffman, R.F., and Forsman, W.C., J. Polym. Sci., Part A2, 8, 1847 (1970).

27. Gilliland, E.R., and Gutoff, E.B., J. Phys. Chem., 64, 407 (1960).

28. Silberberg, A., J. Phys. Chem., 66, 1872 (1962).

29. DiMarzio, E.A., J. Chem. Phys., 42, 2101 (1965).

30. Silberberg, A., J. Phys. Chem., 66, 1884 (1962).

31. Jenckel, E., and Rumbach, B., Z. Elektrochem., 55, 612 (1951).

32. Hoeve, C.A.J., DiMarzio, E.A., and Peyser, P., J. Chem. Phys., 42, 2558 (1965).

33. Hoeve, C.A.J., J. Chem. Phys., 43, 3007 (1965).

34. Roe, R.J., J. Chem. Phys., 43, 1591 (1965).

35. Rubin R.J., J. Chem. Phys., 43, 2392 (1965).

36. Motomura, K., and Matuura, R., J. Chem. Phys., 50, 1281 (1969).

37. Silberberg, A., J. Chem. Phys., 46, 1105 (1967).

38. Silberberg, A., J. Chem. Phys., 48, 2835 (1968).

39. DiMarzio, E.A., and Rubin, R.J., J. Chem. Phys., 55, 4318 (1971).

40. Hoeve, C.A.J., J. Polym. Sci., Part C, 34, 1 (1971).

41. Hoeve, C.A.J., J. Polym. Sci., 30, 361 (1970).

42. Napper, D.H., Polymeric Stabilization of Colloidal Dispersions, Academic Press (1983).

43. Fleer, G.J., and Scheutjens, J.M.H.M., J. Phys. Chem., 83, 1619 (1979).

44. Fleer, G.J., and Scheutjens, J.M.H.M., J. Phys. Chem., 84, 178 (1980).

45. Fleer, G.J., and Scheutjens, J.M.H.M., Adv. Colloid Interface Sci., 16, 341 (1982).

46. Tabor, D., andWinterton, R.H.S., Proc. Roy. Soc. London, A312, 435 (1969).

47. Issraelachvili, J.N., and Tabor, D., Proc. Roy. Soc. London, A331, 19 (1972).

48. Israelachvili, J.N., and Adams, G.E., Nature, 262, 774, (1976).

49. Israelachvili, J.N., and Adams, G.E., J. Chem. Soc. Faraday Trans, 174, 975 (1978).

50. Pashley, R.M., and Israelachvili, J.N., Colloids Surfaces, 2, 169 (1981).

51. Pashley, R.M., and Israelachvili, J.N., J. Colloid Interface Sci., 101, 511 (1984).

52. Israelachvili, J.N., and Pashley, R.M., J. Colloid Interface Sci., 98, 500 (1984).

53. Bowen, B.P., Epstein, N., J. Colloid Interface Sci., 72, 81 (1979).

54. Krupp, H., Adv. Colloid Interface Sci., 1, 111 (196[illegible]).

55. Visser, J., J. Colloid Interface Sci., 3[illegible], [illegible] (19[illegible]).

56. Visser, J., J. Colloid Interface Sci., 55, 66[illegible] (19[illegible]).

57. Cleaver, J.W., and Yates, B., J. Colloid Interface Sci., [illegible], [illegible] (19[illegible]3).

58. Dahneke, B., J. Colloid Interface Sci., [illegible], 89 (19[illegible]).

59. Dahneke, B., J. Colloid Interface Sci., [illegible], 19[illegible] (19[illegible]).

60. Zimmer, S.L., and Dahneke, B., J. Colloid Interface Sci., 54, 329 (1976).

61. Goren, S.L., J. Fluid Mech., 26, 325 (1971).

62. Hubbe, M.A., Colloids and Surfaces, 16, 249 (1985).

63. Kolakowski, J.E., and Matijevic, E., J. Chem. Soc. Faraday Trans. I, 75, 65 (1979).

64. Kuo, R.J., and Matijevic, E., J. Chem. Soc. Faraday Trans. I, 75, 2014 (1979).

65. Kuo, R.J., and Matijevic, E., J. Colloid Interface Sci., 78, 407 (1980).

66. Hubbe, M.A., Colloids and Surfaces, 16, 227 (1985).

CHAPTER [illegible]

DEPOSITION AND DETACHMENT OF LATEX PARTICLES AT GLASS SURFACES EXPOSED TO FLOW

ABSTRACT

Deposition and detachment of 3 μm polystyrene latex particles on clean and surface treated cover glass slides used as collectors was investigated using the stagnation point flow technique, which was developed to study the deposition of colloidal particles under well controlled hydrodynamic conditions. The deposition can be followed microscopically and recorded on video. This technique allows us to study both particle deposition and particle detachment at the same time.

It was found that the deposition of latex depends on salt concentration but not in the manner predicted by the DLVO-theory, which, combined with transport theory, predicts a sudden change from almost no deposition to fast deposition at a well-defined electrolyte concentration. Instead we find a gradual increase in deposition rates, somewhat below the critical electrolyte concentration. It is very probable that this anomalous deposition behavior is caused by surface protrusions on the latex surface because altering the surface leads to lower deposition rates, despite decreased energy barriers. It is shown that the detachment of particles is governed by a convective-diffusive transport out of an energy minimum, which is enhanced by surface collisions between suspended and deposited particles.

I. INTRODUCTION

By performing model experiments on deposition and detachment of colloidal particles we can deepen our understanding of these important phenomena. Many deposition studies have been performed with model colloids on well-defined surfaces. Marshall, Kitchener and co-workers [1,2] used the rotating disk technique which provides well-defined hydrodynamic conditions. In their experiments, a problem with the experimental observations of deposition rates is that some of the particles, initially deposited on a surface, may be removed in the process of rinsing or preparing the surface under investigation for microscopic observation. To avoid such problems it is essential to detect the deposition of particles directly by microscopic observations during the deposition process. Dabros and van de Ven [3] reported results using a new experimental technique in which a direct observation of the deposition process can be realized. It consists of creating a stagnation point flow in a confined impinging jet. Such a flow field is very similar to the flow near a rotating disk, but has the advantage of a stationary collector surface, making it relatively easy to observe the surface while particle deposition takes place. Some papers have been published on the impinging jet method [4,5], containing experimental work dealing with barrierless deposition rates as a function of particle dimension and flow intensity. The present paper reports measurements on the deposition of latex particles on glass surfaces for various flow rates and electrolyte concentrations. In subsequent papers we will deal with the effects of polymer absorption on deposition which was our primary objective. While comparing polymer coated latexes with bare ones, it turned out that the behavior of model latexes is much more complex than envisaged. In this paper we report on our findings on bare latexes.

The removal of particles already attached to the surface is quite a distinct problem which has also recently received some preliminary study. Visser [6] proposed that an attached particle is disloged by a component of hydrodynamic force acting parallel to a flat substrate in shear flow. Cleaver and Yates [7] proposed a model in which a lifting force arises due to stagnation point flow in a viscous sublayer of turbulent shear. Pelton et al. [8] employed Poiseuille flow in the case of polystyrene particles attached to the inner wall of a capillary. Hubbe [9] used the coaxial shearing method to detach samples of uniform colloidal TiO_2 spheres from cellulose and glass. In all these experimental techniques there is a tendency toward unstable flow and turbulence. In this paper we report on direct observations of the detachment of particles from a flat surface exposed to a stagnation point flow. It turns out that surface collisions can play an important role in the detachment process.

The paper is divided into five sections. In section II the fluid flow field and kinetics of mass transfer are described. The experimental technique and conditions are specified in section III. In section IV, results of deposition-detachment experiments are presented and discussed. Finally, in section V we present our concluding remarks.

II. THEORETICAL

Fluid flow field

The flow due to impingement of a confined laminar axisymmetric jet onto a flat surface has been discussed by Law and Masliyah [10]. They were interested in the effect of the presence of a confinement plate on the mass transfer in a laminar jet in the stagnation point flow and the wall-jet regions. The impinging jet system consists of a jet of liquid exiting through a circular tube of diameter d with an average velocity U into a region bounded by a confinement and an impingement plate. The confinement plate is located parallel to and at a distance h from the impingement plate. Law and Masliyah [10] numerically solved the transport equations for this geometry. They calculated the variations of the local Sherwood number along the impingement plate for different Reynolds numbers in the range of 400 to 1900 for various jet-to-plate spacings.

Their impinging jet system is very similar to ours, but our observations are restricted to the region near the stagnation point where the fluid flow field takes on a simple form.

The impinging jet system used in this paper is schematically shown in Fig. 1. A dispersion of colloidal particles suspended in a fluid medium of viscosity η is pumped at a volumetric flow rate Q through the smaller inner tube A and exits it through an orifice made in the center of a thin plate covering tube A. The stream of suspension flowing out of the orifice impinges on a flat collector plate and runs down the cell

Fig. 1 Schematics of deposition cell (a) and details of the geometry of the system (b).

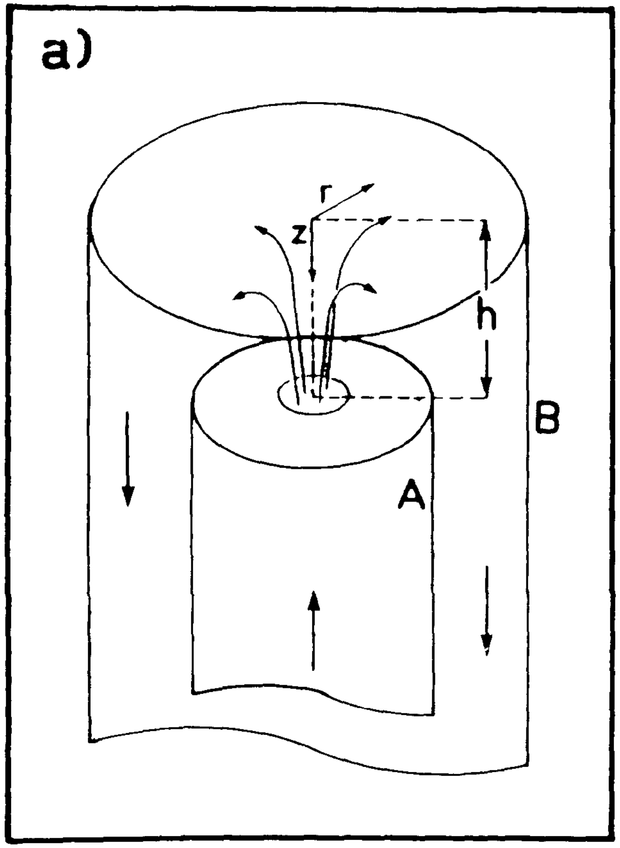
a)
r
z
h
B
A

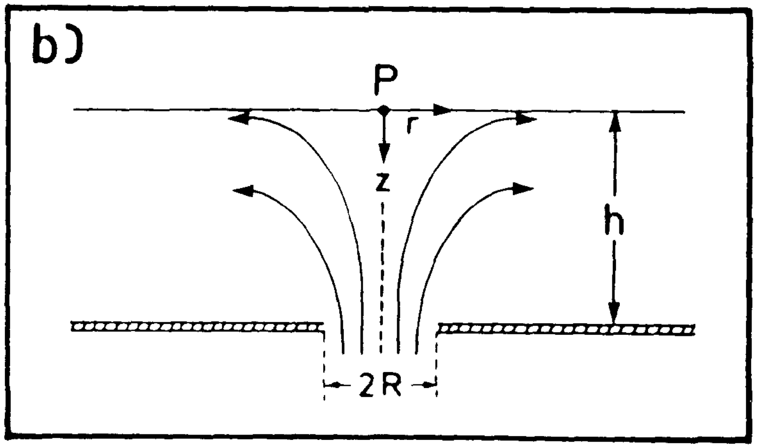
b)
P
r
z
h
2R

through the larger outer tube B, (Fig. 1(a)). The geometry of the deposition cell is shown in Fig. 1(b). The radius of the hole is denoted by R and the distance between the top and the bottom plate by h.

To find the flow field in the area of observation of the experimental set-up, Dabros and van de Ven [3] solved the stationary Navier-Stokes equation assuming axial symmetry of the system. They assumed that the fluid is incompressible and Newtonian. Due to the symmetry of the system, they introduced the vorticity ω and the stream function ψ, which are defined (in dimensionless form) by

$$\omega = \frac{\partial V_r}{\partial z} - \frac{\partial V_z}{\partial r} , \qquad (1)$$

$$V_z = \frac{1}{r} \frac{\partial \psi}{\partial r} , \qquad V_r = - \frac{1}{r} \frac{\partial \psi}{\partial z} . \qquad (2)$$

Here z and r are non-dimensionalized by R and V_z and V_r by the mean velocity in the exit hole. The governing Navier-Stokes equation can be formulated as

$$\bar{\omega} = \frac{1}{r^2} \left[- \left(\frac{\partial^2 \psi}{\partial r^2} + \frac{\partial^2 \psi}{\partial z^2} \right) + \frac{1}{r} \frac{\partial \psi}{\partial r} \right] \qquad (3)$$

$$r^2 \left[\frac{\partial}{\partial z} \left(\bar{\omega} \frac{\partial \psi}{\partial r} \right) - \frac{\partial}{\partial r} \left(\bar{\omega} \frac{\partial \psi}{\partial z} \right) \right] - \frac{1}{Re} \left[\frac{\partial}{\partial z} \left(r^3 \frac{\partial \bar{\omega}}{\partial z} \right) + \frac{\partial}{\partial z} \left(r^3 \frac{\partial \bar{\omega}}{\partial r} \right) \right] = 0 \qquad (4)$$

where $\bar{\omega} = \omega / r$ and $Re = UR/\nu$ is the Reynolds number, U is the average velocity in the exit hole, R is the radius of the exit hole, and ν is the fluid kinematic viscosity.

Eq. (4) with the appropriate boundary conditions was solved numerically using the overrelaxation finite-difference method described in detail by Dabros and van de Ven [3].

An example of the flow profile in the confined impinging jet is given in Fig. 2 for the particular case of Re = 60. Locally, near the symmetry point P (see Fig. 1(b)), the flow closely resembles a stagnation point flow, which can be expressed as

$$v_r = \bar{\alpha} r \qquad (5a)$$

$$v_z = - \bar{\alpha} z \qquad (5b)$$

The parameter $\bar{\alpha}$ is a dimensionless constant characterizing the intensity of the stagnation point flow which depends on the cell geometry and the volume flow rate, but does not depend on the radial coordinate r. From Eqs. (1) and (5) it follows that [illegible] $= \bar{\alpha} r$ or

$$[illegible] = \bar{\alpha} \qquad (6)$$

in this region. In order to estimate the extension of the region in which Eqs. (5) applied, Dabros and van de Ven [3] calculated $\bar{\alpha}$ as a function of r. They found for distances up to 10% of the exit hole radius, $\bar{\alpha}$ is constant, and concluded that the flow in that region is a pure stagnation point flow. In our system, the radius of the exit hole equaled 1 mm. The deposition region analyzed extended radially up to 450 μm, i.e. 0.45 R. This is outside the range where one has a pure stagnation point

Fig. 2 Calculated streamlines in flow cell for Re = 60 for cell geometry h/R = 2.3. The numbers on the right refer to the value of the stream function ψ, which varies from 0 on the lower plane to − 0.5 on the top plane.

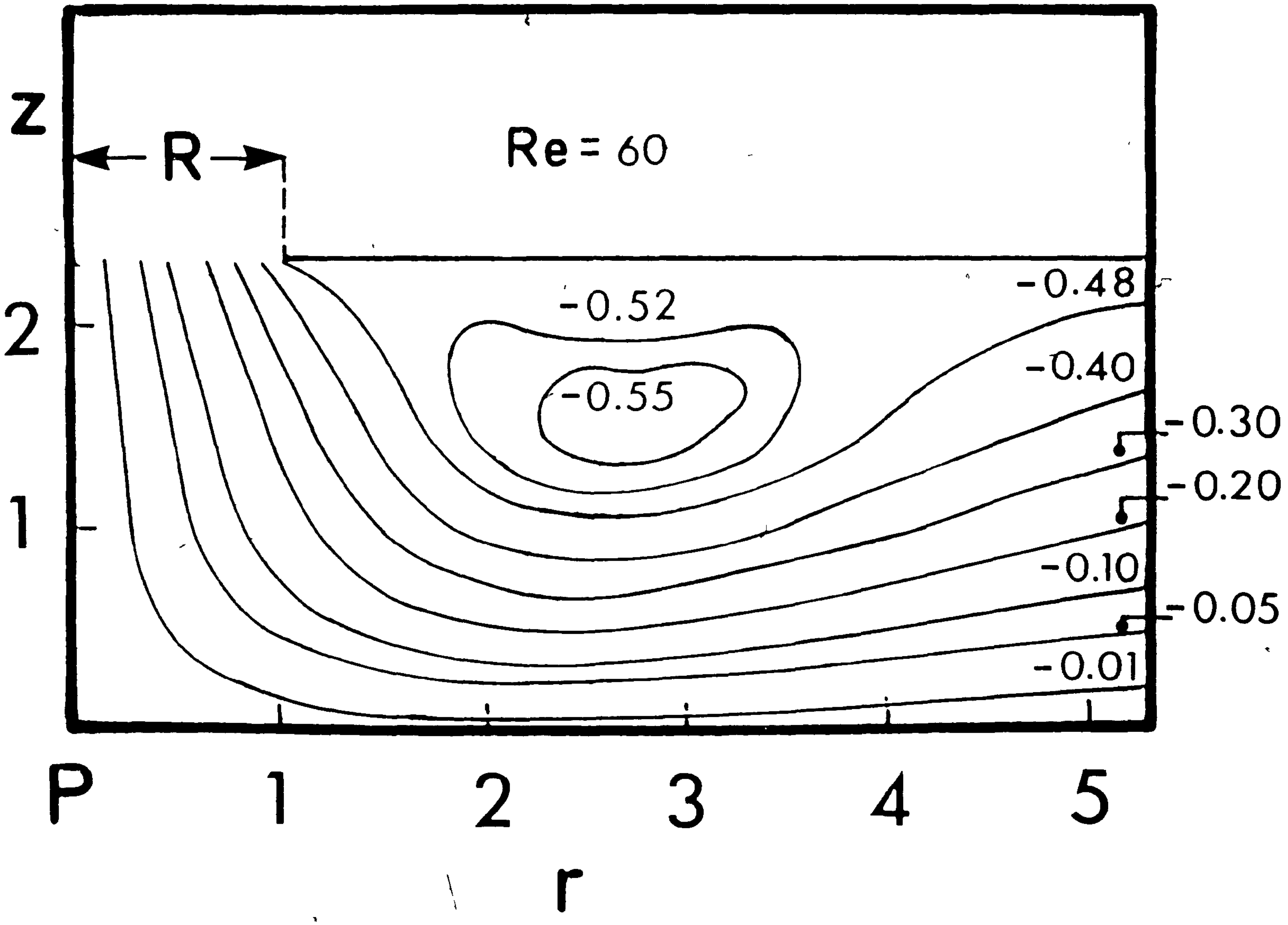
z
R
Re = 60
2
1
-0.52
-0.55
-0.48
-0.40
-0.30
-0.20
-0.10
-0.05
-0.01
P
1
2
3
4
5
r

flow. According to the exact flow field [3] at r = 450 μm, $\bar{\alpha}$ is about 15% lower than at the center. When needed, corrections to account for the non-constancy of $\bar{\alpha}$ have been made. In general $\bar{\alpha}$ is a function of the Reynolds number and the geometry of the deposition cell. For our experimental impinging jet, the separation between the collector cover glass and the outflow plate was h = [illegible].3 mm and the ratio h/R equaled [illegible].3. Numerically calculated values of $\bar{\alpha}$, found by comparing the numerically calculated flow field with eqs. ([illegible]), are given in Table I. When Re < 1[illegible], $\bar{\alpha}$ can be approximated by:

[illegible]

For higher Reynolds numbers, we can calculate $\bar{\alpha}$ from the relationship given by Dabros and van de Ven [illegible] obtained from numerical results of Law and Masliyah [1[illegible]] which show that $\bar{\alpha}$ becomes approximately proportional to $Re^{1/2}$. When h/R = [illegible].3 and Re > 1[illegible] the value of $\bar{\alpha}$ can be found from

$$\bar{\alpha} = [illegible].1\, Re^{1/2} . \qquad ([illegible])$$

The values of $\bar{\alpha}$ are also given in Table I for high Reynolds number.

In our cell the value of V depends on the radius R of the exit hole and the fluid volumetric flow rate Q according to the relationship:

$$V = Q/\pi R^2 \qquad (8)$$

and can be easily varied within broad limits by changing Q.

TABLE I

Values of the parameter $\bar{\alpha}$ describing the strength of the flow in an impinging jet near the stagnation point, for h/R = 2.3.

Re	$\bar{\alpha}_1$ [a]	$\bar{\alpha}_1$ [b]
[illegible]	[illegible]	
[illegible]	.9	
[illegible]	[illegible]	
[illegible]	.99	
[illegible]	1.[illegible]	
[illegible]	1.[illegible]	1.[illegible]
[illegible]		1.43
[illegible]		1.56
[illegible]		1.71
381		1.95
[illegible]		2.33
907		3.01

[a] - from Eq. (7a).

[b] - from Eq. (7b).

Transforming Eqs. (5) into dimensional velocities results in the same equations with $\bar{\alpha}$ replaced by α given by

$$\alpha = \frac{\bar{\alpha}U}{R^2} . \qquad (9)$$

Hence α can be determined from the measured velocity U. From α we can calculate the wall shear rate. For a particle at the wall, the wall shear rate G equals

$$G = \frac{\partial v_r}{\partial z} = \alpha r \qquad (10)$$

where we have now expressed all parameters in dimensional form, G in (s^{-1}), α in ($m^{-1}s^{-1}$) and r in (m). It can be seen from Eq. (10) that the shear rate is zero at the stagnation point and increases linearly with distance. Goldman, Cox and Brenner [11] calculated the force and torque exerted by a creeping shear flow on a sphere rigidly attached to a wall. For the force on a sphere of radius a they found

$$F = C\eta a^2 G \qquad (11)$$

where C is a constant which equals 1.7 x 6π. Inserting (10) in the formula for the force yields

$$F = C\eta\alpha r a^2 . \qquad (12)$$

Eq. (12) provides the tangential hydrodynamic force acting on a particle firmly deposited at a distance r from the stagnation point. Hence by measuring α and r_{crit} (i.e. the critical distance where a deposited particle detaches from the surface), we can calculate the hydrodynamic forces exerted on the deposited spheres prior to detachment.

Mass transfer in a stagnation point flow

The mass transfer of spherical particles towards the impingement plate near the stagnation point is described by the convective diffusion equation, which, for steady state, can be written as

$$[illegible] \qquad (13)$$

where [illegible] is the diffusion constant of a sphere which depends on the distance between the sphere and the surface, n is the number concentration of spheres in suspension, and $\underline{u}$ is the velocity of the spheres, which is the sum of the hydrodynamic velocity given by Eqs. (5), but corrected for particle-wall interactions and a velocity due to colloidal and external forces. Eq. (13) was solved in ref. 3. From the solution the flux of particles j towards the surface can be calculated. Usually the flux is expressed in dimensionless form in terms of a Sherwood number Sh, defined as

$$Sh = \frac{ja}{D_0 n_0} \qquad (14)$$

where a is the sphere radius and D_0 and n_0 are the diffusion constant of an isolated sphere and the bulk concentration of spheres respectively.

D_0 can be found from the Stokes-Einstein equation

$$D_0 = \frac{kT}{6\pi\eta a} . \tag{15}$$

In general Sh is a function of various dimensionless parameters·

$$Sh = f(Pe, Ad, \bar{\lambda}, D\ell, \tau, Gr) \tag{16}$$

where the Péclet number, defined by

$$Pe = \gamma a^3 / D_0 , \tag{17}$$

is the ratio of hydrodynamic to diffusion effects,

Ad is the dimensionless adhesion number characterizing the influence of dispersion forces defined as

$$Ad = \frac{A}{6kT} , \tag{18}$$

A being the Hamaker constant of the system particle-fluid-collector,

$\bar{\lambda}$ is the parameter accounting for retardation in dispersion forces,

$$\bar{\lambda} = \lambda / a \tag{19}$$

λ being the London retardation wavelength, $D\ell$ is the dimensionless double-layer number

$$D\ell = \frac{4\pi\varepsilon\varepsilon_o\zeta_1\zeta_2 a}{kT} \qquad (20)$$

where ζ_1, ζ_2 are the electrokinetic potentials of the particle and collector surfaces, ε is the dielectric constant of the medium and ε_o is the permittivity of free space, $\tau = \kappa a$, where κ is the Debye reciprocal length parameter (or reciprocal double layer thickness), Gr is the dimensionless gravity number accounting for sedimentation effects defined as

$$Gr = \frac{2}{9}\,\frac{\Delta\rho\, g\, a^3}{\eta D_o} \qquad (21)$$

where $\Delta\rho$ is the apparent density of the particles and g the acceleration due to gravity.

The flux to the collector surface, when energy barriers are absent and gravity is the only external force, can be approximated as, neglecting the opposing effects of hydrodynamic resistance and van der Waals attraction [3]

$$Sh_{fast} = \frac{\exp\left[-\frac{Pe}{6}(\delta+1)^3 - Gr\,\delta\right]}{\int_\delta^\infty \exp\left[-\frac{Pe}{6}(H+1)^3 - Gr\,H\right]dH}\ , \qquad (22)$$

where δ is the primary minimum distance and H the distance between the sphere center and the wall, both rendered dimensionless by the sphere radius.

In analogy with coagulation [12] it is convenient to define a deposition efficiency α_d as

$$Sh = \alpha_d Sh_{fast} , \tag{23}$$

where Sh is the Sherwood number in the presence of an energy barrier and corresponds to the dimensionless deposition rate obtained experimentally.

For our experimental conditions, the gravity number was $Gr = -2.3$, the adhesion number for a Hamaker constant $A =$ [illegible] $\times 10^{-20}$ J corresponded to $Ad = 0.8$ and $\bar{\lambda} =$ [illegible]. Theory predicts (almost) no deposition at $\tau < \tau_{crit}$ and fast deposition at $\tau > \tau_{crit}$. For our system $\tau_{crit} \approx 650$. Fast deposition will occur when no energy barrier is present.

Notice that Sh does not depend on the distance r from the stagnation point flow, which means that the particle flux is predicted to be uniform over the total collector surface. This is a direct consequence of Eq. (5b) which states that the normal fluid velocity is independent of r. The coating density N_d can be expressed as

$$N_d = \int_0^t j \, dt = Sh \frac{D_0 n_0}{a} t , \tag{24}$$

i.e. it is predicted to be a linear function of time and n_0. In reality the deposition is always non-linear, caused by blocking and escaping effects. Including these effects, the coating density can be approximated by [13]

$$N_d(t) = \frac{J}{\beta} \left[1 - \exp \left\{ - \beta t \right\} \right] \tag{25}$$

where

$$\beta = \beta_m + \beta_e \, . \qquad (26)$$

Here β_m is a masking or blocking coefficient defined as a product of the initial flux j and the surface blocked per particle

$$\beta_m = \pi a^2 \gamma j = \pi a \gamma' j_0 n_0 \mathrm{Sh} \qquad (27)$$

γ is a dimensionless coefficient expressing the number of particle cross sections blocked per particle. Dabros and van de Ven [13] estimated that the surface effectively blocked by deposited particles may be 20 to 30 times greater than their geometrical cross section. Escape of the particles from a primary minimum due to thermal motion depends on the value of the escape coefficient β_e [13]

$$\beta_e = \mathrm{Sh} \frac{D_0 e^{V/kT}}{a \Delta h} \qquad (28)$$

where V is the energy minimum in the interaction between a particle and the collector, kT the thermal energy, and Δh the width of primary minimum region.

Effect of surface collisions on particle escape

In this study we found that particles could not only be dislodged by hydrodynamic forces exerted on them, but also by collisions between freely suspended particles and deposited particles. During a surface collision the probability that a particle is dislodged is considerably increased. The probability that particles can escape from a surface by surface collisions is usually not considered in particle detachment mechanisms. No mention of it is made in a recent summary of detachment mechanisms by Hubbe [14].

To know the efficiency of the detachment process by the mechanism of surface collisions, we must first estimate the number of collisions a particle deposited on the surface will suffer per unit time. Because a collision in a fluid flow field is an ill-defined concept, we define a collision in a manner analogous to the definition by Smoluchowski for the collision between two spheres in simple shear [15]. Neglecting all hydrodynamic and colloidal particle-wall and particle-particle interactions, a collision between a suspended and a deposited particle is defined to occur when the center of a moving particle enters the collision sphere around the immobile particle.

The collision frequency in stagnation point flow can be calculated from the flow field defined previously

$$V_z = -\alpha z^2 = dz/dt \qquad (29)$$

$$V_r = \alpha r z = dr/dt \,. \qquad (30)$$

Dividing Eq. (29) by Eq. (30) we obtain

$$\frac{dz}{dr} = -\frac{z}{r} \,. \qquad (31)$$

Integration of Eq. (31) results in

$$z = \frac{C}{r} \tag{32}$$

where C is the constant of integration. For the limiting trajectory the constant C is determined by the condition that the trajectory has one point in common with the collision sphere (see Fig. 3(a)). This condition leads to a fourth order equation which has no analytical solution. An approximate solution can be found when d >> a, d being the distance between the center of the deposited particle and the stagnation point. A sphere on the limiting trajectory goes approximately through point r = d, z = 3a and hence

$$3a = \frac{C}{d} \quad \text{or} \quad C = 3ad . \tag{33}$$

At $z = \ell$

$$\ell = \frac{3ad}{r_\ell} \quad \text{or} \quad r_\ell = \frac{3ad}{\ell} . \tag{34}$$

The top view at $z = \ell$ is illustrated in Fig. 3(b) showing that

$$\tan\gamma = \frac{a}{d} \approx \frac{S}{r_\ell} . \tag{35}$$

When d >> a we can write

$$\gamma \approx \frac{a}{d} \approx \frac{S}{r_\ell} . \tag{36}$$

Fig. 3 Schematic representation of collision cross section in stagnation point flow. (a) Side view. The broken lines around the particle with radius a denote the collision sphere. The solid curve lines represent the limiting trajectory of the suspended particles in the jet. (b) Top view.

a)

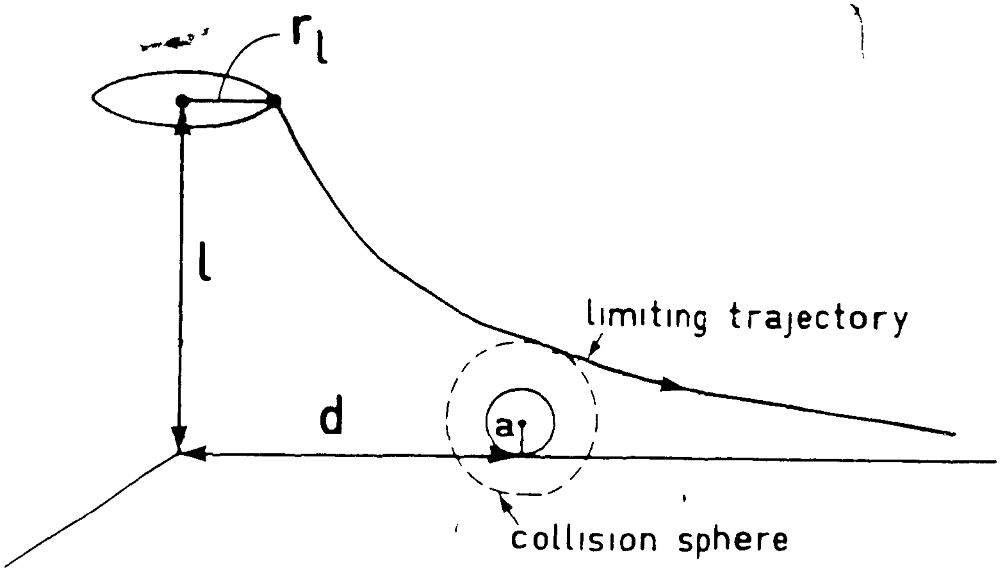

r_l
l
limiting trajectory
d
a
collision sphere

b)

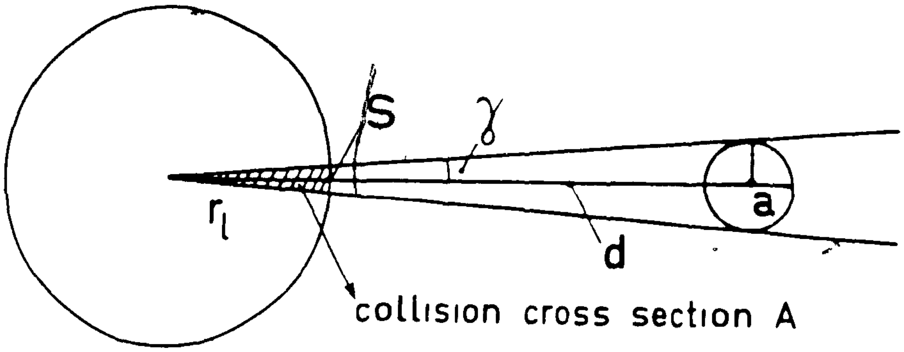

S
γ
r_l
a
d
collision cross section A

The collision cross section A equals

$$A \simeq Sr = \frac{ar_{\ell}^2}{d} . \qquad (37)$$

Combining (34) and (37) yields

$$A = \frac{9a^3d}{\ell^2} . \qquad (38)$$

The number of particles passing through A per second equals

$$I = V_z nA = 9\alpha a^3 dn . \qquad (39)$$

Eq. (39) gives the number of collisions per deposited particle per second when d >> a. This number is linearly proportional to the distance from the stagnation point and to particle concentration. From Eq. (39) one can calculate the surface collision efficiency σ, defined as the ratio of the number of particles removed and the total number of surface collisions:

$$\sigma = \frac{x}{9\alpha a^3 dnt} \qquad (40)$$

where x is the fraction of particles removed after t seconds (at distance d). Or when the particle concentration is expressed in terms of the volume fraction ϕ

$$\sigma = \frac{4\pi x}{27\alpha\phi dt} . \qquad (41)$$

When a deposited particle suffers a collision with a suspended particle its probability of escape is increased. Assuming that the duration of a collision t_c is short compared to the time T between collisions, we can express the probability of escape p as

$$p = \frac{p_0(T - t_c) + p_c t_c}{T} \qquad (42)$$

where p_0 and p_c are the probability of escape in the absence and presence of collisions respectively. From the collision frequency per particle (Eq. (39)) we can express T in terms of the shear rate and volume fraction as

$$T = \chi_0 (G\phi)^{-1} \qquad (43)$$

where $\chi_0 = 4\pi/27$.

Because $t_c \propto G^{-1}$ we have

$$\frac{t_c}{T} \simeq \chi\phi \ , \qquad (44)$$

where χ is a constant of order unity.

Hence Eq. (42) can be rewritten as

$$p \simeq p_0 (1 - \chi\phi) + \chi\phi p_c \ . \qquad (45)$$

We further assume that the release of particles is exponential and hence

FIG. [illegible] (a) Model of latex particle bound to the surface by an elastic force in the x direction.

(b) Energy minimum [illegible] which a particle is captured. In the absence of a hydrodynamic force, the particle is at the origin with energy depth V_m. A particle subjected to a hydrodynamic force is at position x_o with an energy depth of V_o. A particle subjected to a surface collision is at x_c with energy V_c.

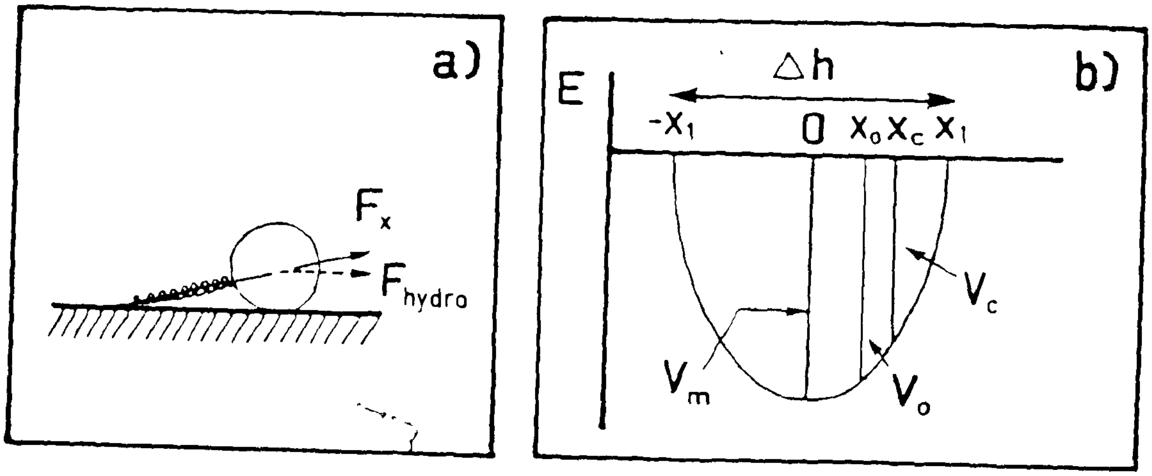
a)
F_x
F_{hydro}
b)
Δh
E
$-x_1$
0
x_o
x_c
x_1
V_c
V_m
V_o

$$p_o \propto e^{V_o/kT}$$

and (46)

$$p_c \propto e^{V_c/kT} .$$

We can model the link between a particle and the surface as an elastic bond which is stretched when a hydrodynamic force is exerted on the sphere (see Fig. 4(a)). We know that the larger the flow rate, the more likely it is for a particle to escape and, furthermore, that surface collisions increase the probability of escape. The hydrodynamic force and the surface collisions are effectively making the energy minimum less deep, (see Fig. 4(b)). In Eq. (46), V_o and V_c are the depth of the minimum for a sphere subjected to a hydrodynamic force F and to a surface collision respectively.

For the elastic energy we can write

$$V_{elastic} = V_m + \tfrac{1}{2}kx^2 . \tag{47}$$

Assuming that when $V_{elastic} = 0$ the bond is broken then

$$k = 8|V_m|/\Delta h^2 \tag{48}$$

where Δh is the width of the energy minimum.

When a hydrodynamic force is acting on the particle, the particle is at x_o given by

$$F = kx_o \qquad (49)$$

where F is the component of the hydrodynamic force in the x-direction. Hence

$$x_o = \frac{F\,\Delta h^2}{8\,|V_m|} \qquad (50)$$

and from Eqs. ([illegible]), (48) and (50)

$$V_o = V_m + \frac{F^2\,\Delta h^2}{16\,|V_m|} \quad . \qquad (51)$$

Similarly, the potential for surface collisions V_c is

$$V_c = V_m + \frac{F_c^{\,2}\,\Delta h^2}{16\,|V_m|} \qquad (52)$$

where F_c is the force exerted on the particle during a surface collision, which is proportional to (but larger than) F

$$V_c = V_m + \frac{\xi F^2\,\Delta h^2}{16\,|V_m|} \qquad (53)$$

where ξ is a constant. Assuming that during a collision the force exerted on a sphere is about twice as large, $\xi \approx 4$. From Eqs. (45), (46), (51) and (53) the escape time τ_{esc} (inversely proportional to p) can be expressed as

$$\tau_{esc}^{-1} \propto (1 - \chi\phi)\, e^{(V_m + CE^2)/kT} + \chi\phi e^{(V_m + \xi CE^2)/kT} \qquad (54)$$

where

$$C = \frac{\Delta h^2}{16\pi V_m} .$$

III. EXPERIMENTAL

Materials and preparations

A monodisperse polystyrene latex suspension was used, prepared by Dow Chemical Co., consisting of spherical particles of uniform size with a mean diameter of 2.99 μm and a standard deviation of 0.21 μm. To clean the latex suspension, successive centrifugation was performed until the conductivity of the distilled water was in the range of 2-3 x 10^{-6} Ω^{-1} m^{-1}. The latex suspension used in the deposition experiments was obtained by ultrasonically dispersing 0.2 cm^3 of concentrated latex in 197.8 cm^3 of distilled water. Before each experiment, 2 cm^3 of sodium chloride solution of various molarity was added to the latex dispersion.

The deposition cell was filled with the suspension and a peristaltic pump was used to circulate the suspensions around the system. The suspension was prepared immediately before each experiment and was used for only one experimental run that lasted about twenty minutes. The concentration of particles in the latex dispersions was obtained by particle counting in a calibrated hemacytometer cell under dark field illumination and was found to be equal to $1.4 \cdot 10^{14}$ particles m^3 ± (5%).

As a collector surface we used Fisherbrand microscope cover glass slides (Fisher Scientific Co.), made of finest optical glass, with uniform thickness and size 25 x 25 mm, uniformly flat and corrosion resistant. A new cover slide was used for each experiment. Each cover glass slide was cleaned by treating it successively for two hours in a concentrated nitric acid solution and for a half-hour in a concentrated hydrochloric acid solution. Subsequently, the slides were rinsed with large quantities of distilled water. Before use they were kept in distilled water. After this treatment, an analysis of electron and scanning microscope photographs of the treated and non-treated cover glass slides showed no cracks, scratches or any other particular features. Both had relatively smooth surfaces, with a surface roughness below 2 nm. Even with this low value for the surface asperities, the effect of surface roughness has to be considered because the theory outlined above is valid for perfectly smooth particles and collector surfaces.

Determination of deposition and detachment rates

The rates of particle deposition and release were obtained using the deposition cell, schematically illustrated in Fig. 5, similar to the one described by Dabros and van de Ven [5]. More details can be found in

Fig. [illegible] Experimental set-up.

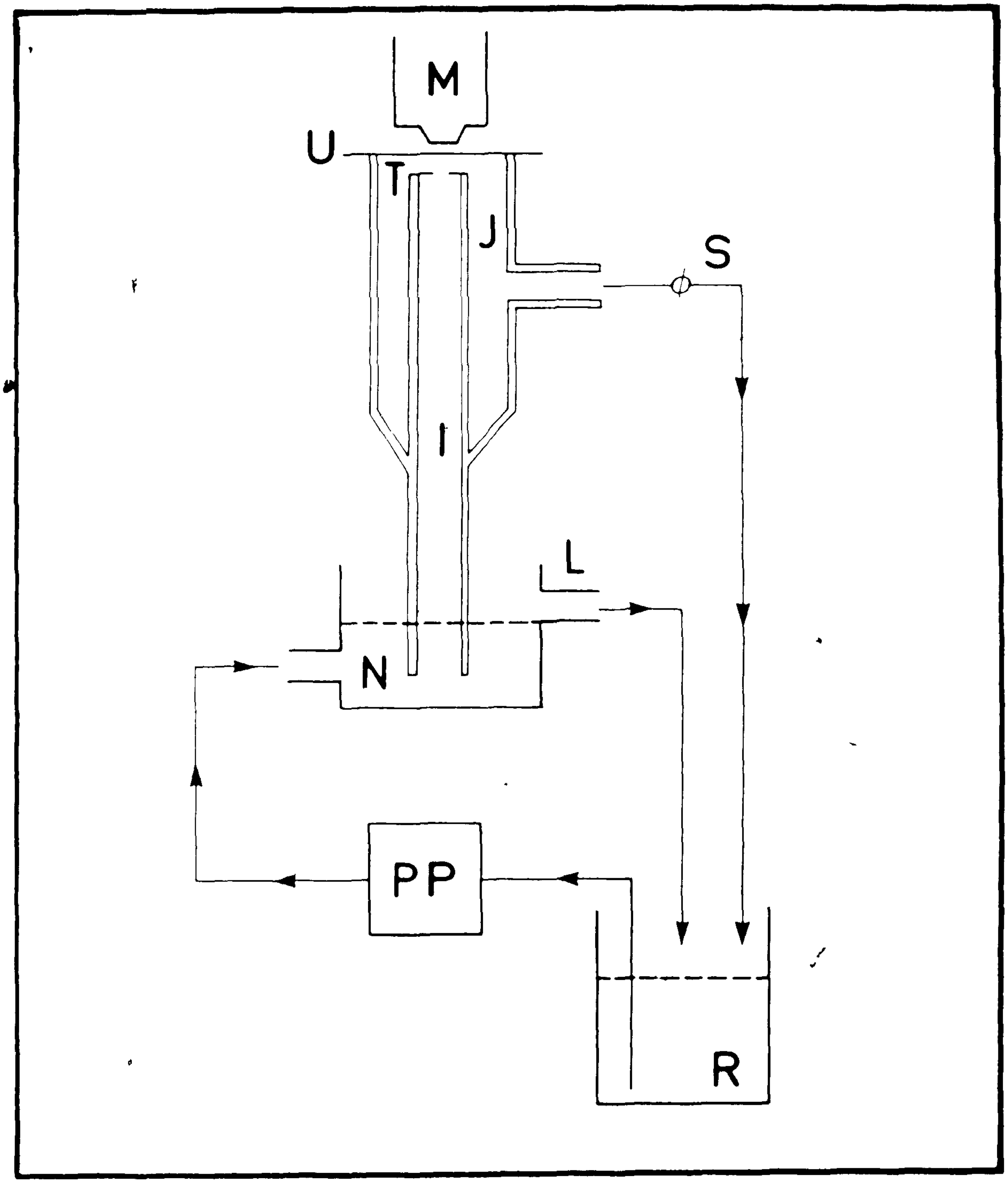
M
U
T
J
S
I
L
N
PP
R

ref. [16]. A colloidal suspension flows (under the action of gravity) from vessel N, through tube I, and eventually leaves the cell by tube J to exit in container R. At the upper end of the central tube a thin stainless steel plate with a 2 mm orifice in the center is fused to the glass. The stream of suspensions flowing out of the orifice impinges on a microscopic cover glass slide used as the collector. The cover slide remains fixed in position at the top of the outer tube owing to the under-pressure prevailing inside the cell. The intensity of the flow can be controlled by using a precision valve to provide a wide range of different flow rates. A pump was used to circulate the suspensions around the system from vessel R to N. The excess fluid in vessel N exits through tube I and falls into vessel R. This experimental set-up was designed to allow a smooth flow near the stagnation point. With it we measured particle deposition by microscopic observations by placing the cell under an optical microscope M. Observations were performed with dark field illumination from above using a Zeiss-Ultraphot II microscope equipped with a TV camera. The microscopic image was recorded on video and afterwards analyzed in detail. In the experiments, an objective EPIPLAN HD 8/0.2 was used. The total magnification of the microscope/TV camera system used in the experiment was about 170 times. The area of observation that was analyzed had a radius of 450 μm. The stagnation point for laminar flow was stationary and was set at the center of the area under observation. From an analysis of the deposition process, it was possible to determine the coating density N_d by counting the particles deposited per unit area; typically N_d ranged from 0 to 40 x 10^8 m^{-2}. The total observation region was divided into 3 regions:

$$0 < r < 150 , \qquad \bar{r} = 75$$

$$150 < r < 300 , \qquad \bar{r} = 225$$

$$300 < r < 450 , \qquad \bar{r} = 375$$

where r is the distance from the stagnation point and $\bar{r}$ the average distance expressed in micrometers. The area S_i of each region for different r is determined by geometry

$$S_i = \pi r_i^2 - \pi r_{i-1}^2$$

where $r_0 = 0$, $r_1 = 150$, $r_2 = 300$ and $r_3 = 450$ μm. The coating density is defined as

$$N_{d_i} = n_{p_i} / S_i$$

where n_{p_i} are the number of particles deposited in each region i. The total number of particles deposited for the total observation region n_p where

$$n_p = \sum_{i=1}^{3} n_{p_i}$$

was usually between 800 and 1500 at the end of an experiment (~ 20 min).

Zeta-potentials

The zeta-potential of the polystyrene particles was determined from mobility measurements using a Rank Bros. Mark II microelectrophoresis apparatus with a flat rectangular cell fitted with blacked platinum electrodes. The electrophoretic mobility is found by timing individual particles over a fixed distance (ca. 500 μm) on a calibrated eye piece scale. Ten readings were made in both directions at the stationary level of the cell. The electrophoretic mobility measurements were converted to zeta-potentials using the Helmholtz-Smoluchowski equation. No corrections for retardation or relaxation were necessary because in all cases $\kappa a >> 1$.

Electrophoretic mobility measurements give information about the charge density at the surface of slip. The measured particle mobility and the derived electrokinetic potential (zeta-potential) depend on the ionic strength of the aqueous phase and the counterion charge. Fig. 6 shows zeta-potentials (ζ) for latex polystyrene as a function of electrolyte concentration.

The ζ-potential of the cover slides, identical to the surface collectors used in [3], was found by measuring the potential of crushed glass and corresponded to − 50 mV. Haller et al [17] reported on electrokinetic potentials of several glasses of well-defined bulk composition in aqueous electrolyte solutions computed from streaming current measurements. Their glass samples were cleaned with boiling concentrated HNO_3 and washed with distilled water. For one sample similar to ours, they measured the electrokinetic potential as a function of pH for various electrolyte concentrations. At pH = 5.0 for 10^{-3} and 10^{-2} M NaCl, the ζ-potential was, respectively, − 67 and − 42 mV. In our study most deposition-detachment experiments were performed at 4 mM NaCl which corresponds approximately to a ζ-potential for pH = 5.0 of − 55 mV.

Fig. 6 Observed ζ-potential of 3μm polystyrene latex particles as a function of salt concentration (Mole/l).

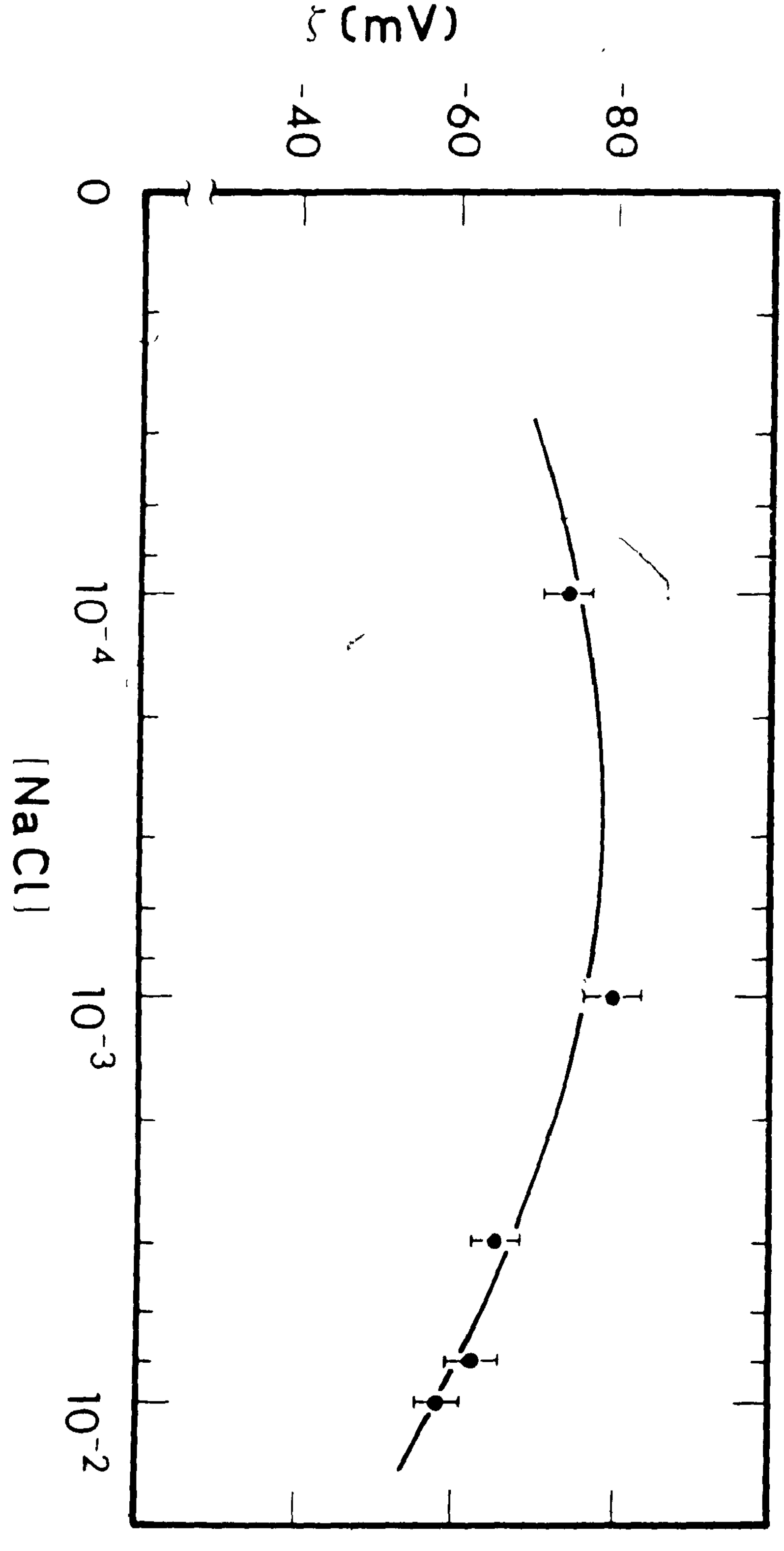
ζ (mV)
-80
-60
-40
0
10^{-4}
10^{-3}
10^{-2}
[NaCl]

IV. RESULTS AND DISCUSSION

Particle deposition

Deposition experiments of dispersions of polystyrene latex were analyzed by determining the coating density N_d (expressed as the number of deposited particles per unit area) as a function of time for various flow intensities. Typical examples are shown in Fig. 7. In all experiments this dependence was found to be non-linear, in agreement with previous experimental studies [3,13]. In ref. [13] many reasons were discussed for such non-linearity. From that discussion we can conclude that the non-linearity observed in Fig. 7 is mainly due to particle escape and effects of blocking of the already deposited particles. When the non-linearity of the flux is caused by blocking and escape, the coating density can be approximated by Eq. (25). In Fig. 7, the solid lines, corresponding to Reynolds numbers 54, 36, and 24 respectively, were calculated from Eq. (25) using the experimentally determined value for j and a best fit value for β.

In these experiments no escape of particles was observed for the range of Reynolds number given in Fig. 7. One can conclude that $\beta_e = 0$, which follows also from the detachment experiments described below, and thus $\beta = \beta_m$. From Eq. (27) we can then calculate the value of the masking parameter γ as a function of Re. Results are given in Fig. 8. It can be seen that γ decreases with increasing Re. Since the blocking arises from a repulsion between the deposited and the mobile particles [18], it can be expected that the relative importance of the repulsion

Fig. 7 Coating density N_d as a function of time for various Reynolds numbers Re. [NaCl] = 4 mM, pH = 5.5, $0 < r < 150$ μm. The solid lines are calculated from Eq. (25) with $\beta = 0.13$, 0.08 and 0.07 min^{-1} and $\gamma = 5.34$, 2.70 and 1.65 ($\times 10^8$ m^{-2} min^{-1}) for Re = 54, 36 and 24 respectively.

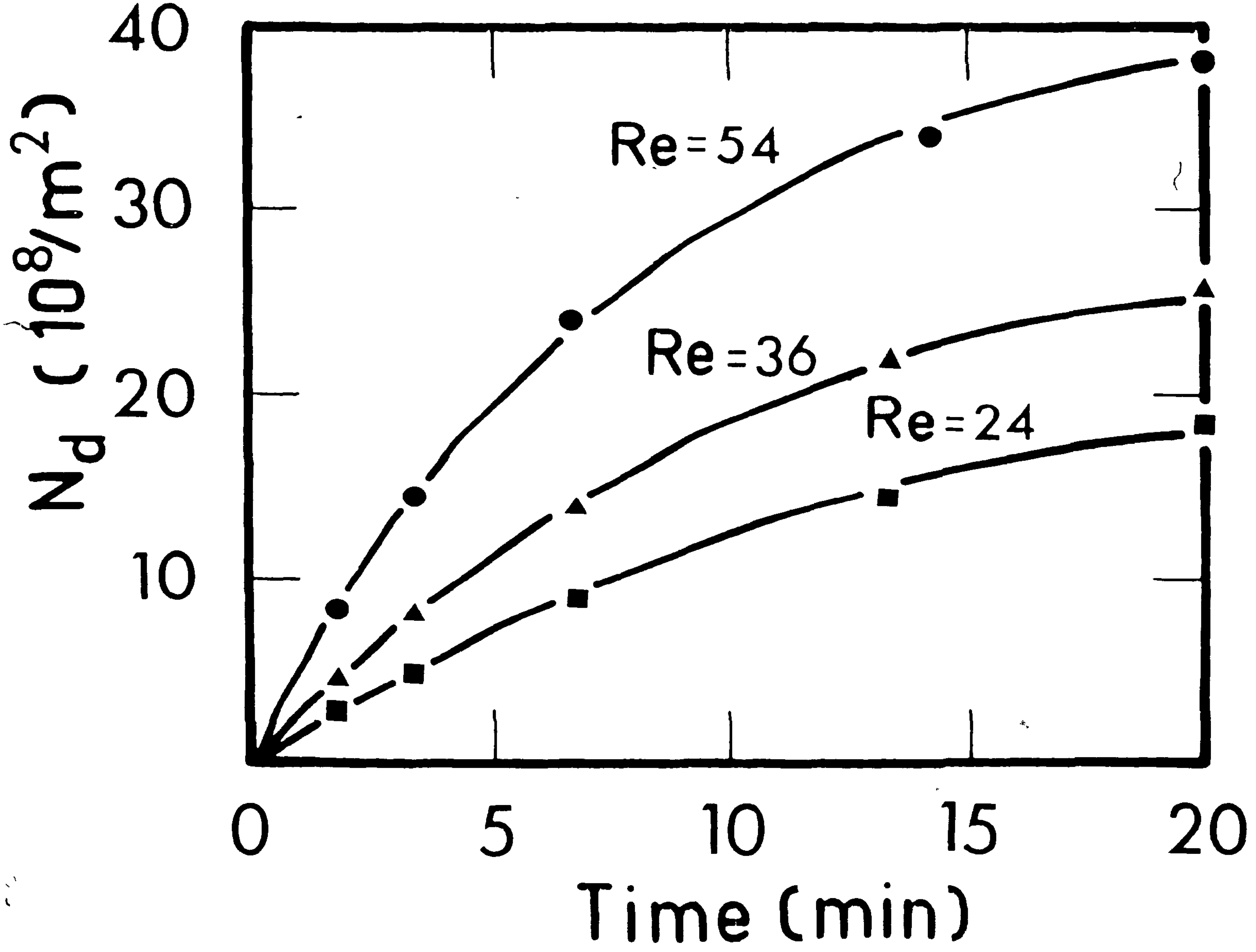
Re = 54
Re = 36
Re = 24
N_d ($10^8/m^2$)
40
30
20
10
0
5
10
15
20
Time (min)

Fig. 8 Blocking parameter γ as a function of Reynolds number for $0 < r < 150$ μm.

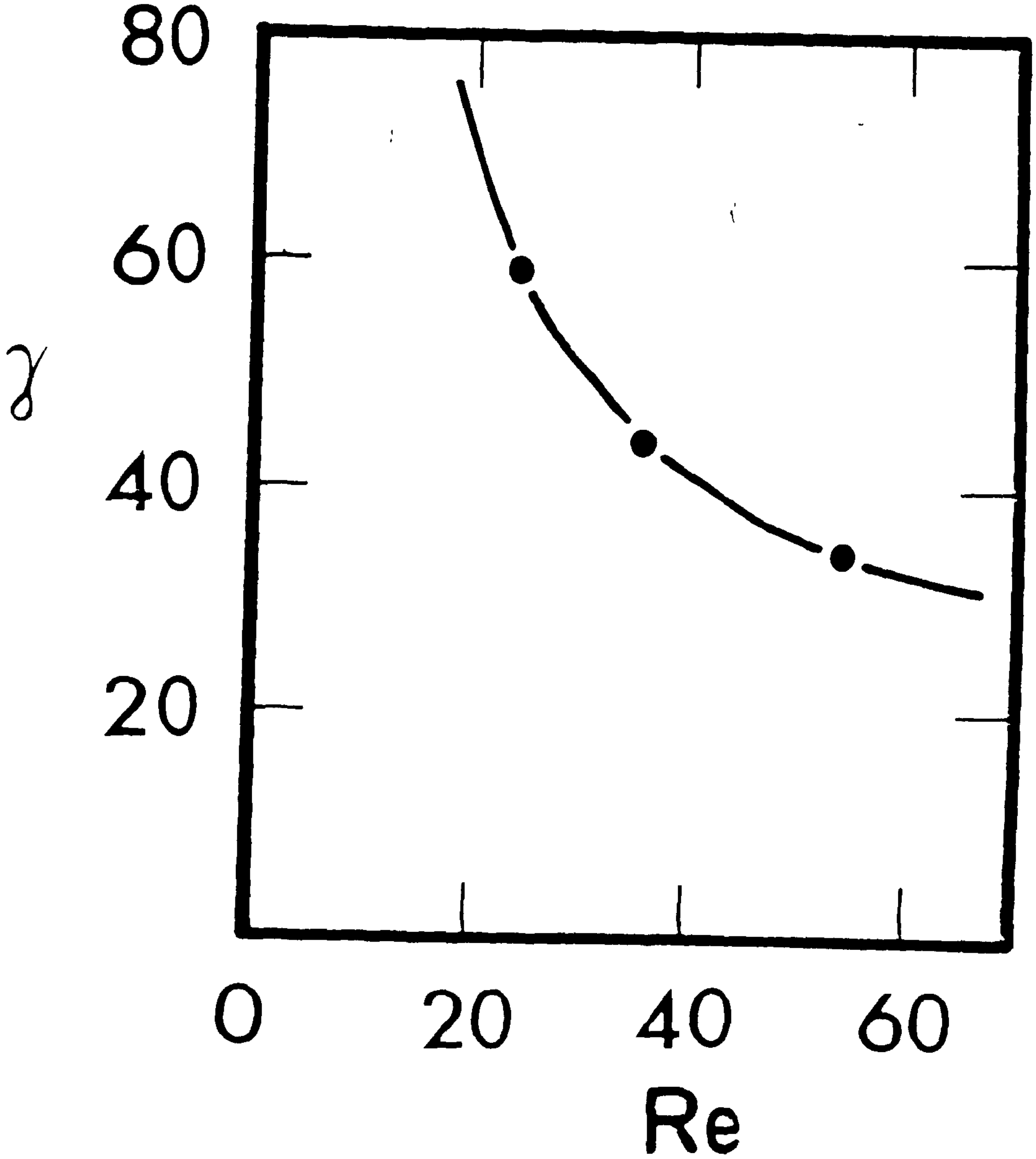
80
60
40
20
γ
0
20
40
60
Re

diminishes with increasing Reynolds number. Our values of γ are substantially larger than those reported by Dabros and van de Ven [13] for 0.5 µm latex particles, indicating a large effect of particle size on blocking effects. From the value γ it can be concluded that the final surface coverage is in the range 2-3%, in agreement with experiment.

The initial slope of the coating density vs time curves provides information about the flux to the collector surface. We observed that as we increased the volumetric flow rate, j inceased also. Fig. 9 presents the dependence of the Sherwood number as a function of Péclet number for [NaCl] = 4 mM. Sherwood and Péclet numbers were found on the basis of Eqs. (14) and (17) from experimentally determined values of particle diameter, concentration of the colloid, initial flux to the surface and the intensity of the flow. The solid line in this figure was calculated from a numerical integration of Eq. (22). It can be seen that under these conditions fast deposition ($\alpha_d \simeq 1$) occurs for low Péclet numbers and close to the stagnation point. At higher Péclet numbers and away from the stagnation point, the deposition rate is considerably lower. The deposition efficiency decreases with increasing Péclet number, from about one hundred percent at low Péclet number to zero at Pe > 11 (as can be concluded from measurements at higher flow intensities).

If we plot the initial flux j as a function of the radial distance from the stagnation point r, Fig. 10 shows that as we increase r, j decreases. This finding is in disagreement with theory which predicts a uniform deposition, independent of the distance from the stagnation point. The variation is much larger than can be explained by the small variation in $\bar{\alpha}$. We can think of three possible reasons that could

Fig. 9 Values of Sherwood number Sh calculated from Eq. (22) (solid line) as a function of Péclet number Pe for Gr = − 2.25, together with experimental data for [NaCl] = 4 mM. ● $\bar{r}$ = 75 μm, □ $\bar{r}$ = 225 μm; ○ $\bar{r}$ = 375 μm.

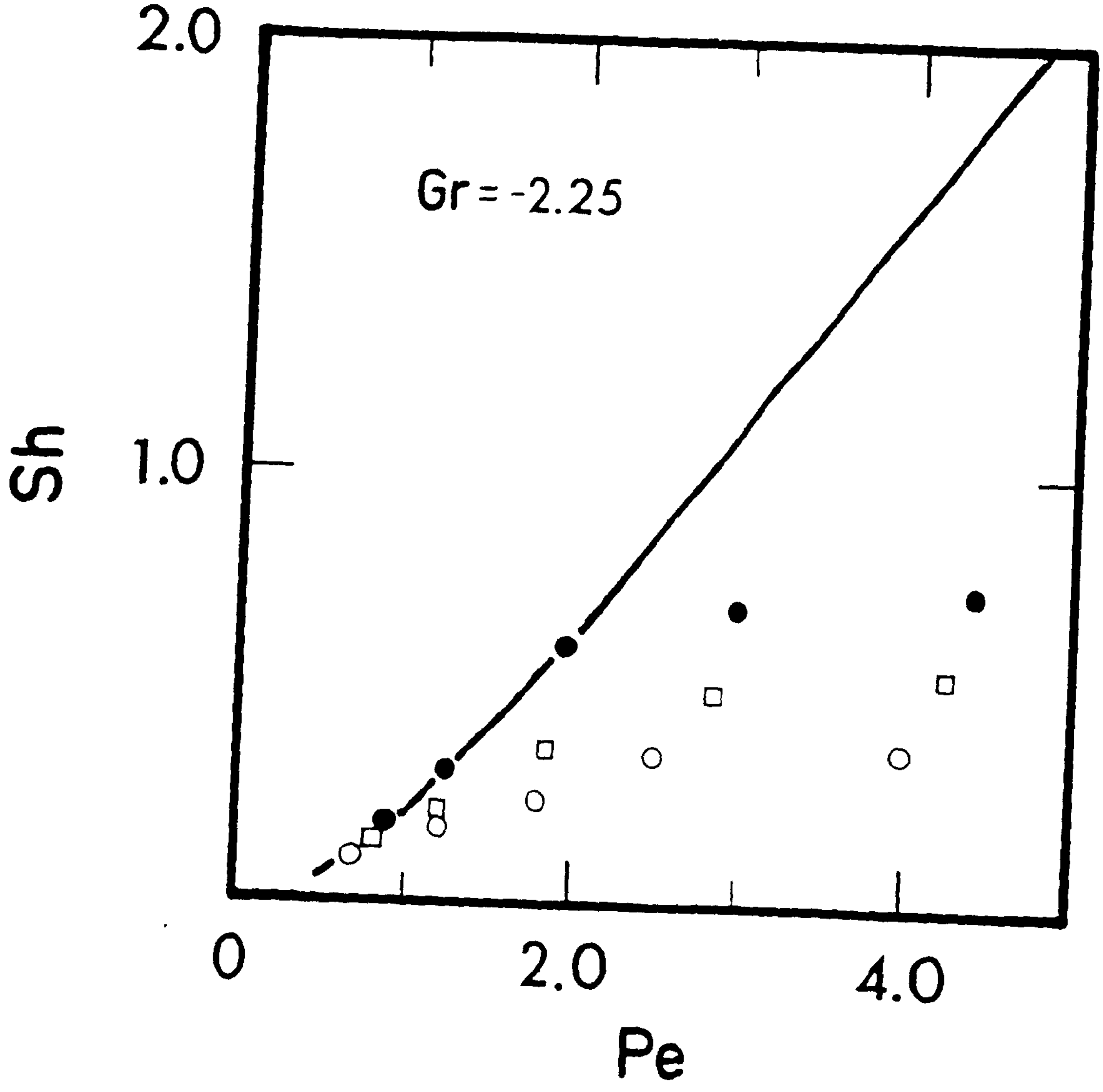
2.0
Gr = -2.25
Sh
1.0
0
2.0
4.0
Pe

Fig. 10 Initial deposition rate j as a function of the distance from the stagnation point $\bar{r}$ for different Reynolds numbers Re. Curve 1: Re = 54, curve 2: Re = 36, curve 3: Re = 24.

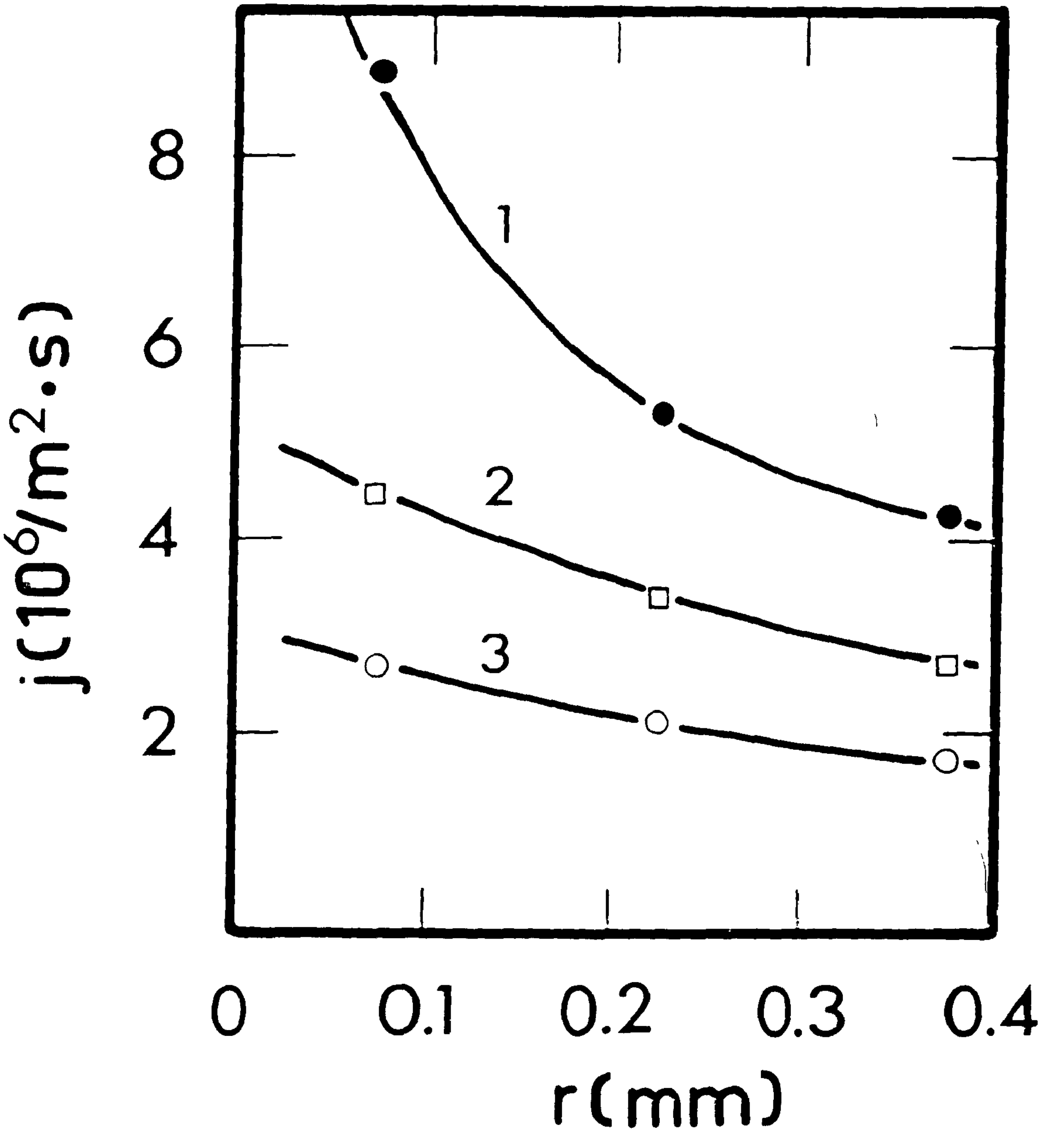

j(10⁶/m²·s)
8
6
4
2
1
2
3
0
0.1
0.2
0.3
0.4
r(mm)

explain these results. (i) We know that the shear rate G is zero at the stagnation point and increases as the radial distance increases from the stagnation point. As the shear rate increases, the contact time (between the particle and a site on the surface) may become less than that required to form a bond, (ii) Particle rotation increases with increasing shear rate, thus also shortening the contact time, (iii) Another explanation, given by Dabros and van de Ven [5] is that weak bonds are formed which have a finite probability to break up shortly after formation. If they survive for a certain initial time, they survive forever. In the system studied in [5], a fraction of particles was observed to leave the surface within the first few seconds after attachment. In our system, no such detachment was observed, making the third explanation (aging of bonds) very unlikely.

We also measured the coating density as a function of radial distance from the stagnation point and the results are given in Fig. 11. We observed, as the wall shear rate increases, a net decrease in the coating density, being maximum near the center and decreasing significantly with radial distances from the stagnation point. Fig. 11 can be explained by assuming that γ is a function of r (or G). No more particles can get to the surface because of blocking.

Fig. 12 shows the curves obtained for the accumulation of latex particles onto a collector when the concentration of electrolyte was varied at constant pH (= 5.0-5.2) conditions. It can be seen that as the NaCl concentration increases, the initial deposition rate (given by the slope of the dashed lines) also increases. This tendency is explained qualitatively by two effects. Firstly, because $\kappa \propto \sqrt{c}$ (c being the

Fig. 11 Coating density N_d as a function of the radial distance from the stagnation point r for different Reynolds numbers Re. Curve 1: Re = 54; curve 2. Re = 36, curve 3 Re = 24.

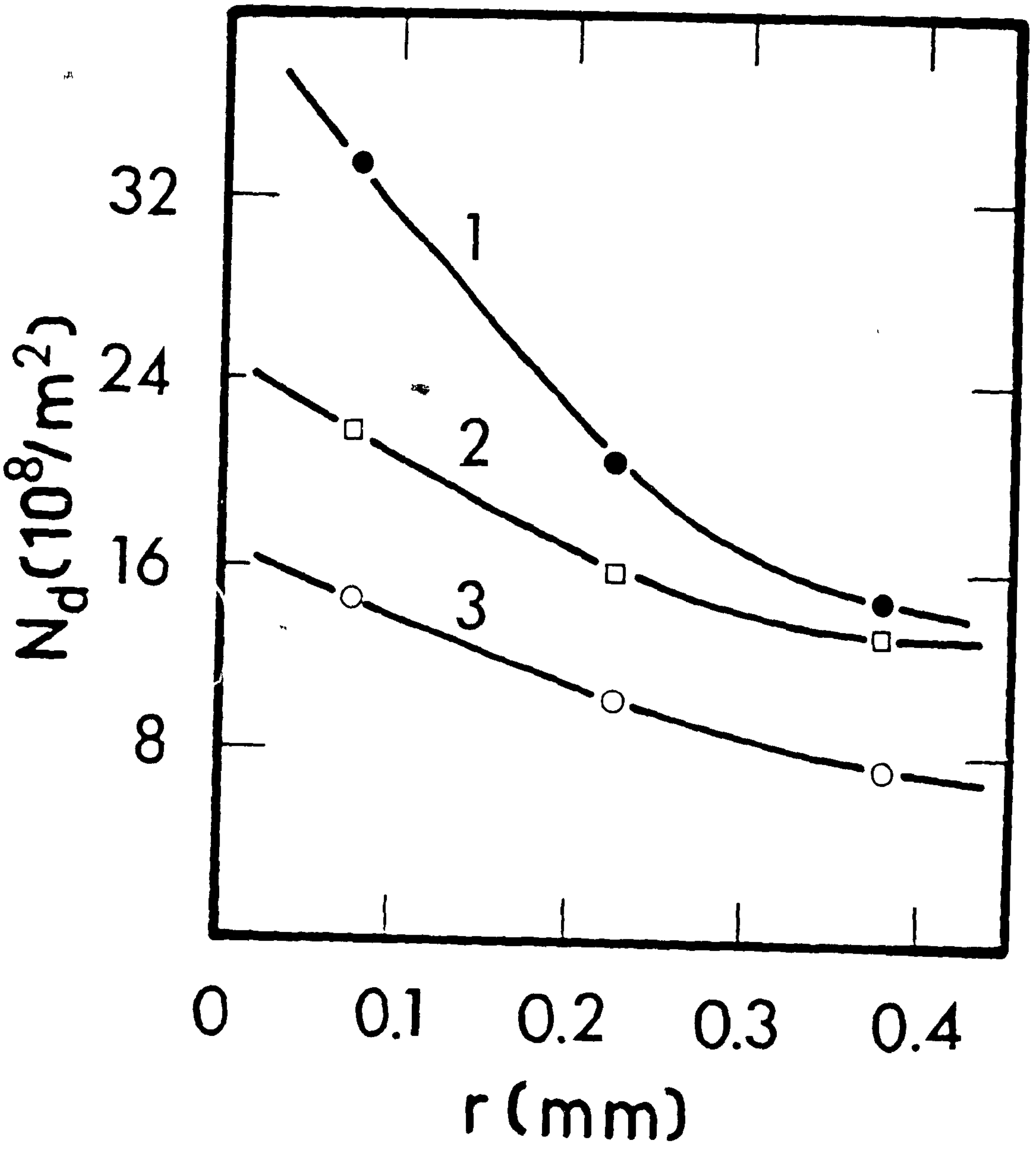

$N_d(10^8/m^2)$
32
24
16
8
0
0.1
0.2
0.3
0.4
r (mm)
1
2
3

Fig. 12 Effect of salt concentration on deposition of polystyrene latex on glass surface. Curve 1: [NaCl] = 0, curve 2: [NaCl] = 1.0 x 10^{-4} M; curve 3 [NaCl] = 1.0 x 10^{-3} M; curve 4: [NaCl] = 4.0 x 10^{-3} M. Results are expressed for $0 < r < 150$ μm. Re = 54.

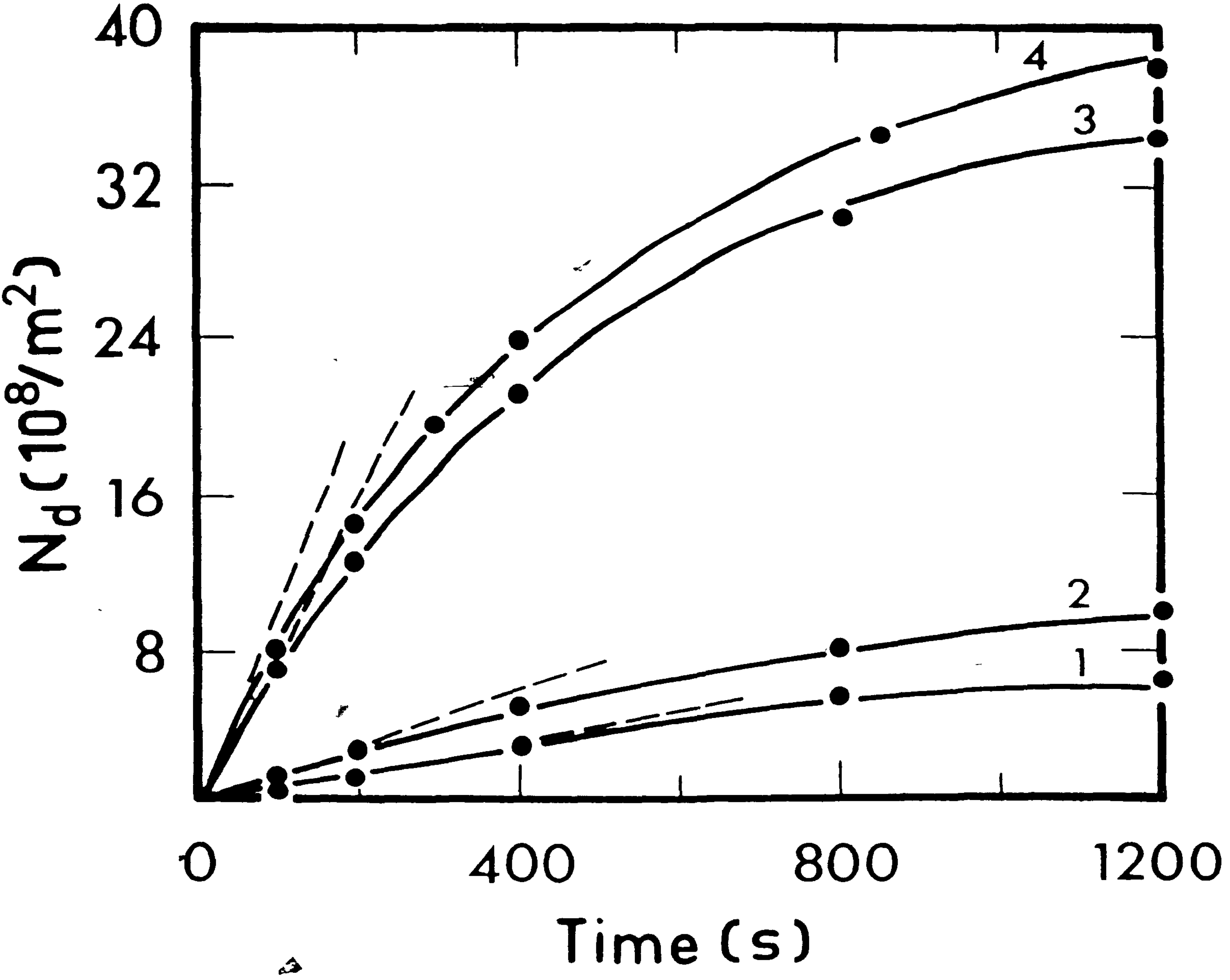

N$_d$ (10^8/m^2)
40
32
24
16
8
0
400
800
1200
Time (s)
4
3
2
1

Fig. 13 Experimental values of the Sherwood number Sh as a function of salt concentration. Curves 1, 2, 3 are for $\bar{r}$ = 75, 225 and 375 μm respectively. Re = 54.

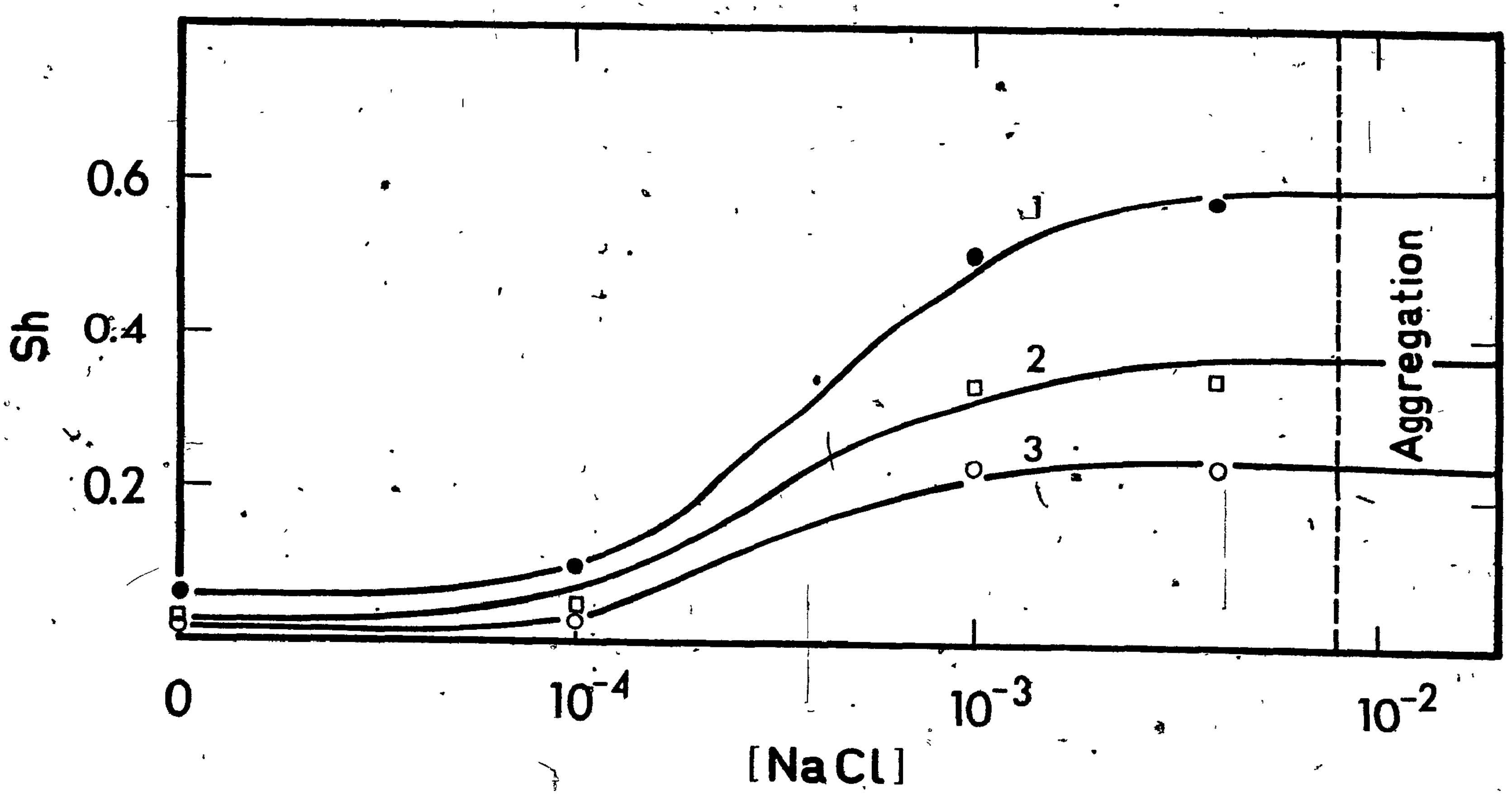
Sh
0.6
0.4
0.2
0
10^-4
10^-3
10^-2
[NaCl]
1
2
3
Aggregation

salt concentration), increasing the salt concentration decreases the double-layer thickness κ^{-1}. As a result, the height and width of the interaction energy barrier is reduced, thus reducing the resistance to deposition. Secondly, increasing the salt concentration also lowers the ζ-potential, as shown in Fig. 6, which also lowers the energy barrier resulting in higher deposition rates. However, according to theory, no deposition should occur until a critical range of salt concentration is reached beyond which fast deposition takes place (deposition efficiency 100%). Theoretically one can either prevent coagulation by increasing the double-layer number $D\ell$ beyond a critical value $D\ell_{crit}$ or by decreasing the parameter τ below τ_{crit}. In the system studied by Dabros and van de Ven [3], $D\ell_{crit} \simeq 120$ when $\kappa a = 60$. From their results we conclude that for our system, for which $D\ell_{crit} = 850$, $\tau_{crit} \simeq 650$. Hence theory predicts no deposition in all experiments because τ is always lower than τ_{crit} (cf. Table II). In our system we observe a gradual increase of deposition as we increase the salt concentration, as shown in Fig. 13. At the CCC (critical coagulation concentration) our suspension flocculates and we are unable to perform experiments with an electrolyte concentration for which theory predicts fast deposition. Only near the stagnation point is the regime of fast deposition reached, but it occurs for $\tau > 400$ rather than $\tau_{crit} > 650$, as predicted by theory. Also contrary to theory, the fast deposition regime is reached gradually rather than suddenly at some critical deposition concentration, and even at very low salt concentration some deposition is observed, while theory predicts that $\alpha_d \simeq 0$ for $\tau < \tau_{crit}$. The reason for the anomalous deposition behavior could be that our latexes are "hairy", i.e. they contain

TABLE II

Deposition rates for different salt concentrations.

[NaCl] (mM)	ζ_1 (mV)	κ^{-1} (nm)	κa	$D\ell$ a)	j^{exp} ($10^6/m^2s$)	Sh^{exp}
0.1	- 74	34.9	43	936	1.5	0.1
1.0	- 80	9.6	156	1012	7.8	0.51
4.0	- 65	4.3	348	822	8.9	0.58
8.0	- 62	3.4	440	784	- b)	- b)
10.0	- 58	3.0	492	734	- b)	- b)

a) - we assumed $\zeta_2 = -55$ mV, independent of salt concentration.

b) - formation of aggregates.

polymeric filaments or segments protruding from their surfaces. The salt dependence of deposition rate could be caused by electrostatic interaction between the glass surface and the hairs. Another possible explanation worth mentioning is the following: there exists an additional short range repulsion (besides DLVO considerations) between two hydrophilic surfaces (hydration force) and an additional short range attraction between two hydrophobic surfaces (hydrophobic force). In our system we have a hydrophobic surface (polystyrene) and a hydrophilic surface (glass). It is not known whether or not there also exists an additional short range force between two such surfaces.

Beside the anomalous deposition rates, the deposited particles also show a strange irregular motion around their attachment site. We observed that a large fraction (sometimes up to 50%) of the latex particles deposited on a collector surface executed lateral motion of up to 3 or 5 micrometers when subjected to a high Reynolds number flow, in which case the flow is unstable (characterized by an irregular motion of the stagnation point). The movement of aggregates or single particles followed the movement of the fluid. The fluctuating motion was observed during each experimental run. The motion of the particles over the surface suggests that the polystyrene latex particles are bound to the surface by a long, invisible, flexible connection. The motion of the particles over the surface is similar to the one observed by Pelton et al. [8] for glass and latex beads stuck to glass surfaces by high molecular weight polymers. However in our system no polymers were added to the system. Dabros and van de Ven [19] also observed this motion of the particles when subjected to turbulent flow. They observed flexible bonds only with latexes and not with TiO_2 particles, which makes it highly unlikely that impurities in water or other artifacts could be responsible for this phenomenon. The same phenomenon was observed for surfaces other than glass. The irregular motion around deposition sites could be related to the anomalous deposition rates.

The possibility that latex particles are "hairy" has been proposed by several people [20] in order to explain anomalous behavior. Here we also mention the work by Takamura et al. [21], who observed that two particles colliding in a shear flow ran into a large energy barrier at a separation of about 12 nm; a possible explanation is the presence of hairs on the surface of polystyrene latex spheres.

To prove the hypothesis that our latexes are hairy, we treated them by heating them above the softening temperature of polystyrene (~ 100°C). In most experiments we used a temperature of 116°C for a one-day period, during which the latex was kept in a closed air-tight vessel.

If the latex is hairy, it can be assumed that the charge groups on the surface are spread out in a shell around the particle, rather than all being located on the surface. By heating, this diffuse charge layer can be expected to collapse, resulting in a better defined surface charge layer with a higher ζ-potential. The ζ-potential of polystyrene equaled − 65 mV before treatment (t = 0) and we observed that when we treated the latex surface, the ζ-potential varied with treatment time. Treating the latex suspension for 1, 24 and 48 hours resulted in ζ-potentials of − 68, − 54 and − 23 mV respectively. Ross and Takamura [22] used the same procedure and found a substantial increase in the ζ-potential after the treatment for their polystyrene latex. The initial rise observed in our system, can be explained by the expected contraction of the surface charge layer when we increase the temperature. The subsequent lowering of the ζ-potential can be explained by the desorption of certain charge groups. At room temperature these are impossible to desorb by repeated centrifugation, but at elevated temperatures desorption is possible. That desorption of charge groups really takes place can be concluded from the conductivity of the supernatant of a centrifuged sample of the treated latex, which was found to increase with heat treatment.

Deposition experiments with the heat-treated latexes, which have a lower ζ-potential than the untreated ones, show a decrease in deposition rate with treatment, especially near the stagnation point (cf. Table III). Hence despite a lower energy barrier in the energy of interaction between a particle and the surface (from which one would predict a higher deposition rate), a lower deposition rate is observed. It is clear that deposition is not governed by electrostatic particle-wall interactions alone. As treated latexes are expected to have a less hairy surface than untreated ones, the reduction in hairiness can account for the decrease in deposition.

Particle release

Experiments were performed to determine the rate of escape of previously deposited particles by changing the original suspension (latex, salt), after twenty minutes of deposition, for a solution with similar electrolyte properties. A release measurement of this circulating salt solution is shown in Fig. 14 where the jet is changed at point A. This figure shows that without surface collisions and at moderately

TABLE III

Deposition rates for heat-treated (for 1 day) and non-treated latexes, at different distances $\bar{r}$ from the stagnation point, Re = 54.

$\bar{r}$ (μm)	j ($10^6/m^2 \cdot s$)	
	non-treated	treated
75	8.9	7.5
225	5.3	5.2
375	4.2	4.2

Fig. 14 Coating density as a function of time for polystyrene latex (run I-2) showing release measurements. Point A is the starting point for detachment experiments performed with a jet without suspended particles.

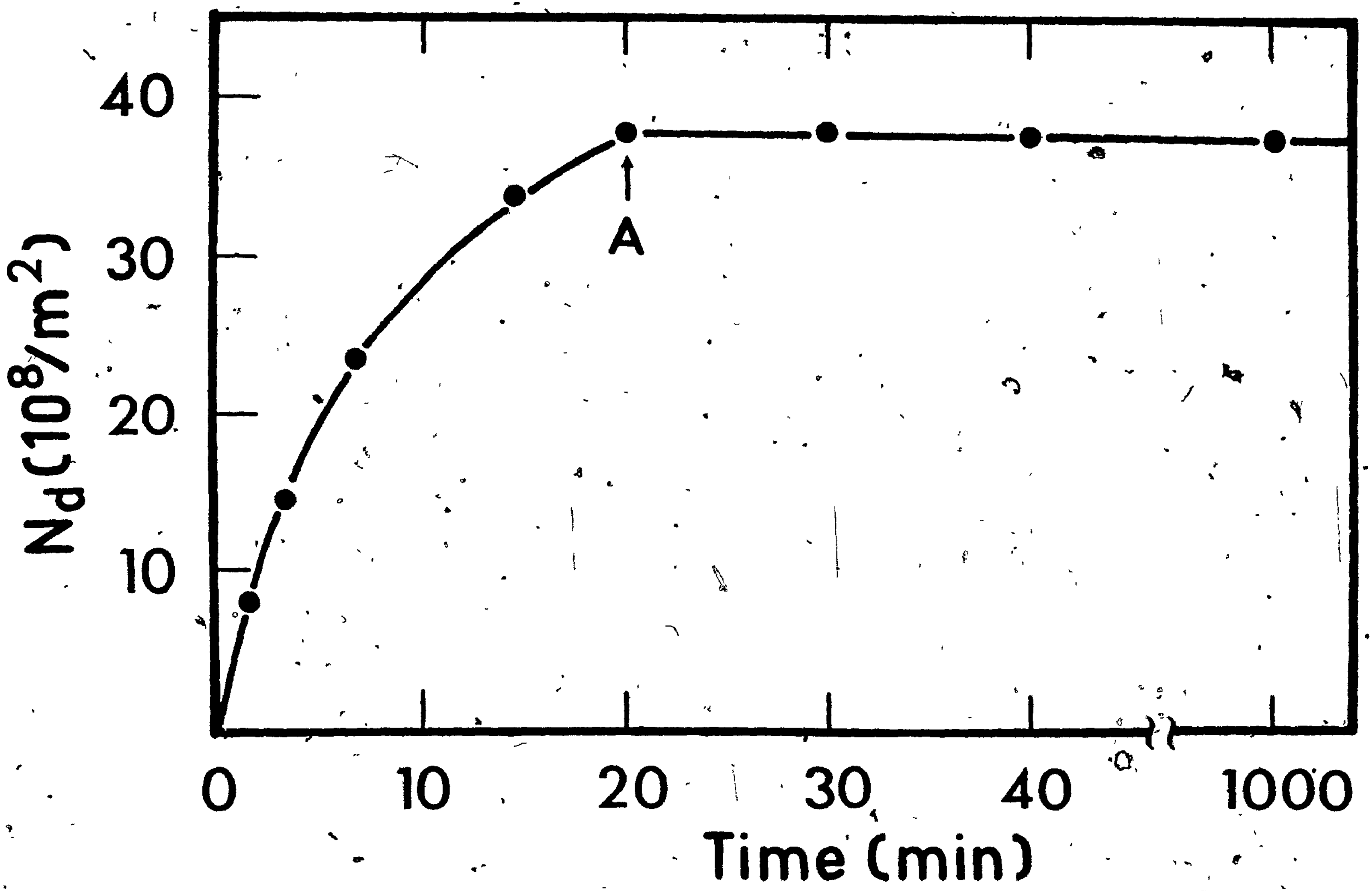

40
30
20
10
$N_d(10^8/m^2)$
0
10
20
30
40
1000
Time (min)
A

low Reynolds numbers (Re = 54) almost no particles detached from the surface after one day. Similar experiments were done by Bowen and Epstein [23] with spherical particles of silica. They found that the rate of detachment of previously deposited particles was negligible in the range of 18 hours. These results suggest that the adhesion force acting to hold particles on the surface in the primary minimum of the potential energy curve was too strong to permit a significant escape from the surface.

Hydrodynamic forces (high Re or unstable flow) and collisions of deposited particles by suspended particles are responsible for the detachment of the particles. Detachment experiments were performed for different systems: (i) by changing the flow rate to unstable flow after twenty minutes of deposition, and (ii) by comparing the percentage of detachment for systems with and without surface collisions (corresponding to a jet with or without suspended particles).

Instabilities in the stagnation point flow have been observed for Reynolds number larger than 120. In the range 120 < Re < 200, experiments were difficult to interpret because we observed both deposition and detachment. For Re > 200, $\alpha_d = 0$; particles can survive at the surface for some time but cannot stick to it permanently.

Table IV is a summary of various detachment experiments. We found that by increasing the Reynolds number from 109 to 907, depending on the wall shear rate, between 33 and 66% of the particles were removed within two hours. By adding particles to the jet, resulting in surface collisions, for the same flow rates (Re = 109-907), between 77 and 90% of the particles were removed in two hours. We found in both types of detach-

TABLE IV

Fraction of dislodged particles at various Reynolds number.

Run[a]	Re_a[b]	Re_b[b]	F[c] (pN)	Time (hr)	τ_{esc}[c] (min)	Fraction Escaped[c] (%)
I-1	54	54	0.2, 0.6, 1.0	6	-, 6, 3[d]	0, 4, 7
I-2	54	54	0.2, 0.6, 1.0	24	49, 16, 10[d]	2, 6, 9
I-3	54	206	1.3, 3.7, 6.0	2	840, 360, 240	13, 27, 40
I-4	54	907	12, 34, 55	2	348, 270, 132	29, 36, 60
I-5	93	907	12, 34, 55	2	324, 234, 114	31, 40, 64
I-6	109	907	12, 34, 55	2	300, 210, 108	33, 43, 66
II-1	54	242	1.7, 4.8, 7.7	1	570, 174, 84	10, 29, 52
II-2	54	292	2.2, 6.3, 10	1	300, 144, 66	18, 34, 59
II-3	54	381	3.3, 9.4, 15	1	216, 114, 47	24, 41, 72
II-4	54	544	5.7, 16, 26	1	150, 60, 36	33, 62, 81
II-5	54	907	12, 34, 55	0.5	47, 36, 21	47, 56, 75
II-6	79	907	12, 34, 55	3	138, 108, 84	73, 81, 88
II-7	109	907	12, 34, 55	1	84, 55, 41	50, 66, 77
II-8	109	907	12, 34, 55	2	84, 66, 52	77, 84, 90

Notes:

a) - series I and II, without and with surface collisions.

b) - Re_a and Re_b are the Reynolds number during deposition and the removal process.

c) - the results are expressed for different distances from the stagnation point, corresponding respectively to $\bar{r}$ = 75, 225, 375 μm.

d) - τ_{esc} in days, all other data in minutes.

ment experiments (with or without surface collisions) that when the Reynolds number increases, the percentage of particles released increases. These examples show the importance of hydrodynamic conditions and surface collisions.

From our observations, it is possible to estimate surface collision efficiencies from Eq. (41).

We found that surface collision efficiencies are very low, e.g. $\sigma = 1.35 \times 10^{-4}$ at $\bar{r} = 75$ µm and $\sigma = 4 \times 10^{-6}$ at $\bar{r} = 375$ µm (runs I-4 and II-5). The surface collision efficiency increases near the stagnation point. Despite these low efficiencies, surface collisions strongly affect the average lifetime of a particle on the surface because of the large number of collisions per deposited particles.

From the data in Table IV one can estimate the half-life or the escape time τ_{esc} for a particle on the surface from the relation

$$n_p = n_o e^{-t/\tau_{esc}} . \tag{55}$$

The values for τ_{esc} are given in Table IV. By comparing runs I-4 to I-6 it can be seen, somewhat surprisingly, that the particles deposited at the highest Reynolds number have the shortest escape time and thus are the easiest to remove. The reason for this is not clear. By comparing run I-4 with run II-5 it can be seen that surface collisions have a dramatic effect on escape times. The results are summarized in Fig. 15. It can be seen that in all cases surface collisions decrease the escape time dramatically, despite the low efficiency per collision. It can be seen that the data with and without surface collisions fall near two reason-

Fig. 15 The escape time τ_{esc} (min) as a function of shear rate (s^{-1}) and force (nN) for two series with or without collisions. ∇: run I-4; Δ: run I-5; o: run I-6; ●: run II-2; ◆: run II-3; :■ run II-4; □: run II-5.

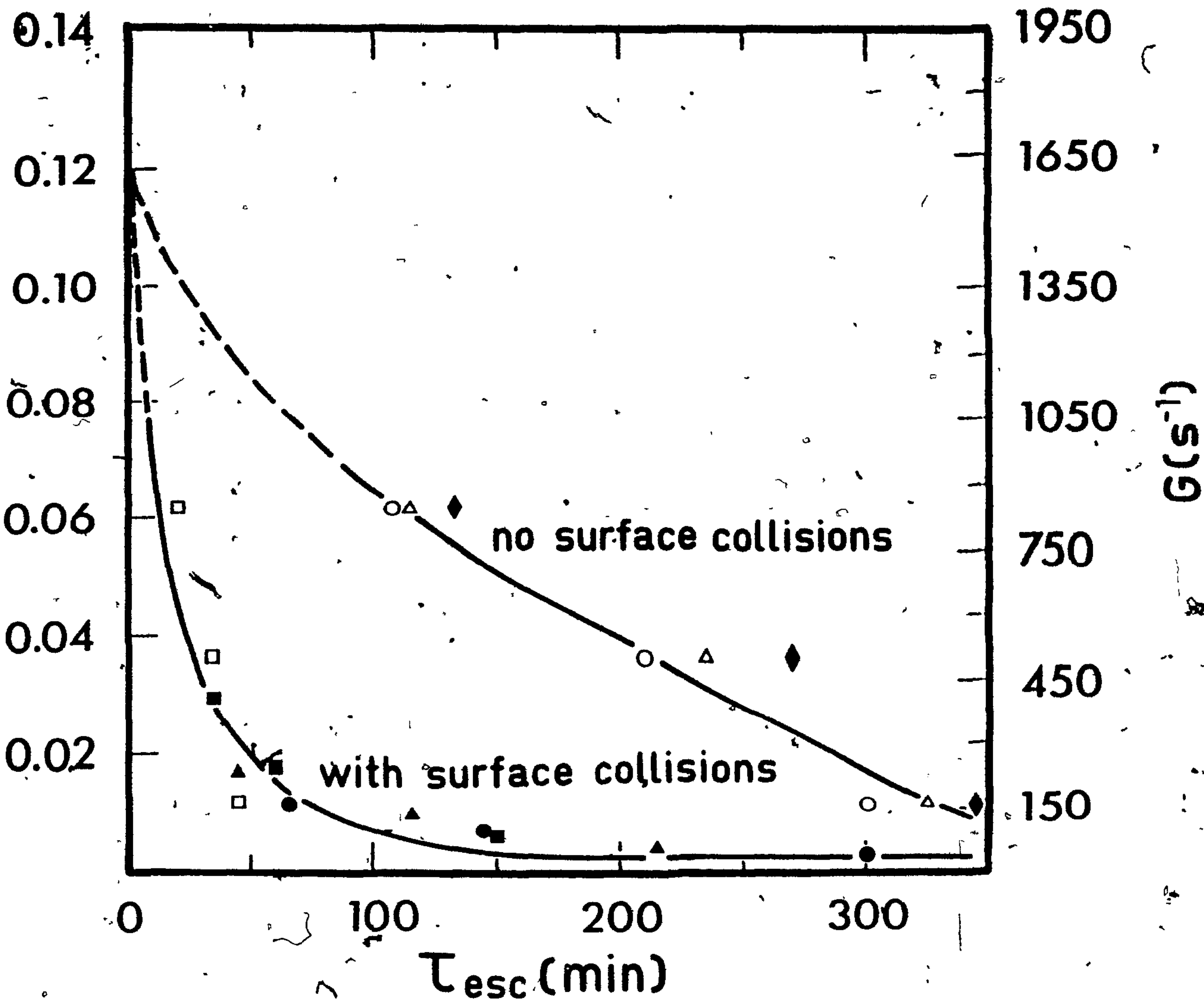
F(nN)
0.14
0.12
0.10
0.08
0.06
0.04
0.02
$G(s^{-1})$
1950
1650
1350
1050
750
450
150
0
100
200
300
τ_{esc}(min)
no surface collisions
with surface collisions

ably well-defined curves, indicating that the bondstrength does not vary much with hydrodynamic conditions. By extrapolating both curves to zero escape time, it can be concluded that all particles will be removed almost instantaneously at a shear rate of about 1600 s^{-1}, corresponding to hydrodynamic forces of about 0.12 nN.

We can determine the depth of the primary minimum in which the particles are captured by finding the slope of the relation between τ_{esc} and F^2 (cf. Eq. (54)). Fig. 16 shows the logarithm of τ_{esc} as a function of the square of the hydrodynamic force. The two curves refer to the cases with and without surface collisions. It can be seen that the behavior under laminar flow conditions is very different from that for unstable flow conditions. The escape rate changes steeply at the onset of the instability. For laminar flow $\ell n \tau$ changes steeply with F^2. From the initial slope (in the laminar flow region) and assuming that Eq. (54) holds, one finds large values of Δh for reasonable values of V_m; e.g. when $V_m = -20$ kT, $\Delta h \simeq 100$ nm. This could be due to large elastic connections or, alternatively, the shape of the energy minimum is different from the one assumed (Eq. (47)). Under unstable flow conditions the rate at which particles escape is slowed down. This can be the result of various factors. The bond between a particle and the surface is no longer stretched all the time since the fluctuations in the flow will move the particle in all directions over the surface. The lower escape rate further implies that the chaotic motion about its attachment point results in a stronger bond.

We also looked at the detachment process for the heat-treated latex to see if the fraction of escaped particles remains the same after

Fig. 16 Logarithm of τ_{esc} (min) as a function of the square of the hydrodynamic force F^2. With (Δ) or without ($\square$) surface collisions.

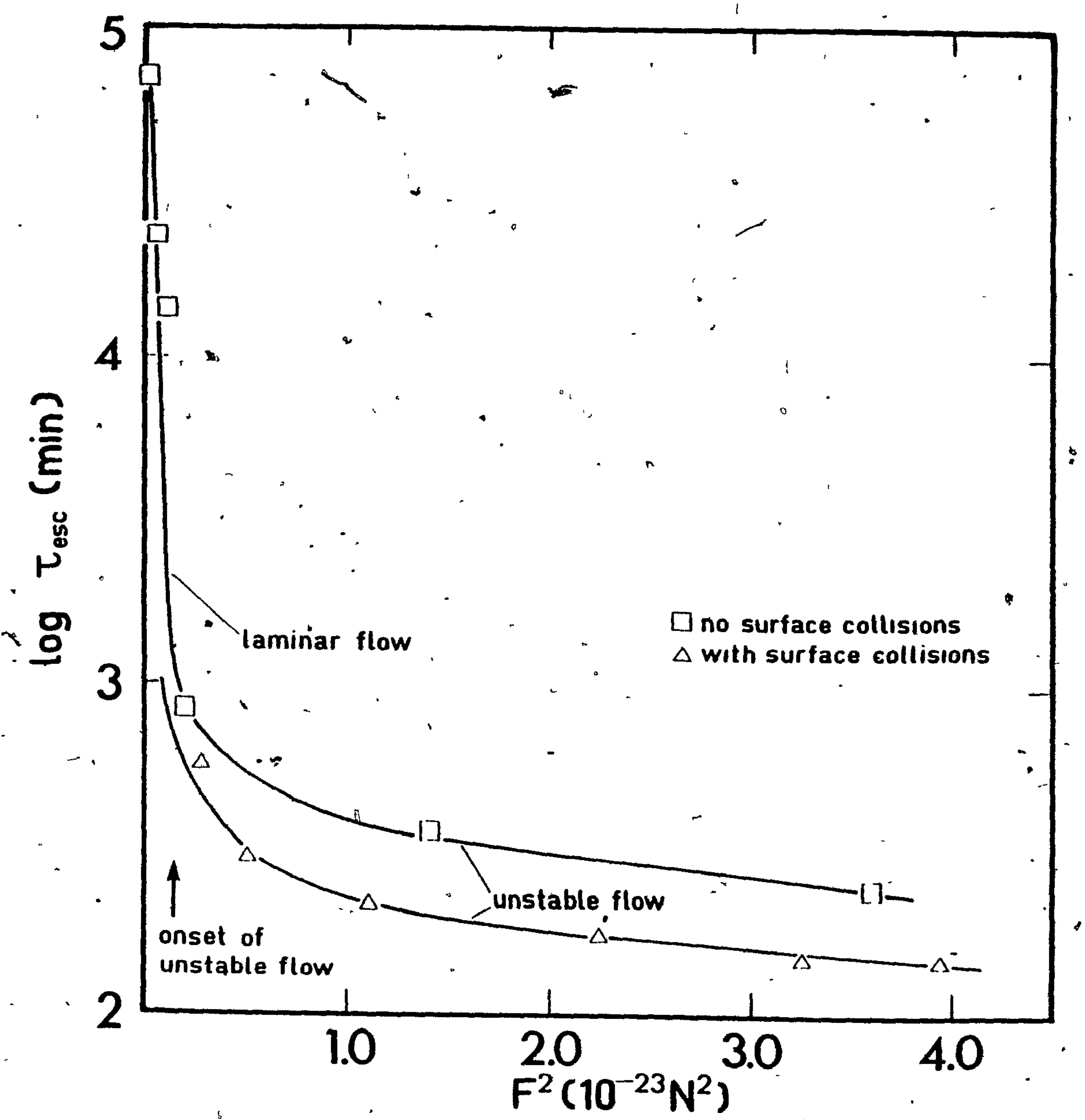
log τ_{esc} (min)
5
4
3
2
1.0
2.0
3.0
4.0
$F^2 (10^{-23} N^2)$
laminar flow
unstable flow
onset of unstable flow
□ no surface collisions
△ with surface collisions

treatment. The detachment experiment was performed with surface collisions at high Reynolds number (Re = 907) and after half an hour we obtained for the fraction of escaped particles, depending on the wall shear rate, 64, 75, 92%. Compared with the results for untreated latexes, we found about 20% more release after heat-treatment. As treated latexes are expected to have a less hairy surface than untreated ones, the reduction of hairiness can account for the enhancement in the removal process.

V. CONCLUDING REMARKS

Deposition experiments in a confined impinging jet indicate that even for such a model system as polystyrene latex, the nature of interactions at small particle collector separations are not governed by the DLVO-theory alone. It is very probable that anomalous deposition rates and surface motions are caused by surface protrusions on the latex surface because altering the surface by heat treatment leads to lower deposition rates, despite a lower energy barrier, which can be explained by the expected reduction of hairness.

It was shown that particle escape is governed by a convective-diffusive transport out of an energy minimum, and that surface collisions between suspended and deposited particles play an important role in the detachment process. Hydrodynamic forces exerted on a deposited particle effectively makes the minimum in which the particle is captured less deep, thus increasing the probability of escape. During a surface collision the hydrodynamic force on a deposited particle is increased, thus increasing even further the probability of escape.

ACKNOWLEDGEMENT

The authors wish to thank Dr. T. Dabros for performing numerical calculations of the flow field.

REFERENCES

1. Marshall, J.K., and Kitchener, J.A., J. Colloid Interface Sci., 22, 342 (1966).
2. Hull, M., and Kitchener, J.A., Trans. Faraday Soc., 65, 3093 (1969).
3. Dabros, T., and van de Ven, T.G.M., Colloid Polym. Sci., 261, 694 (1983).
4. Adamczyk, Z., Zembala, M., Siwek, B., and Czarnecki, J., J. Colloid Interface Sci., 110, 188 (1986).
5. Dabros, T., and van de Ven, T.G.M., Physico Chem. Hydr., 8, 161 (1987).
6. Visser, J., J. Colloid Interface Sci., 34, 26 (1970).
7. Cleaver, J.W., and Yates, B., J. Colloid Intereface Sci., 44, 464 (1973).
8. Pelton, R.H., Nugent, H., and Allen, L., J. Colloid Interface Sci., 99, 387 (1984).
9. Hubbe, A., Colloids & Surfaces, 12, 151 (1984).
10. Law, H.S., and Masliyah, J.H., Ind. Eng. Chem. Fundam., 23, 446 (1984).
11. Goldman, A.J., Cox, R.G., and Brenner, H., Chem. Eng. Sci., 22, 653 (1967).
12. van de Ven, T.G.M., and Mason, S.G., Colloid Polym. Sci., 255, 468 (1977).
13. Dabros, T., and van de Ven, T.G.M., J. Colloid Interface Sci., 89, 232 (1982).

14. Hubbe, A., Colloids & Surfaces, 16, 249 (1985).

15. Smoluchowski, M., Z.Phys. Chem., 92, 129 (1917).

16. Varennes, S., Appendix I, Ph.D. Thesis, McGill University, 1987.

17. Jednacak, J., Pravdic, V., and Haller, W., J. Colloid Interface Sci., 49, 16 (1974).

18. Malysa, K., Dabros, T., and van de Ven, T.G.M., J. Fluid Mech., 162, 157 (1986).

19. van de Ven, T.G.M., Dabros, T., and Czarnecki, J., J. Colloid Interface Sci., 93, 580 (1983).

20. Lyklema, J., Advance Colloid Interface Sci., 17, 307 (1982).

21. Takamura, K., Goldsmith, H.L. and Mason, S.G., J. Colloid Interface Sci., 82, 175 (1981).

22. Chow, R.S., and Takamura, K., (private communication) (to appear).

23. Bowen, B.P., Epstein, N., J. Colloid Interface Sci., 72, 81 (1979).

CHAPTER 3

EFFECTS OF NEUTRAL POLYMERS ON THE KINETICS OF PARTICLE DEPOSITION

ABSTRACT

The deposition of polystyrene latex particles in the presence of electrolytes and non-ionic polymers has been studied by measuring the change in coating density with time. The dependence of the deposition rate on polymer concentration and adsorption time shows that the presence of excess free polymer decreases the deposition rate. In the absence of excess free polymer, but with all particles fully coated with polymer, we found a linear relationship between the deposition rate and the concentration of latex particles, as predicted by theory. The dependence of the deposition rate on electrolyte concentration shows that the coated particles follow the predictions of the DLVO theory more closely than the bare particles.

I. INTRODUCTION

The kinetics of the deposition of colloids on a solid surface is of importance in many industrial processes, and monitoring the rate of deposition under well-defined conditions can yield valuable insight into the nature of specific surface interactions.

In the past most fundamental experiments [1,2] have made use of the rotating disk technique for which the hydrodynamic flow field can be readily calculated. Its major disadvantage is that it is very difficult to monitor the deposition process continuously. A direct measurement of the force between the particles and a solid surface is possible using the impinging jet technique developed by Dabros and van de Ven [3]. In this technique a jet of the suspension impinges on a stationary surface thus allowing one to monitor the deposition process continuously. The deposition process can be video-recorded and afterwards individual particles can be counted.

In Chapter 2 we reported measurements, using the impinging jet technique, of the deposition of latex particles on glass surfaces for various flow rates and electrolyte concentrations. Here we want to study the effects of polymer, either adsorbed on latex particles or free in solution, on the deposition process.

Published data are available on the adsorption characteristics of polymer onto solid surfaces in aqueous media. Pelton [4] and Hubbe [5] studied the strength of bonds formed between particles and a solid surface in the presence of polyelectrolytes. In this chapter we study the deposition of polystyrene latex particles on glass in the presence of polyethylene oxide (PEO). Neutral linear polymers are of special interest because they are the simplest polymers to consider and they are found to have a large effect on particle deposition. In a subsequent chapter we will deal with the effects of polymers with a more complex structure.

In the present study the deposition rate of a polystyrene latex suspension in the presence of non-ionic polymer and electrolyte has been investigated by measuring the change in the coating density of the latex with time. From these observations we can derive quantitative information concerning the influence of the polymer on the interaction acting between particles and the solid surface.

II. THEORY

The deposition of particles on a surface can be described by (Chapter 2)

$$N_d = N_d^{\infty} \left(1 - e^{-t/\tau}\right) \qquad (1)$$

where N_d is the number of particles on the surface per unit area at time t and N_d^{∞} is the number of particles at $t = \infty$. The deposition time τ usually consists of two contributions; one due to particle escape and one to particle blocking.

$$\frac{1}{\tau} = \frac{1}{\tau_{esc}} + \frac{1}{\tau_{bl}} \quad . \tag{2}$$

Under our experimental conditions $\tau_{esc} = \infty$ (no particle escape) and

$$\tau_{bl}^{-1} = \pi a^2 \gamma j \tag{3}$$

where a is the radius of a particle, j the initial deposition rate and γ the area blocked (i.e. made unavailable for deposition) per particle. As $t \to 0$, Eq. (1) reduces to

$$N_d = jt \tag{4}$$

and thus the initial slope of a plot of N_d vs. t yields the deposition rate j. j can be calculated from the convective diffusion equation (Eq. [13] in [4]) and usually varies from zero in the presence of a sufficiently large energy barrier to the fast deposition rate approximately given by the Smoluchowski-Levich equation (Eq. [22] in [4]).

III. EXPERIMENTAL

The apparatus, general procedures, and the determination of deposition rates were described in ref. [4]. Briefly, the apparatus uses a stagnation point flow created in a confined impinging jet. Deposition is observed in the stagnation point region where the flow field is given by

$$V_r = \alpha r z \qquad V_z = -\alpha z^2 \tag{5}$$

where r and z are the radial and normal directions from the stagnation point, V_r and V_z the fluid velocities in these directions, and α is the strength of the stagnation point flow, which can be determined from the amount of fluid passing through the deposition cell (Chapter 2). The adsorption of polyethylene oxide on latex particles simply added a procedural step. All the deposition experiments were performed with polystyrene latex particles having a mean radius of 1.5 μm (Chapter 2).

Materials

The non-ionic water-soluble polymer used in this study is polyethylene oxide (PEO) with a molecular weight of 5×10^3. A stock solution of the polyethylene oxide was prepared by gradually adding PEO to distilled water while the solution was being stirred magnetically for a few hours. The solution contained 0.1 g/l of PEO.

Adsorption procedure

Solutions were made by diluting a concentrated suspension of latex spheres which, before each experiment, were dispersed in an ultrasonic bath. Various quantities of PEO were added to the systems. The concentration of polymer ranged from 0.25 to 10 mg/l. A typical example of how to prepare a latex dispersion is to add 0.2 cm^3 of concentrated latex in 196.8 cm^3 of distilled water and then add 1 cm^3 of 0.1 g/l PEO.

Agitation was done with magnetic stirring, which was continued, usually, for 48 hours (yielding an adsorption time of two days). Only before deposition experiments, 2 cm^3 of sodium chloride of various molarities was added to the suspension of polymer coated particles.

The glass surfaces acting as collectors were prepared according to the procedures given in Chapter 2.

Measurement of zeta-potentials

Zeta-potentials of coated latex particles with polymer were determined by microelectrophoresis with a flat rectangular cell described in Chapter 2. Mobilities were converted to zeta-potentials by the Helmholtz-Smoluchowski equation. In water, PEO is a neutral polymer and within experimental error the ζ-potential remained constant at a value of - 64 mV with a standard deviation of ± 5% of the mean, independently of the amount of polymer added to coat the latex particles. A reason why the ζ-potential remained constant could be that the charge groups on the latex are in a diffuse layer around the particle and that the short polymers (MW 5000) fill the spaces between the charge groups, thus little affecting the plane of slip.

Turbidity

To evaluate the concentration of free polymer in solution, a method developed by Attia and Rubio [6] was used that is particularly sensitive to low concentrations of PEO in water, in the range 0.1-10 ppm. It consists of measuring the turbidity produced by mixing the polymer solution with a dilute solution of tannic acid in the presence of 1 M NaCl. This causes a change in the turbidity of the solution which can be monitored using an electrophotometer.

A series of sample solutions of known polymer concentrations in the range 0-10 ppm was treated with tannic acid and sodium chloride in separate 50 ml volumetric flasks. The required volumes of the PEO standard solutions were added to each flask already containing 5 ml of a tannic acid solution of 1 g/l and 40 ml of 1 M sodium chloride. The solutions were adjusted to 50 ml with distilled water to make up the final concentrations. The flasks were shaken for about one minute and were then allowed to stand for 15 min. before measuring the turbidity. Measurements were plotted against polymer concentrations to produce the calibration curves for PEO. The calibration curve is linear for 0-2 ppm and gently curved above 2 ppm. Fig. 1 shows the calibration curve, which can be used for determining the polymer concentration of unknown samples. The turbidity of a 10 ppm solution was arbitrarily set at 100.

Using the turbidity technique, the concentration of polymer remaining in the solution after adsorption can be evaluated. Before performing turbidity measurements, we removed the latex particles by microfiltration (1.2 μm pore). By evaporation under vacuum, we concentrated the solution by a factor of four, i.e. to 50 ml. The concentrated filtrate or solution containing free polymer was mixed with a dilute solution of tannic acid in the presence of NaCl and the turbidity was measured and the concentration of free polymer determined using the calibration curve. To be certain that significant results are obtained, we repeated the same procedure in the absence of latex particles with a 1 mg/l solution of PEO. Turbidity measurements for such a solution corresponded to a PEO concentration of 0.98 mg/l. Thus 0.02 mg/l of PEO, i.e. 2% of PEO, was lost in the procedure.

Fig. 1 Calibration curve for PEO-tannic acid electrophotometer analysis in the presence of 1 M NaCl.

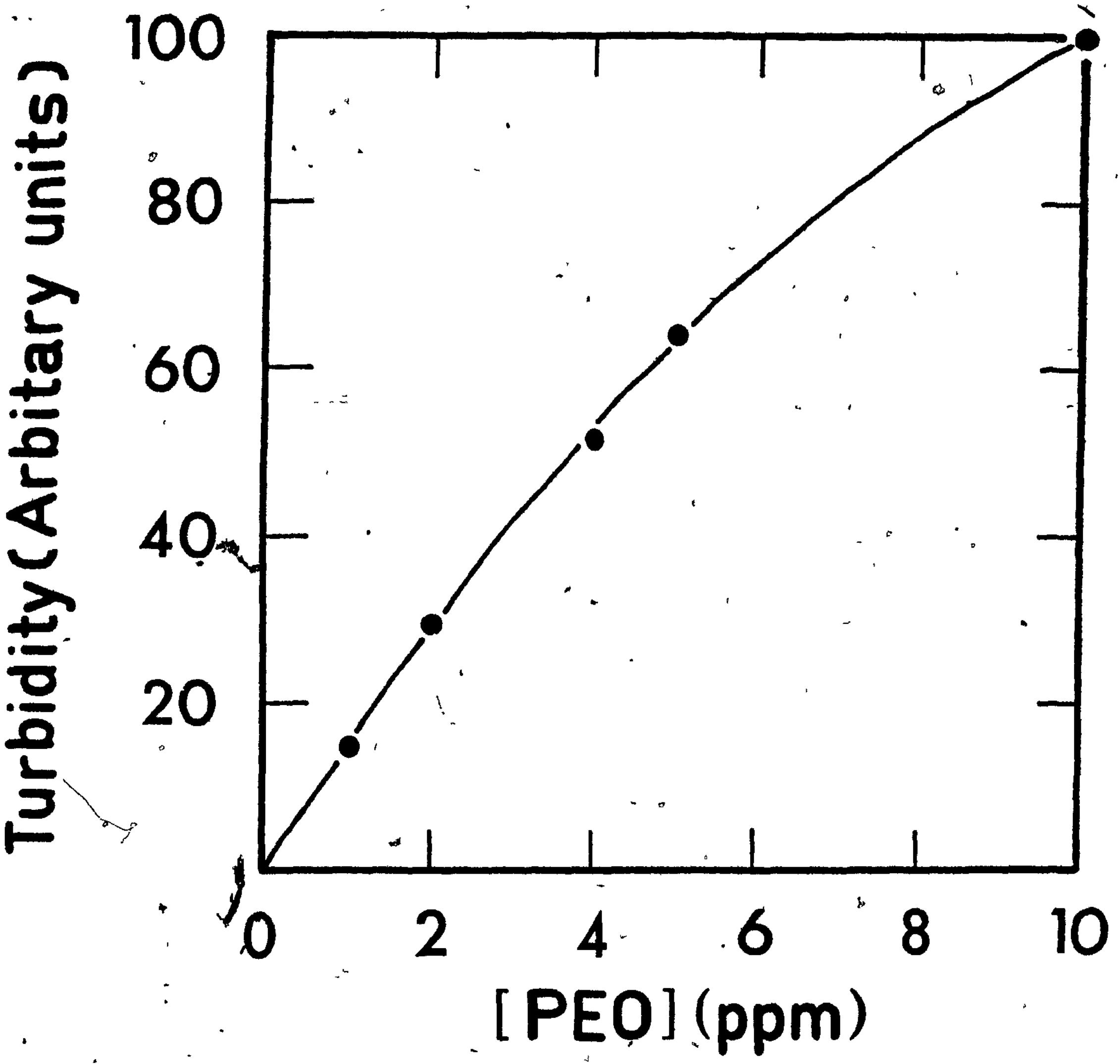
Turbidity (Arbitary units)
100
80
60
40
20
0
2
4
6
8
10
[PEO] (ppm)

IV. RESULTS AND DISCUSSION

Deposition experiments with dispersions of polystyrene latex coated with PEO were analyzed by determining the coating density N_d (expressed as the number of deposited coated particles per unit area) as a function of time. Typical examples are shown in Fig. 2. For the curve with the solid circles, where no polymer was added, we observed a linear increase of coating density with time and a large deposition (see details in ref. [4]). The two other curves correspond to the deposition of coated particles obtained using two different polymer concentrations, 0.5 and 1.0 mg/l. When particles were coated with polymer, the coating density was considerably decreased. It can be seen that the initial deposition rate (given by the slope of the dashed lines) of particles coated with PEO was very much lower than the deposition rate of bare particles.

It was found that the time allowed for the adsorption of PEO on the latex particles was important. Fig. 3 shows the initial deposition rate j as a function of adsorption time for a PEO concentration of 0.5 mg/l. We observed that the deposition rates increase with increasing time of adsorption, ranging from a few hours to a few days. This might be explained by the presence of free polymer preventing deposition. A maximum deposition rate was observed after two days and a slight decrease after 4 days of adsorption. Fig. 3 also shows that the initial flux j decreases with increasing radial distance from the stagnation point r.

We also measured the dependence of the deposition rate j on polymer concentration used for coating the particles after two days of ad-

Fig. 2 The coating density of latex particle deposition as a function of PEO concentration in a solution of 4 mM NaCl at Re = 54. 1. No PEO added. 2. 0.5 mg/l PEO. 3. 1.0 mg/l PEO.

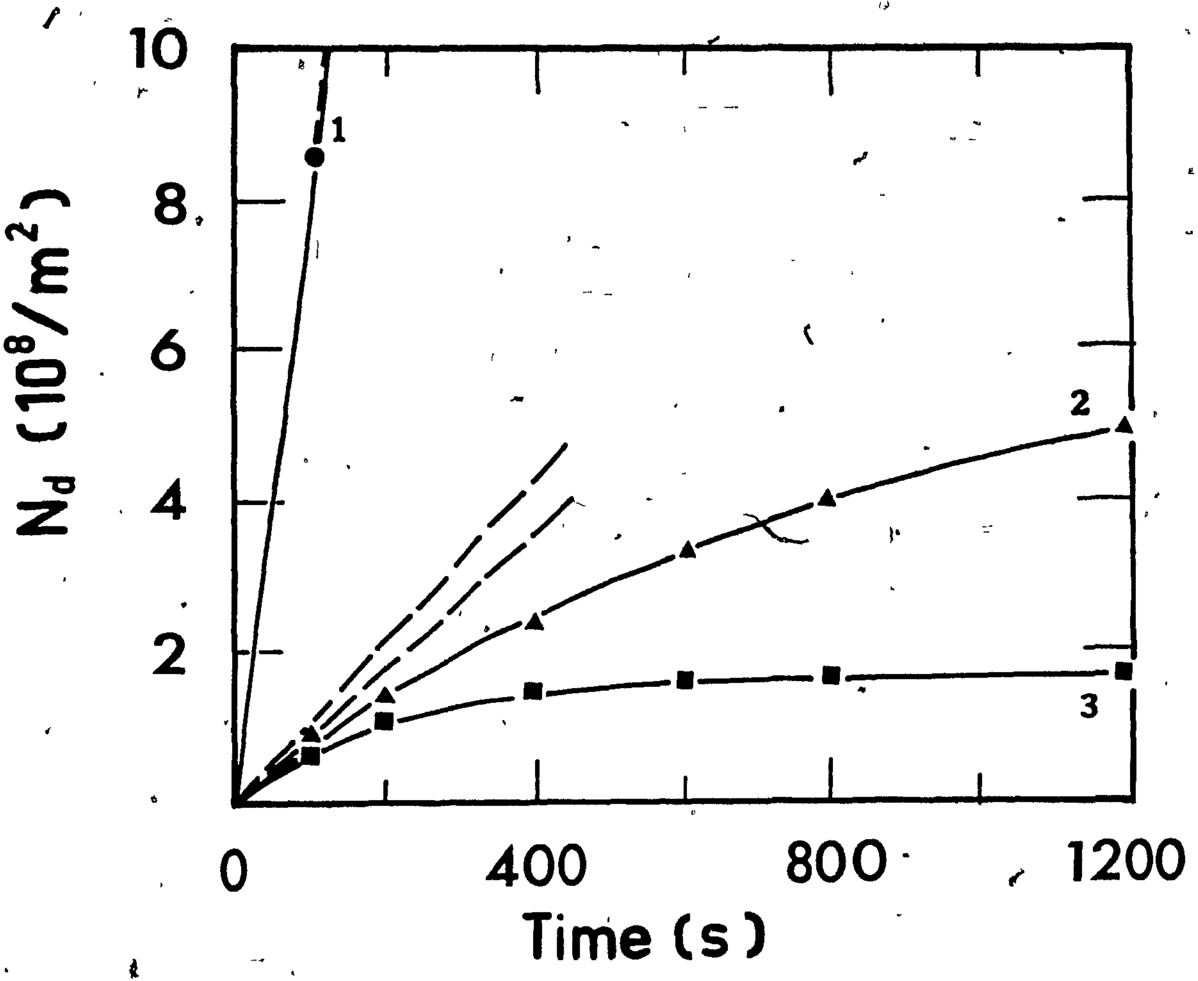

10
8
6
4
2
0
400
800
1200
Time (s)
N_d ($10^8/m^2$)
1
2
3

Fig. 3 Deposition rate as a function of adsorption time for 0.5 mg/l PEO on latex particles. For [NaCl] = 4 mM and Re = 54. ● $\bar{r}$ = 75 μm; Δ $\bar{r}$ = 225 μm; □ $\bar{r}$ = 375 μm.

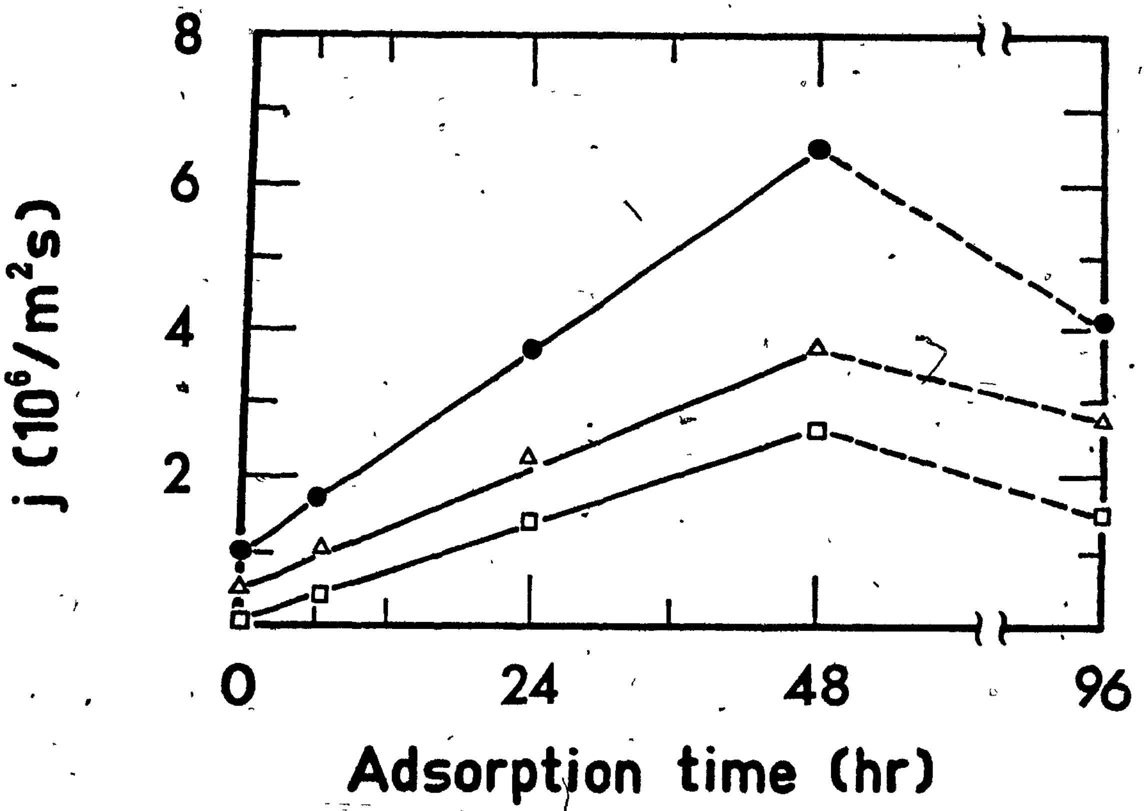
8
6
4
2
j (10^6/m^2s)
0
24
48
96
Adsorption time (hr)

sorption of PEO on latex particles and the results are given in Fig. 4. When no polymer was added we observed a high deposition rate. It can be seen that as the polymer concentration increases, the initial deposition rate decreases linearly. A possible explanation for the lower deposition rate with polymer coated particles is that the bare latex particles are "hairy" (i.e. have polymer segments protruding from their surface) and have a high tendency to stick to the surface (see Fig. 5(a)). After adding polymer these hairs are buried (see Fig. 5(b)). Another explanation is that as we increase the polymer concentration we also increase the concentration of free polymer in the suspension, thus preventing deposition. Consider a dispersion of polymer coated particles surrounded by free polymer (Fig. 6). When deposition occurs, there will be regions on the glass where free polymer molecules are adsorbed on the glass surface. Thus a competition occurs for adsorption sites between segments of polymer adsorbed on spheres and free polymer in solution. This competition prevents high deposition rates.

By the turbidity measurement technique, described in the experimental part, we can evaluate the amount of free polymer in the suspension. Turbidity measurements for a dispersion of coated particles with 0.5 mg/l PEO correspond to a value of 0.05 mg/l of PEO remaining in the dispersion. Thus, for this case, 10% of the polymer remains in the dispersion after two days of adsorption of PEO on latex particles.

According to theory, the initial deposition rate j is proportional to the concentration of latex particles n_ℓ. Deposition experiments were performed on suspensions of latex particles of various concentrations coated with 0.5 mg/l PEO. The initial flux j (= number of particles

Fig. 4 Deposition rate of the coated latex particles as a function of PEO concentration. [NaCl] = 4 mM; Re = 54.
● $\bar{r}$ = 75 μm; Δ $\bar{r}$ = 225 μm; □ $\bar{r}$ = 375 μm.

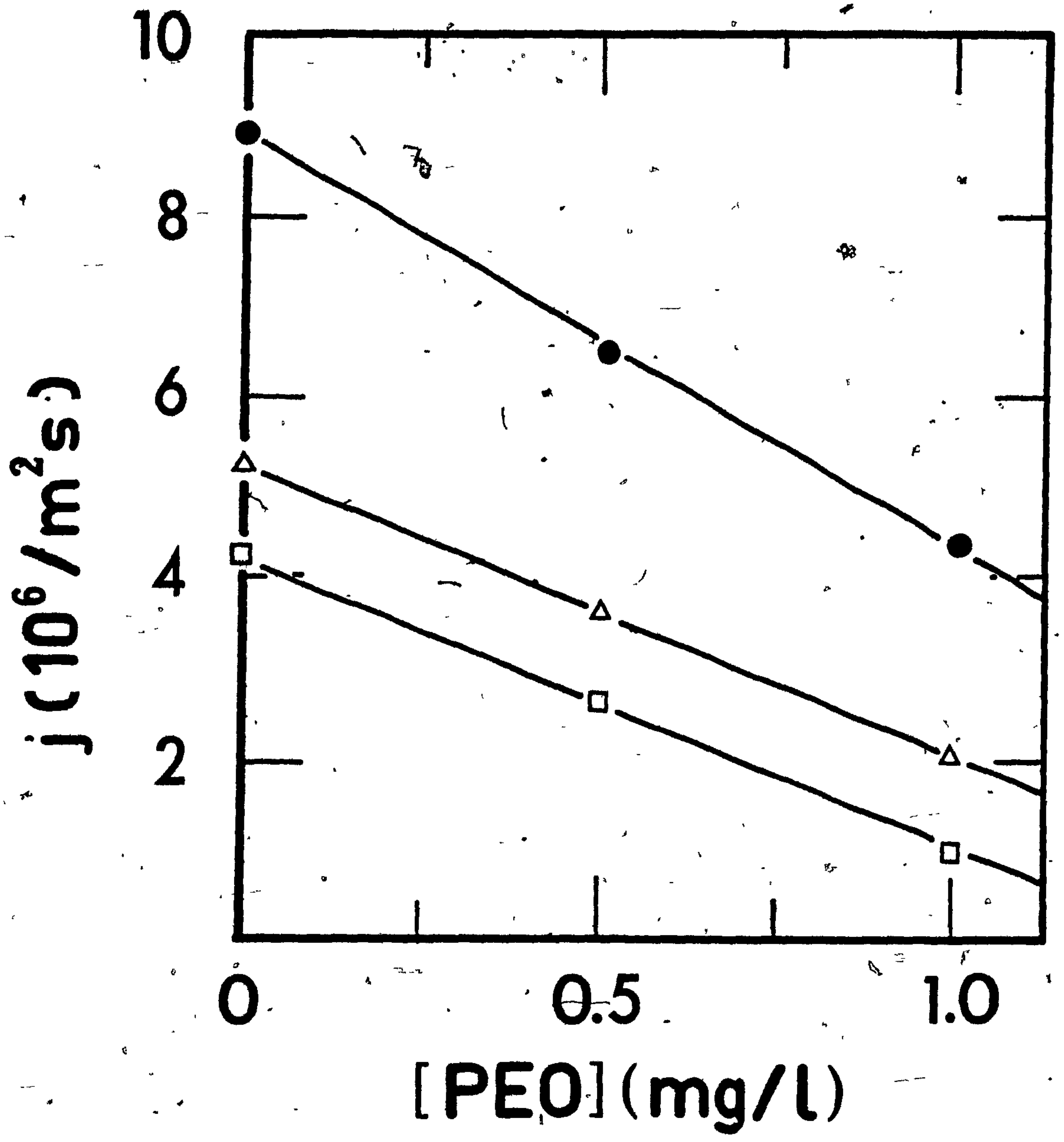
10
8
6
4
2
j (10⁶/m²s)
0
0.5
1.0
[PEO] (mg/l)

Fig. 5 Schematic representation of deposition of polystyrene particles on a glass surface (a) in the absence of PEO, and (b) latex particles are coated with PEO.

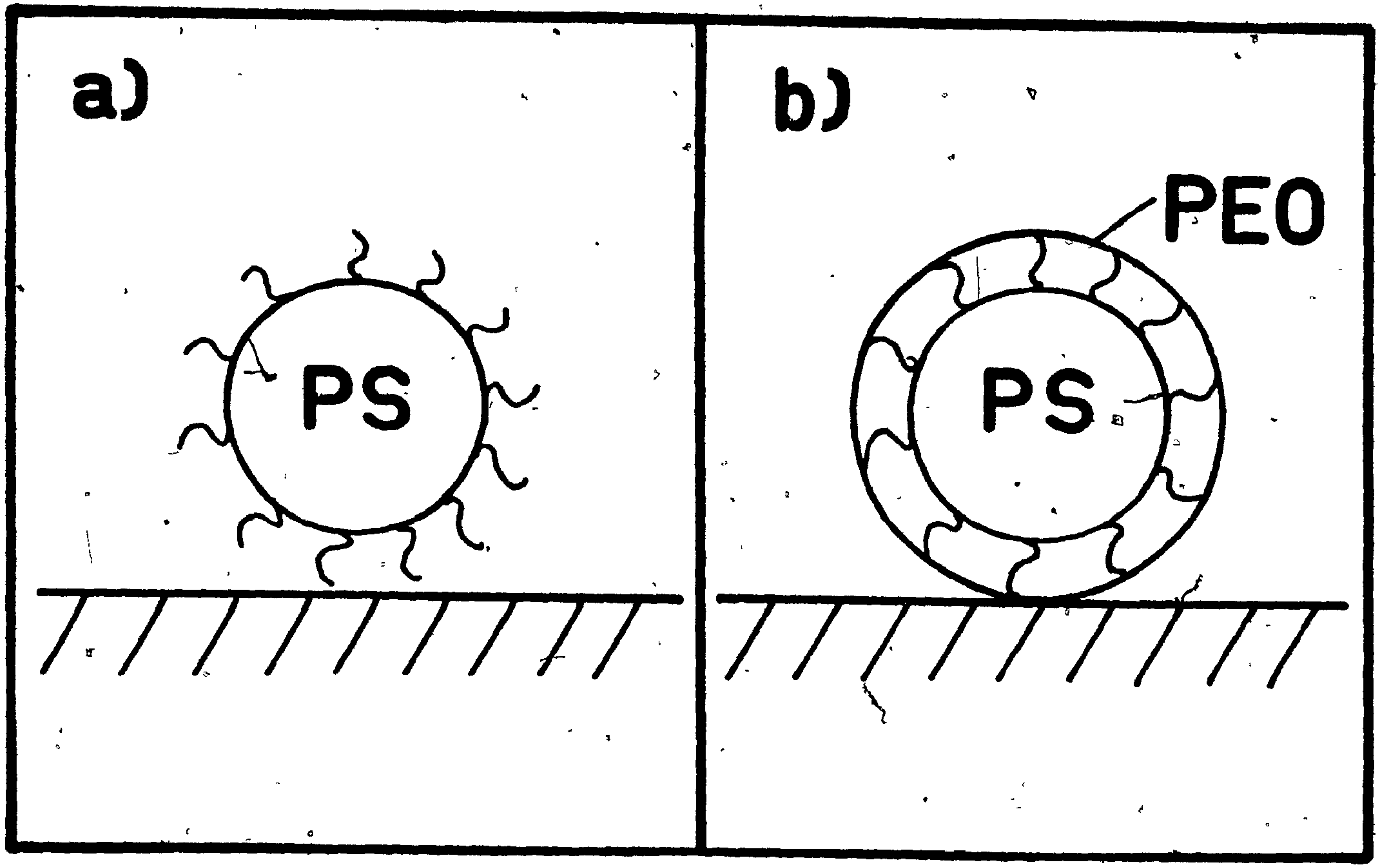
a)
PS
b)
PEO
PS

Fig. 6 Schematic representation of possible mechanism to explain the deposition of latex particles coated with PEO in the presence of free polymer; competition for adsorption sites between polymer adsorbed on latex particles and in solution.

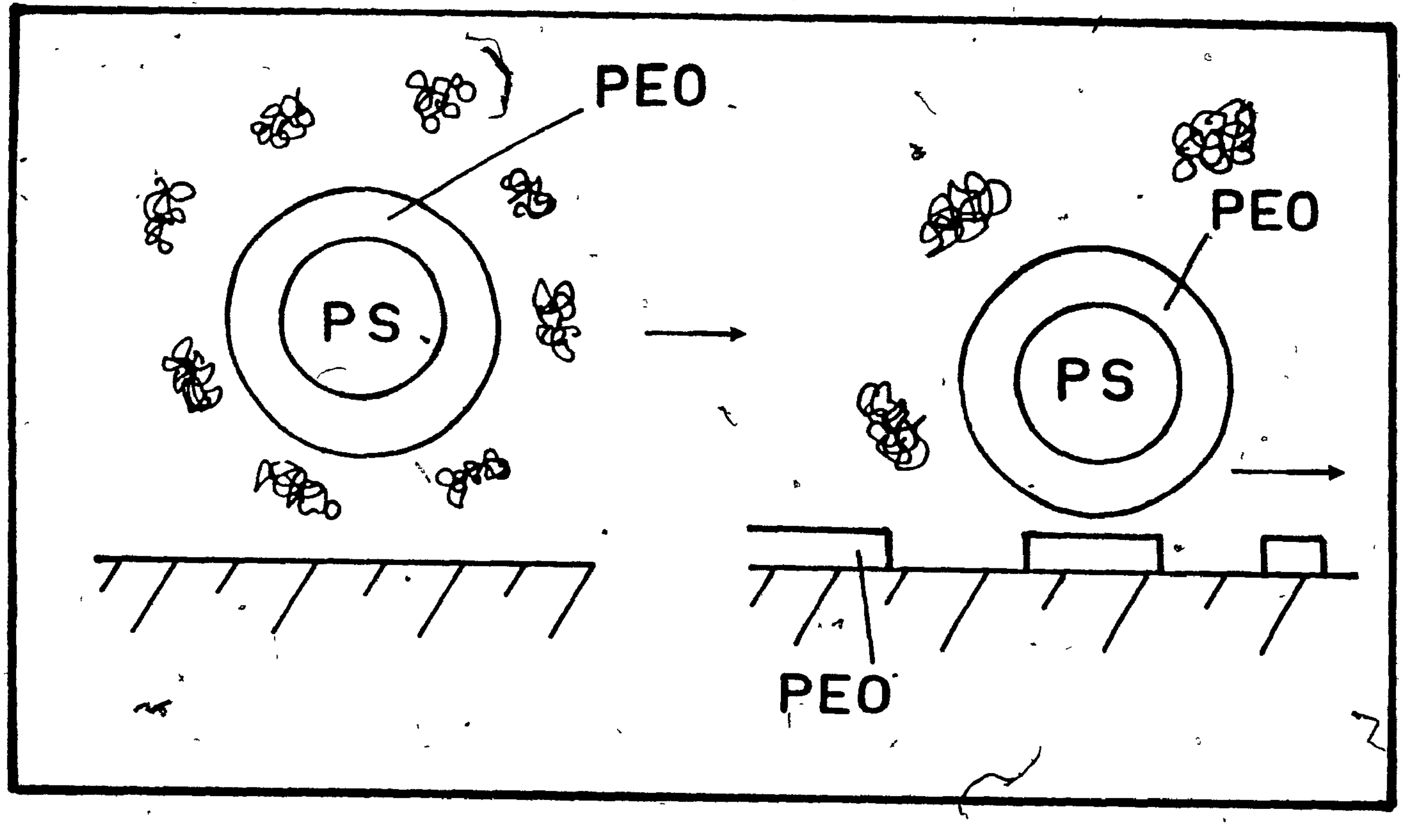
PEO
PS
PEO
PS
PEO

depositing per second per unit area) is a linear function of the concentration of latex particles. Fig. 7 shows that for volume fractions ϕ = 0.1 and 0.05%, j is smaller than expected. By the turbidity measurement technique the percentage of free polymer was determined, for volume fractions ϕ = 0.4, 0.2, 0.1 and 0.05%, respectively, and was found to be 0, 10, 35, and 75% (for 0.5 mg/l PEO). As one can see, dilute suspensions contain a large fraction of free polymer in suspension.

To avoid the problem of having a large amount of free polymer present, we performed deposition experiments with the most concentrated latex suspension (ϕ = 0.4%) coated with PEO (0.5 mg/l). To obtain different concentrations of latex particles, we diluted the original (ϕ = 0.4) suspension by various factors. By this method a linear variation between j and n_1 was found (solid circles in Fig. 7). This shows that free polymer in a suspension of coated particles prevents high deposition. However deposition rates of coated particles in the absence of free polymer are still considerably lower than those of bare particles.

For the remainder of this study we performed deposition experiments with the most concentrated latex suspensions (ϕ = 0.4%) coated with PEO (0.5 mg/l). The adsorption time for all experiments was two days.

We measured the coating density as a function of time for various flow intensities and the results are given in Fig. 8. In all experiments this dependence was found to be non-linear, similar to the deposition of bare latex particles (Chapter 2). In ref. [3] many reasons were discussed for such non-linearity. From that discussion we can conclude that the non- linearity observed in Fig. 8 is mainly due to particle escape and effects of blocking of the already deposited particles. In Fig. 8, the

Fig. 7 The dependence of j on the concentration of latex particles for Re = 54, 0.5 mg/l PEO plus 4 mM NaCl for o < r < 150 μm. ● in the absence of free polymer in solution; ▲ in the presence of free polymer.

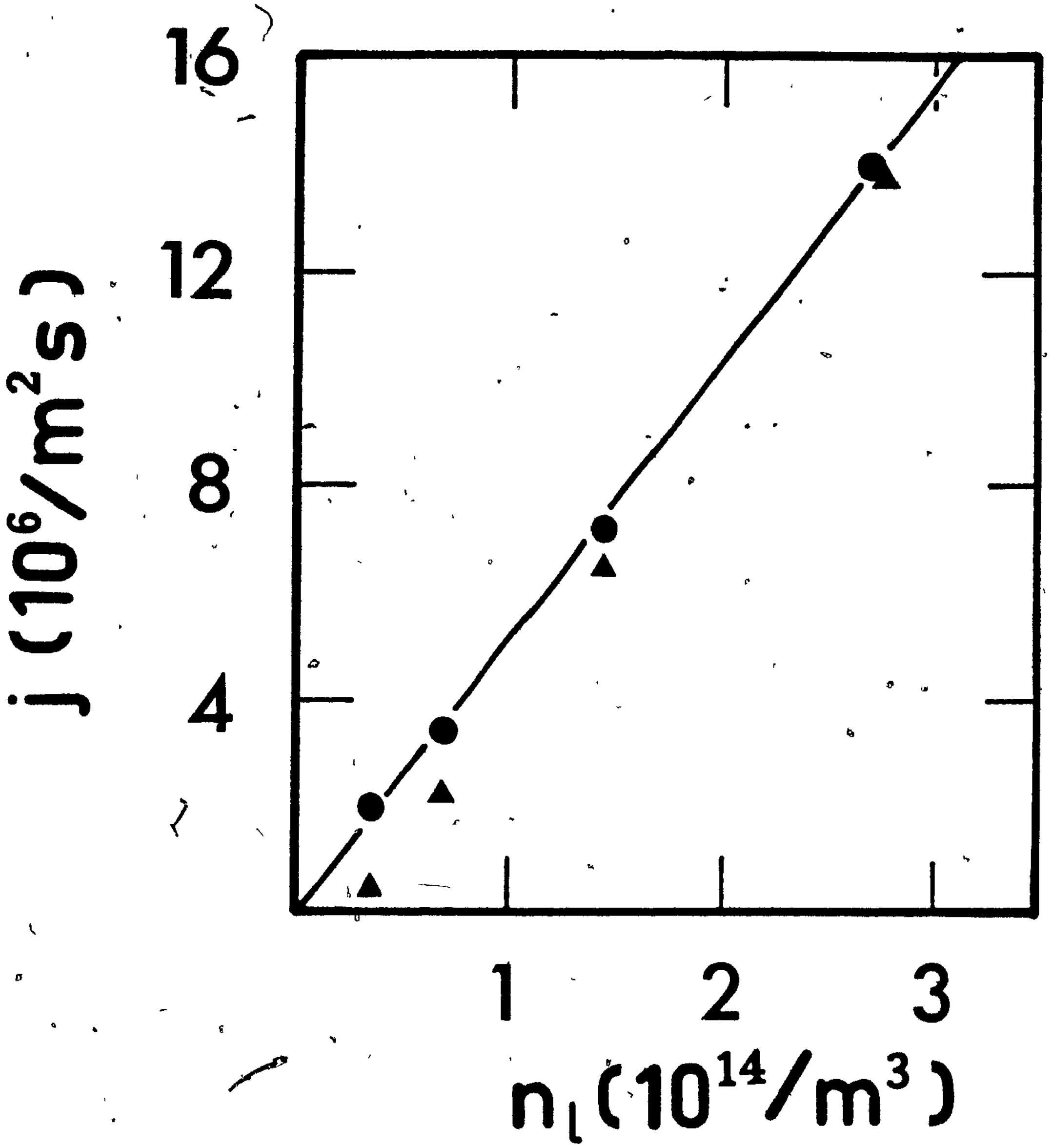
16
12
8
4
j (10^6/m^2s)
1
2
3
n_l (10^14/m^3)

Fig. 8 Coating density N_d vs. time for various Reynolds numbers. [NaCl] = 4 mM; $0 < r < 150$ μm. The solid lines are calculated from Eq. (1) with $\tau = 7.44$, 11.56 and 15.53 min and $j = 4.32$, 2.04 and 1.32 ($\times 10^8$ m^{-2} min^{-1}) for Re = 54, 32 and 24, respectively.

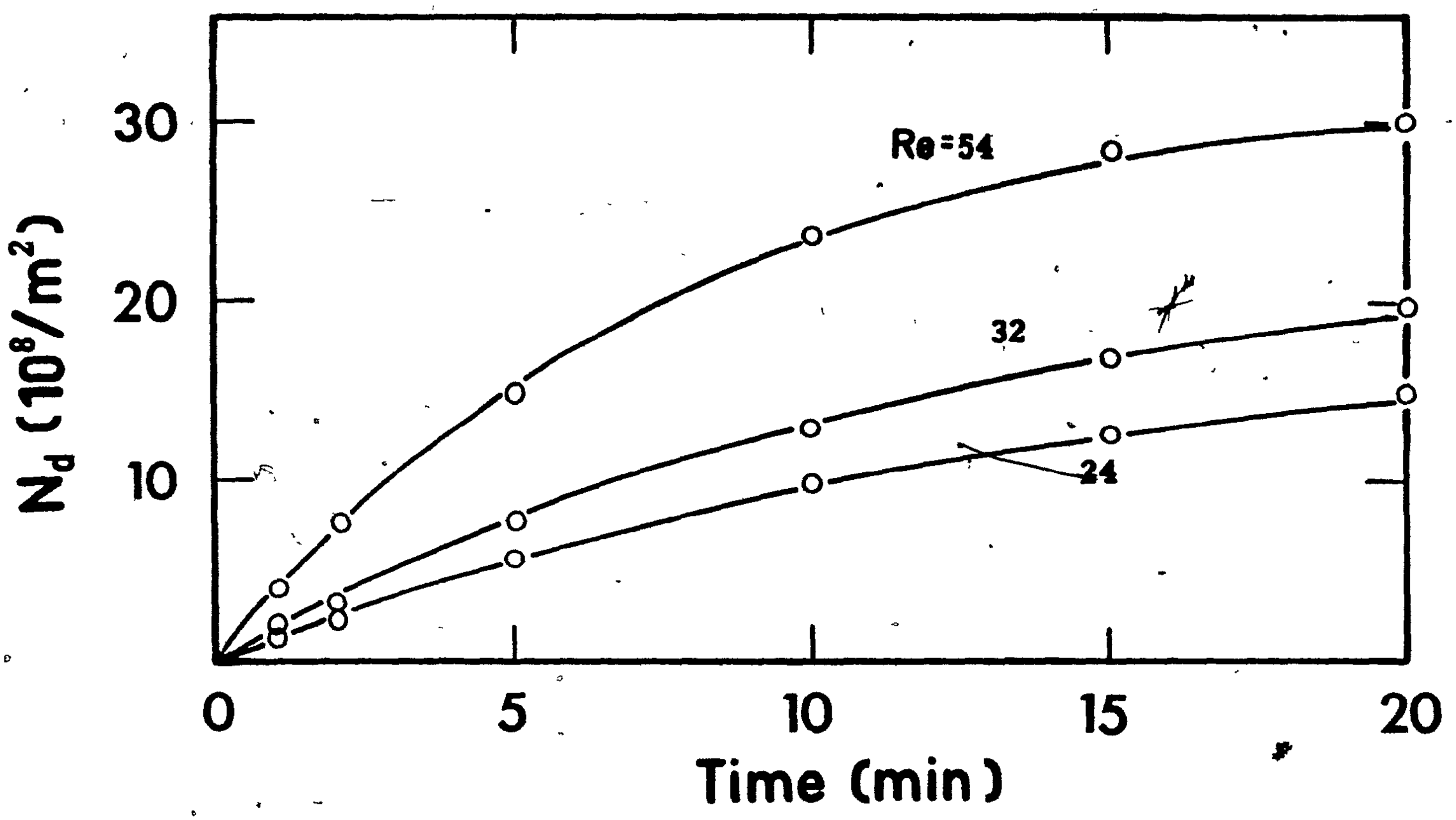

Re=54
32
24
30
20
10
0
5
10
15
20
N_d ($10^8/m^2$)
Time (min)

solid lines, corresponding to Reynolds number 54, 32 and 24, respectively, were calculated from Eq. (1) using the experimentally determined value for j and a best fit value for τ. Compared to the initial deposition rate of bare latex particles, a decrease of about 15% was observed for particles coated with polymer.

Like bare particle experiments, no escape of particles was observed for the range of Reynolds number given in Fig. 8. One can conclude that $\tau_{esc} = \infty$, which follows also from the detachment experiments reported in a later chapter, and thus $\tau = \tau_{bl}$. From Eq. (3) we can calculate the value of the masking parameter γ as a function of Re. Results are given in Fig. 9. Analogous to bare particles (Chapter 2), γ decreases with increasing Re. Our values of γ for polymer coated particles are substantially larger than those for bare latex particles, indicating a large effect of polymer coating on blocking effects. This indicates that the repulsion between two coated latex particles is larger than between bare ones, due to the presence of steric repulsions.

From the initial slopes of experimental N_d vs. t curves (Fig. 8), it is possible to find the initial flux j towards the collector surface. Fig. 10 shows experimental data on the dependence of the initial flux on the Péclet number ($Pe = 2\alpha\ a^3/D_o$), a being the particle radius and D_o the diffusion constant. The solid line in this figure was calculated theoretically from a numerical integration of Eq. (22) in Chapter 2 for the case of particle deposition in the absence of energy barriers. As one can see, the experimental values of Sherwood number Sh, defined as ($Sh = ja/D_o n_o$) where n_o is the bulk concentration of spheres, are lower than theoretical values, especially at higher values of Pe. Away from the

Fig. 9 Masking parameter γ as a function of Reynolds number for $0 < r <$ 150 μm. Curve 1: PEO coated with particles. Curve 2: bare latex particles.

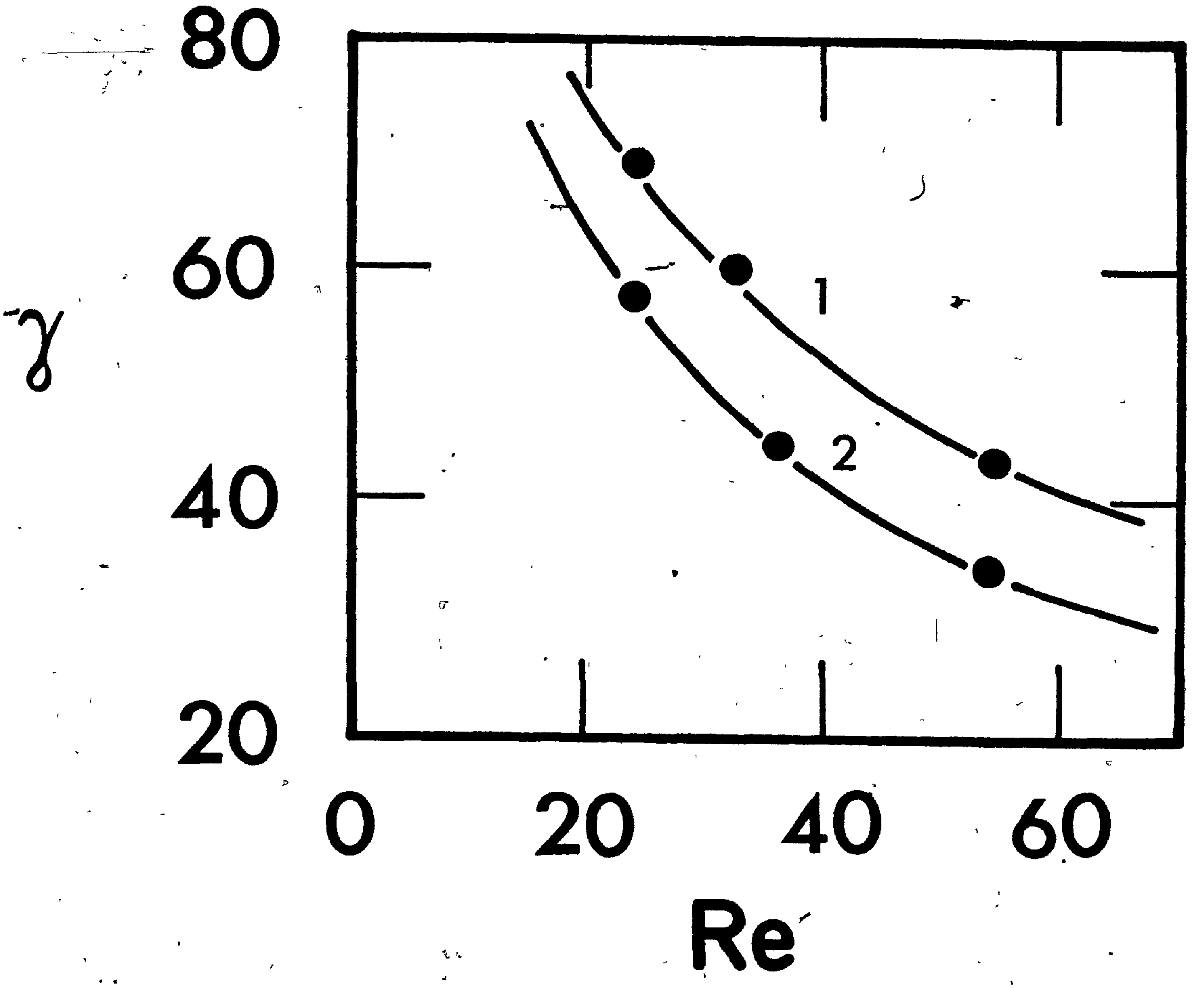
80
60
40
20
γ
0
20
40
60
Re
1
2

Fig. 10 Values of Sherwood number Sh calculated from Eq. (22) in Chap. 2 (solid line) as a function of Péclet number Pe for dimensionless gravity number $G_r = -2.25$, together with experimental data for latex particles coated with PEO, [NaCl] = 4 mM.
● $\bar{r} = 75$ μm; ▲ $\bar{r} = 225$ μm; ■ $\bar{r} = 375$ μm.

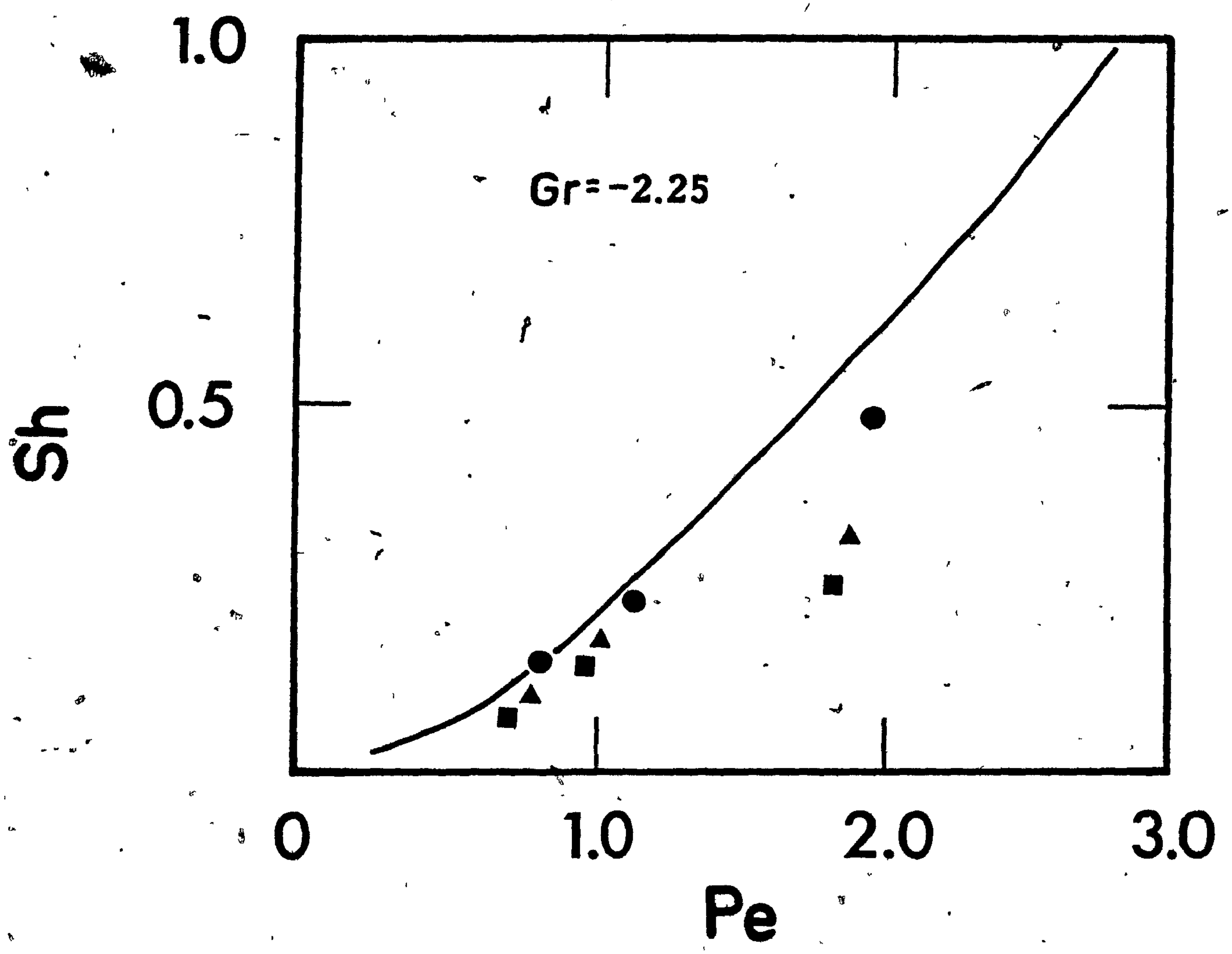
1.0
0.5
Sh
Gr=-2.25
0
1.0
2.0
3.0
Pe

stagnation point, and as Pe increases, the deposition rate is considerably lower. In contrast, for bare latex particles, it can be seen, (Chapter 2), that fast deposition occurs for low Péclet numbers (Pe 2) and close to the stagnation point. Thus, the flux with polymer coated particles indicates the presence of an energy barrier in agreement with predictions of the conventional DLVO theory. Bare particles have the same ζ-potential but deposit faster because of the presence of "hairs" (Chapter 2).

If we plot the initial flux j as a function of the radial distance from the stagnation point r, Fig. 11 shows that as we increase r, j decreases. We found the same dependence with bare latex particles, in disagreement with theory, which predicts a uniform deposition independent of the distance from the stagnation point. In Chapter 2 some reasons were discussed for such non-uniformity. Most likely the contact time (between the particle and site on the surface) may become less than that required to form a bond.

We also measured the coating density as a function of the concentration of latex expressed as the number of particles per cubic meter and the results are given in Fig. 12. We observed, as the concentration of latex increases, that the coating density also increases, being maximum with concentrated suspensions. As $n_\ell \to 0$ we obtain a constant value for N_d^∞ (no particle interactions)(N_d^∞ is the asymptotic coating density obtained when $t \to \infty$). Fig. 12 can be explained by assuming that γ is a function of n_ℓ ($N_d^\infty = 1/\pi a^2\gamma$). It is possible that when a particle is repelled from the surface by a deposited particle, it is again pushed towards the surface by a collision with a suspended particle.

Fig. 13 shows the dependence of the Sherwood number ($Sh = ja/D_o n_o$)

Fig. 11 Initial deposition rate j as a function of the distance from the stagnation point $\bar{r}$ for latex particles coated with PEO for different Reynolds numbers Re.

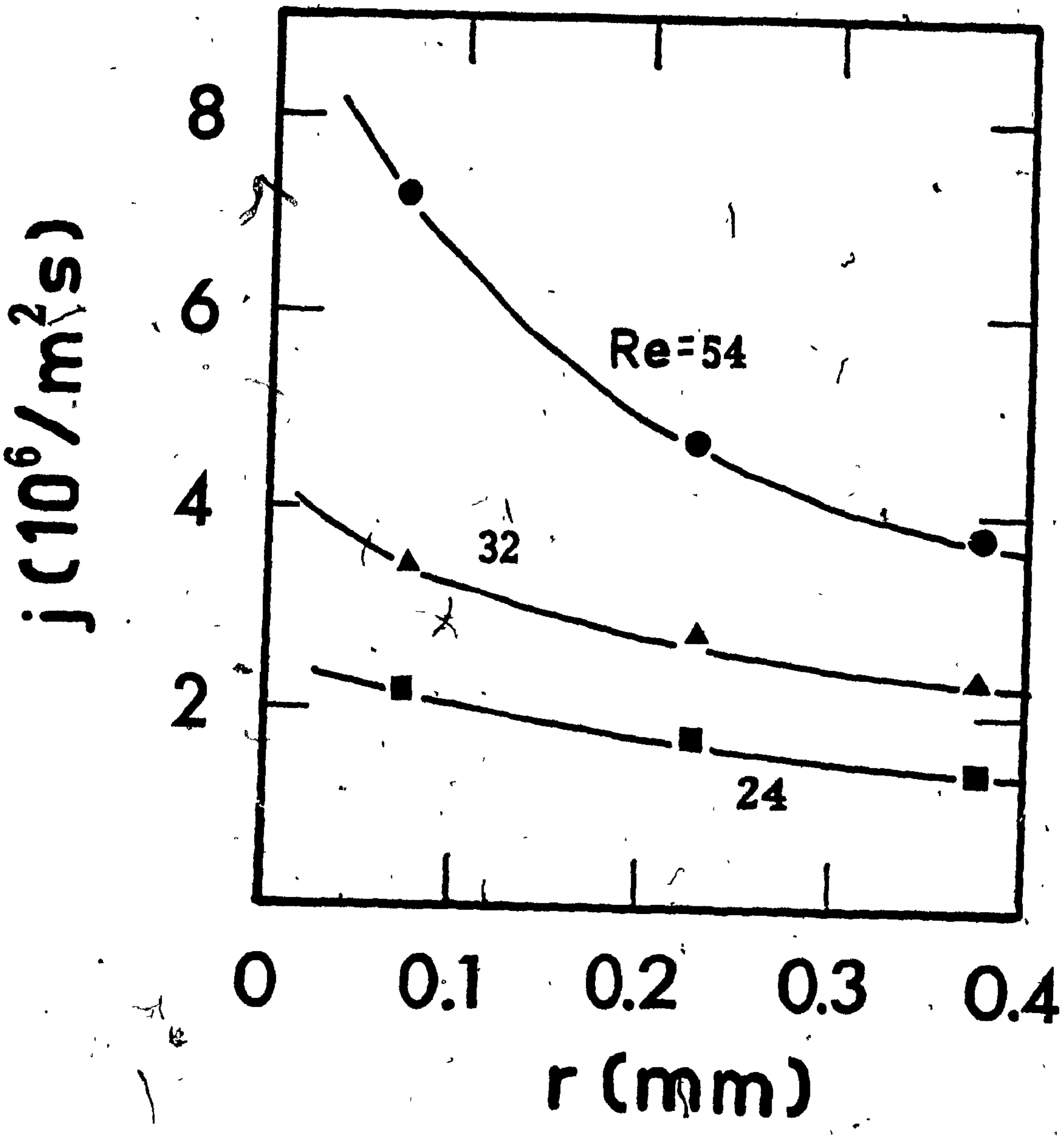

j (10^6/m^2 s)
8
6
4
2
Re=54
32
24
0
0.1
0.2
0.3
0.4
r (mm)

Fig. 12 Coating density N_d^∞ as a function of the concentration of latex coated with PEO for different distance from the stagnation point r. Curve 1: $\bar{r} = 75$ µm; curve 2: $\bar{r} = 225$ µm; curve 3: $\bar{r} = 375$ µm.

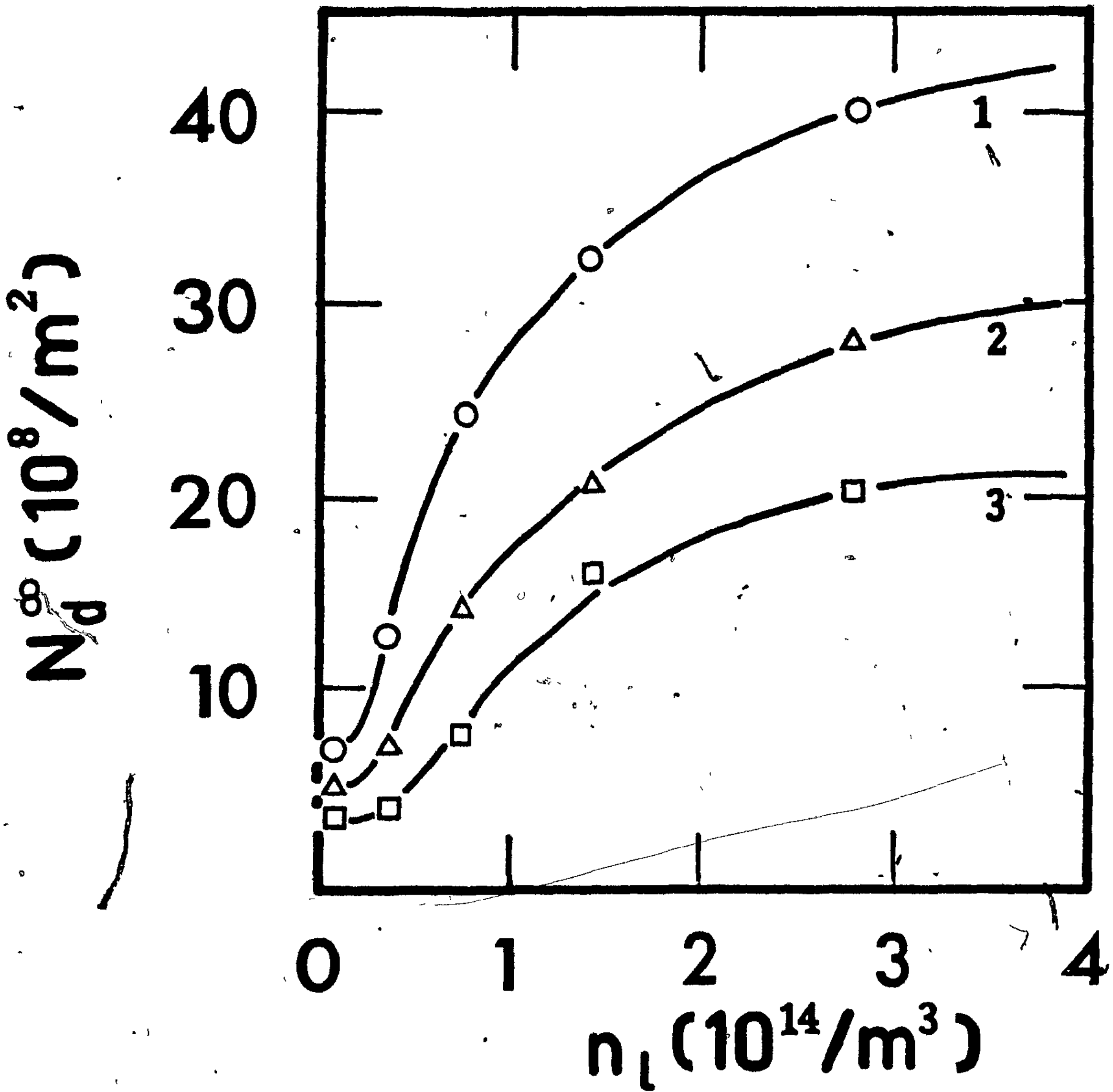

N_d^{∞} ($10^8/m^2$)
40
30
20
10
0
1
2
3
4
n_l ($10^{14}/m^3$)
1
2
3

Fig. 13 Experimental value of Sherwood number Sh for PEO coated particles as a function of salt concentration. Curves 1, 2, 3 are for $\bar{r}$ = 75, 225 and 375 μm, respectively. Re = 54.

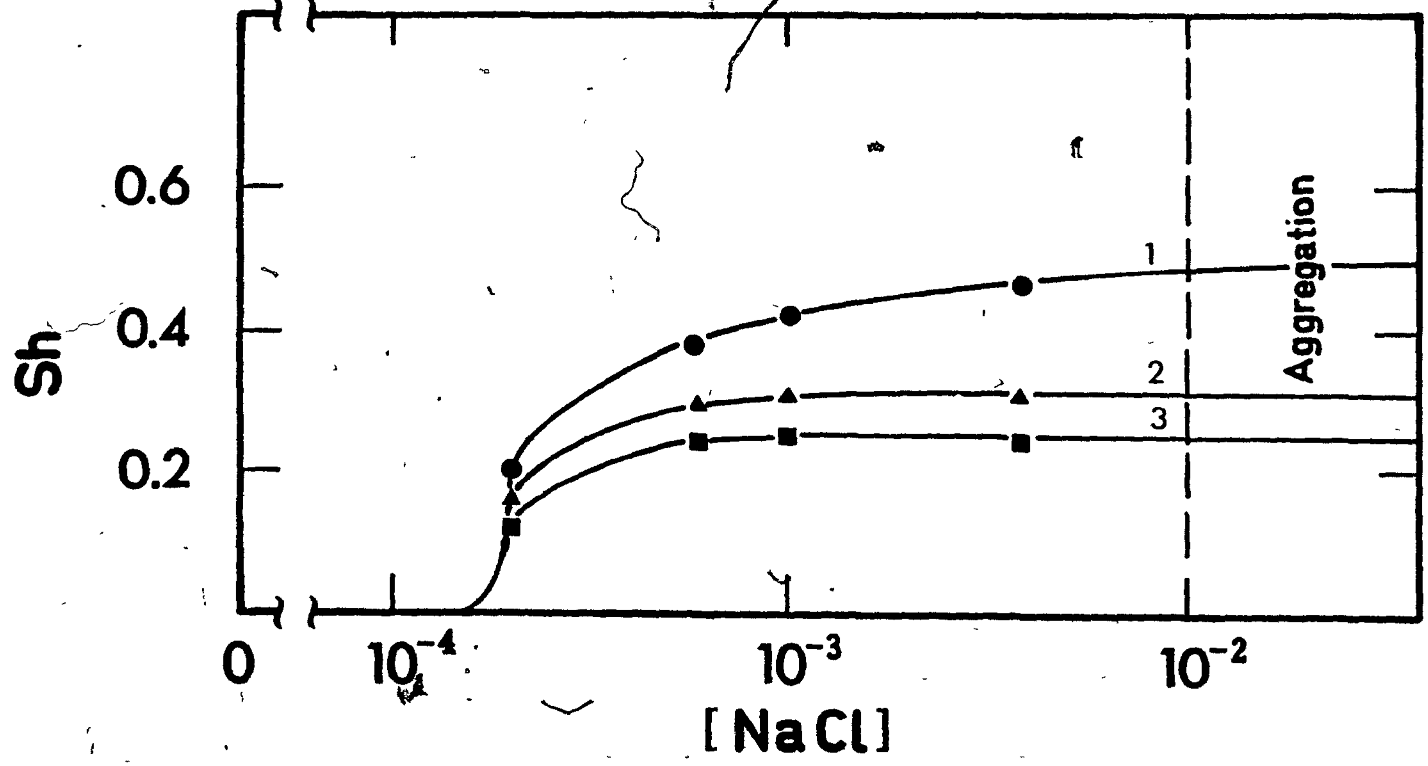

Sh
0.6
0.4
0.2
0
10^{-4}
10^{-3}
10^{-2}
[NaCl]
1
2
3
Aggregation

as a function of electrolyte concentration at constant pH ($\approx$ 5.0-5.2) for average radial distances from the stagnation point equal to 75, 225 and 375 µm. For [NaCl] $\geq$ 0.005 M, the value of the Sherwood number is constant, and for [NaCl] > 0.01 M we observed coagulation. In the range 0 < [NaCl] < 10^{-4} M we observed no deposition. In contrast, for bare latex particles, it can be seen in Chapter 2 that we observe a gradual increase of deposition with increasing salt concentration, and even at the lowest salt concentration do we observe deposition. By coating the particles with polymer, our system behaves more like deposition predictions of DLVO theory, which predicts that no deposition occurs until a critical range of salt concentration is reached. We observed deposition when [NaCl] $\geq$ 10^{-4} M. By adding salt, we decrease the double layer thickness and, as a result, the height of the energy barrier is reduced, resulting in higher deposition. The obtained results reflect the fact that when the energy barrier is higher than a few kT units, it starts to control the flux of particles towards the collector surface.

V. CONCLUSIONS

The deposition on solid surfaces of polystyrene latex particles is decreased by coating them with polyethylene oxide (PEO) of molecular weight 5 x 10^3. The deposition of polymer coated particles on glass surfaces increases with the time allowed for the adsorption of PEO on the latex particles and reaches a maximum after two days. The deposition rate of latex particles coated with PEO decreases with increasing polymer concentration and radial distance from the stagnation point. The polymer concentration dependence of the deposition rate can be explained by the presence of free polymer in the suspension, which deposits on the glass surface resulting in steric repulsion. From turbidity measurements, the percentage of free polymer for different concentrations of coated latex particles (ϕ = 0.4 to 0.05%) was found to be in the range of 0 to 75%. In the absence of free polymer (confirmed by turbidity measurements), we found a linear relation between deposition rate and concentration of latex particles. The dependence of the deposition rate on electrolyte concentration was determined experimentally and, in contrast to bare latex particles, by coating the particles with polymer, the system follows the predictions of the DLVO theory more closely; no deposition occurs until a critical range of salt concentration is reached, beyond which the deposition rates reaches a constant rate.

REFERENCES

1. Marshall, J.K., and Kitchener, J.A., J. Colloid Interface Sci., 22, 342 (1966).
2. Hull, M., and Kitchener, J.A., Trans. Faraday Soc., 65, 3093 (1969).
3. Dabros, T., and van de Ven, T.G.M., Colloid Polym. Sci., 261, 694 (1983).
4. Pelton, R.H., Nugent, H., and Allen, L., J. Colloid Interface Sci., 99, 387 (1984).
5. Hubbe, A.; private communication.
6. Attia, Y.A., and Rubio, J., Br. Polym. J., 7, 135 (1975).

CHAPTER 4

EFFECTS OF POLYMERS ON THE DETACHMENT OF POLYMER COATED LATEX PARTICLES FROM GLASS SURFACES

ABSTRACT

We studied the detachment of polymer coated particles from glass surfaces subjected to a stagnation point flow, generated in a confined impinging jet, with Reynolds numbers, based on the dimension and the mean velocity of the jet, in the range $10 < Re < 1000$. Previously we had established the importance of surface collisions in the detachment process. In this study we investigated the effects of hydrodynamic conditions and of polymers dissolved in the jet. As polymers we used polyethylene oxide (PEO) of various molecular weights. The force of adhesion for particles coated with polymer was much greater than that obtained in the absence of polymer. We found that at moderately low Reynolds numbers, free polymer dissolved in the jet is needed to detach polymer coated particles from glass surfaces. The detachment rate is a strong function of time, being initially zero for a certain induction period, subsequently increasing, then decreasing and, finally, becoming zero again at long times. The rate increases with increasing molecular weight and polymer concentration in the jet.

I. INTRODUCTION

Detachment of colloidal particles from solid surfaces has been studied by various people [1-5] because of its importance to various industrial applications and because it can provide insights in fundamental problems of particle adhesion. For instance, Visser [1,2] showed that the detachment force required to dislodge carbon black and polystyrene particles from cellulose depended on variables such as pH and ionic strength. Hubbe [3] showed that the release of colloidal TiO_2 spheres from cellulose and glass surfaces was a function of the applied shear stress and particle diameter. In these studies the rate of particle deposition and detachment depends on the total interaction energy between two solids in an aqueous medium, which is the sum of London-van der Waals and electrical double-layer energy. The release of adhered particles is facilitated by electrostatic repulsion.

Previously we found experimentally [6] that the deposition of latex particles from glass surfaces is not governed by electrostatic particle-wall interactions alone. It is very probable that the latexes we used were hairy, containing polymeric filaments or segments protruding from their surfaces. In ref. [6] we also studied the detachment of bare latex particles from a glass surface and observed that hydrodynamic effects played an important role in release experiments. As we increase the applied force on deposited particles, the rate at which particles are detached from the surface increases as well. We also found that surface collisions of deposited particles by suspended ones were effective in causing detachment of latex particles from glass surfaces. But when we coat particles with polymer, we change the detachment behavior compared with bare latex particles.

In the present study we describe our experimental work dealing with the detachment rate of polymer coated particles from glass surfaces. The nature of interactions at small particle collector separations are not governed by the DLVO-theory alone, but also by macromolecular bridging.

Our objective is to measure the adhesive strength of polystyrene latex particles bonded to glass with polymer. Particle detachment was studied using the stagnation point flow technique [6]. As polymer we used polyethylene oxide (PEO), a neutral linear polymer.

It will be shown that the presence of polymers dissolved in the jet significantly affects the particle detachment process, a factor not considered in a recent review [3]. To study in more detail the effect of free polymer on the detachment process, experiments were performed for long periods of time (about one day). The molecular weight and polymer concentration in the solution were varied, as well as the Reynolds number (flow rate).

II. THEORETICAL

According to Goldman, Cox and Brenner [7], the tangential force F_H exerted on a spherical particle of radius a in contact with a plane wall in a creeping shear flow is given by the modified Stokes' law:

$$F_H = C\eta a^2 G \tag{1}$$

where C is a constant which equals 1.7 x 6π; η is the viscosity of the liquid, and G the wall shear rate. The wall shear rate can be found from the velocity field $\underline{v}$ near the stagnation point, which can be represented as

$$\begin{aligned} v_r &= \alpha z r \\ v_z &= -\alpha z^2 \end{aligned} \tag{2a}$$

where α is the strength of the stagnation point flow which can be found from flow rate through the cell and the cell geometry [6]. r and z are the radial and normal distances from the stagnation point. The wall shear rate is given by

$$G = \frac{dv_r}{dz} = \alpha r \tag{2b}$$

and increases linearly with radial distance. Detachment occurs when the tangential force acting on a particle (given by eq. (1)) exceeds a critical value related to the force of adhesion.

In this study we found that polymer coated particles could usually not be dislodged by hydrodynamic forces exerted on them, but could be detached in the presence of free polymer in the jet.

The bond strength of PEO coated latex particles adhered to glass in the presence of dissolved polymer in the jet can be determined by measuring the detachment rate as a function of time.

The detachment rate can be expressed as

$$\frac{dn}{dt} = - kn \tag{3}$$

where k is a rate constant proportional to $e^{V_m/kT}$, n is the fraction of remaining particles, V_m is the energy minimum in the interaction between a particle and the collector and kT is the thermal energy. When a hydrodynamic force is acting on the particle, the effective energy minimum is changed [6]

$$V = V_m - V_{hydr} \tag{4}$$

Assuming a constant hydrodynamic force, Eq. (3) becomes

$$\frac{dn}{dt} = \tilde{k} n e^{V_m/kT} , \tag{5}$$

where the effects of the flow are incorporated in the value of modified rate constant $\tilde{k}$. Furthermore

$$V_m \approx - F_{bond} \, \ell \tag{6}$$

where ℓ is a characteristic length over which a bond can be stretched. Taking the logarithm of Eq. (5) results in

$$\ln\left(-\frac{1}{n}\frac{dn}{dt}\right) = \ln \tilde{k} - \frac{\ell}{kT} F_{bond} \qquad (7)$$

where the l.h.s. is experimentally observable. A variation of this term with time is an indication that the bondstrength varies in time.

III. EXPERIMENTAL

Materials

Experiments were performed using polystyrene latex particles with a mean diameter of 3 μm, identical to those used previously [6,8]. The latex was cleaned by successive centrifugation until the conductivity of the supernatant of the centrifuged sample was in the range of 2 - 3 x $10^{-6}\Omega^{-1}m^{-1}$.

We coated latex particles with polyethylene oxide (PEO) (a neutral linear polymer) with a molecular weight of 5000. The adsorption method is given in ref. [8], where we found that the adsorption time was important since it affected deposition rates. The adsorption time for all experiments reported here was two days. Polyethylene oxide of higher molecular weights, 7.9 x 10^4 and 5 x 10^6, were used in release measurements. PEO samples of molecular weight 5 x 10^3 and 7.9 x 10^4 were provided to us by Professor D.H. Napper, while the sample of molecular weight 5 x 10^6 was a commercial one (Seitetsu Kagaku Co. Ltd.). PEO is very soluble in water. To dissolve it we added it gradually to the solution while agitating. In this way PEO will be perfectly wetted and dispersed in water. For the high molecular weight polymer, after dispersion in water, mechanical agitation was continued at moderate speeds for some hours to obtain a homogenous solution. The concentration of the PEO solution was 0.1 g/l.

As substrates we used microscope cover glass slides. Before use, the surfaces were treated with nitric and hydrochloric acid to obtain clean surfaces. For details see ref. [6].

Impinging jet technique

The apparatus used consisted of an impinging jet cell, described in [6,9]. The deposition procedure employed was the same as in the experimental runs described in ref. [8]. In short, the technique consists of depositing particles onto a transparent surface by impinging a dispersion onto it. The surface is observed through a microscope to which a video system is attached. For detachment experiments some procedural steps were added.

Detachment procedure

After twenty minutes of deposition, we stopped the deposition process by closing valves 1 and 2 as illustrated in Fig. 1. We pumped the suspension in the recipient B and emptied the dispersion from containers A and B, which were subsequently thoroughly rinsed with distilled water. Next we filled containers A and B with a solution of polymer and salt or salt only, depending on the type of release experiment. We placed another recipient under valve 3 to collect the original suspension remaining in the deposition cell at the beginning of the removal experiment. The intensity of the flow was controlled by valve 3. This allowed the Reynolds number to vary over a wide range in the experiments. To start

Fig. 1 Schematic representation of the experimental set-up. A: reservoir to collect outflowing dispersion; B: colloidal dispersion; C: collector (cover slide); M: microscope; 1: entrance valve; 2: outflow valve; 3: flow speed control valve.

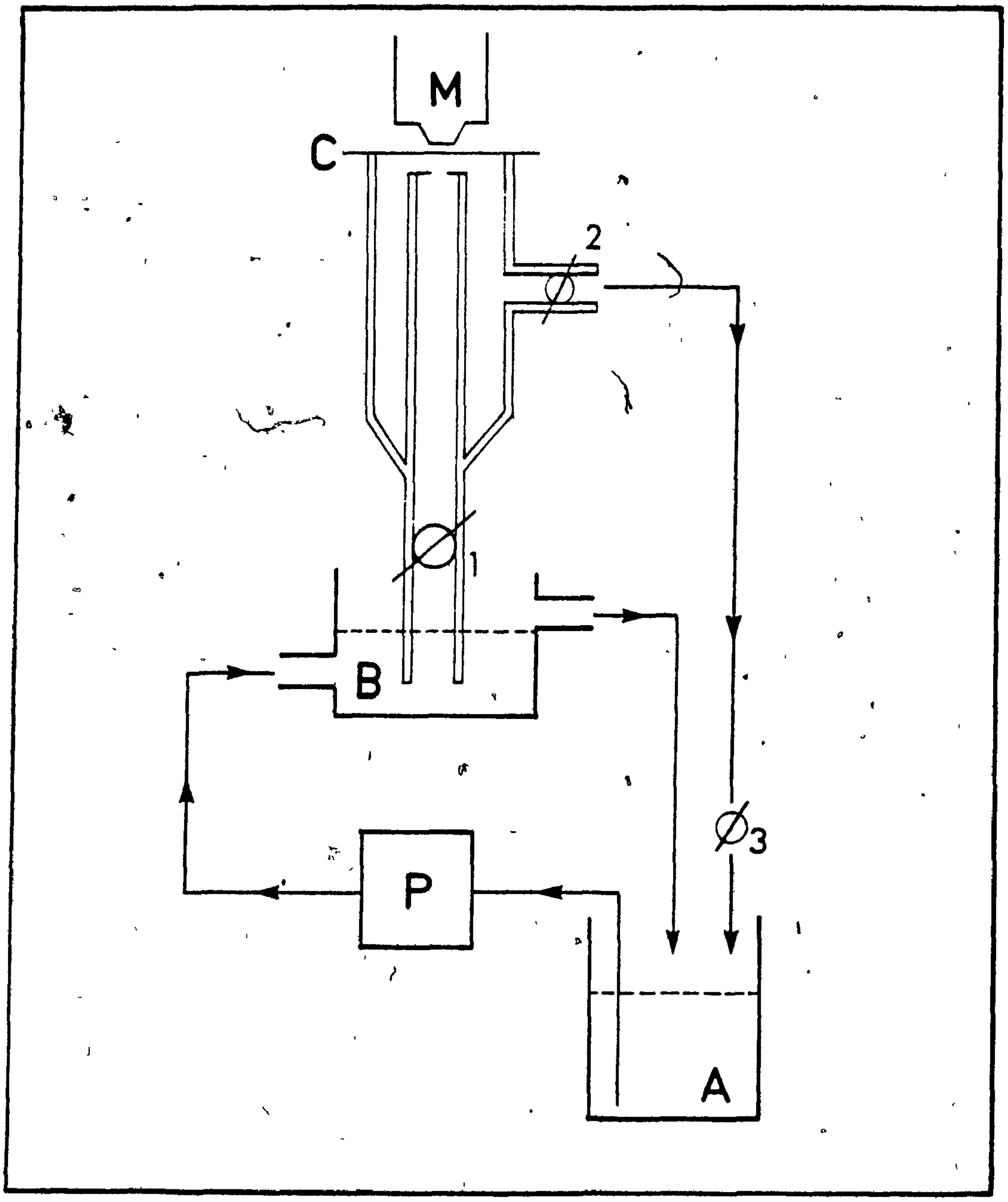
M
C
2
1
B
3
P
A

the detachment process we opened valves 1 and 2 simultaneously and observed the detachment of particles as a function of time. This procedure was repeated for various Reynolds numbers. From an analysis of the detachment process, it was possible to determine the fraction of escaped particles as a function of time. An initial count of adhering particles was made routinely prior to the detachment process. Counts were made through an optical microscope/TV camera system described in [6]. We divided the observation region into three areas, one near the stagnation point (up to 150 μm), one far from the stagnation point (300-450 μm), and an intermediate region (150-300 μm).

IV. RESULTS AND DISCUSSION

Particles coated with PEO (of molecular weight 5000) suspended in an aqueous electrolyte solution were deposited on a glass surface for a period of 20 minutes. Subsequently experiments were performed to determine the fraction of escaped particles by changing the original suspension to a solution containing (i) salt, or (ii) particles and salt, or (iii) polymer and salt. The same flow rate, corresponding to Re = 54, was applied before and after each removal experiment. In case (i), no particle detachment was observed and the coating density (number of deposited particles per unit area) remained constant; in case (ii), deposition was increased similar to the case of deposition of bare particles and there was no evidence of detachment. In case (iii), a slow decrease in the number of particles was observed, especially far from the stagnation point. Thus polymer was involved in the detachment process of the particles. These qualitative observations are summarized in Fig. 2.

Experiments were performed to determine the bond strength of polystyrene spheres—PEO-glass systems by changing the flow rate to unstable flow (prior to the onset of turbulent flow) after 20 minutes of deposition for four different systems: (i) Coated particles (for circulating solution) and clean cover slide (acting as solid surface); no particle detachment was observed under unstable flow, the coating density remaining constant. If we compare this to similar conditions for the detachment of bare latex particles from glass, in which case we observed a fraction of escaped particles in the range 0.5 to 0.75 depending on the wall shear rate, we can conclude that strong bonds were formed between coated latex particles and glass; (ii) Cover slide coated with PEO and bare latex particles circulating in the flow; during the 20 min. of deposition we observed less deposition compared to case (i) and more particle escape in the deposition/detachment process. Under unstable flow, particles detach very easily from the surface. Hence under these conditions the formation of weak bonds occurs. The most effective bonding must result when the initial adsorption takes place on the surface having a lower affinity for the polymer. This order of treatment maximizes the strength of the weaker link in the solid-polymer-solid bond; (iii) Same as (ii) but after 20 min. of deposition we let the particles sit on the surface for one day (in contact with the solution) and then apply the unstable flow. Under these conditions no particles detach. Some particles are seen to escape at very high flow rates correspoding to Re =

Fig. 2 Schematic representation of the detachment of latex polystyrene particles coated with PEO from a glass surface at Re = 54 in the presence of a solution containing (a) salt, (b) polymer and salt.

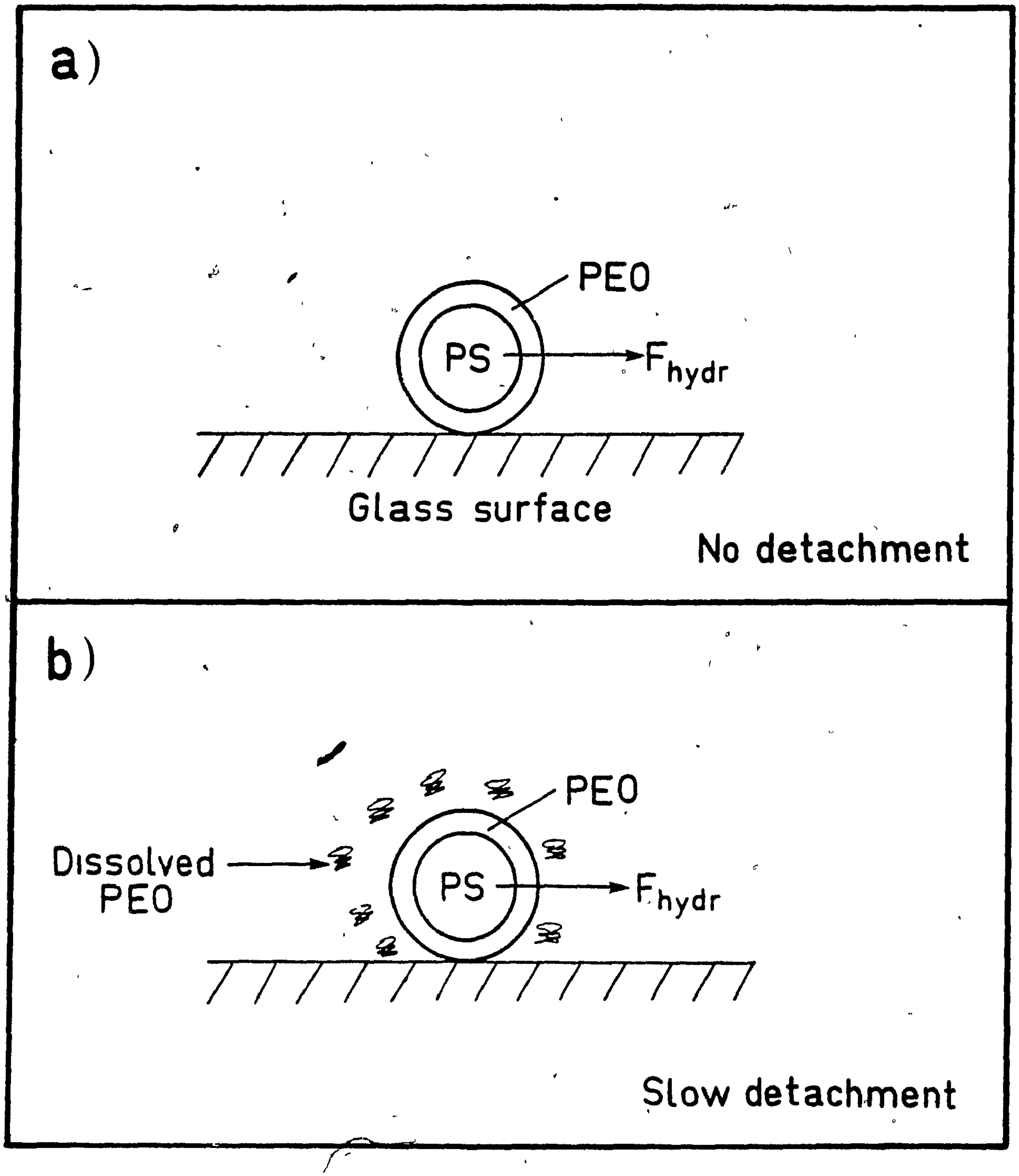
a)
PEO
PS
F hydr
Glass surface
No detachment
b)
PEO
Dissolved PEO
PS
F hydr
Slow detachment

900. After one day the polymer adsorbed more strongly on the surface, probably because more polymer segments were bridging both surfaces, resulting in the formation of stronger bonds than case (ii); (iv) Both the cover slide and the latex particles were coated with PEO. In this case no deposition was observed, due to steric repulsion between the particle and the surface. These observations are summarized schematically in Fig. 3.

To study in more detail the effects of free polymer on the detachment process, experiments were performed for long periods of time (about 1 day). By changing the amount of polymer in the solution, and also by changing the Reynolds number (flow velocity), we can determine if these factors accelerate the process of detachment.

Table I contains data on the release of PEO coated polystyrene particles from glass for various flow rates in the presence or absence of polymer in the jet. In Table I the results are expressed in terms of the fraction of remaining particles. This fraction is given for three different shear rates G (corresponding to the mean of three regions near the stagnation point). G increases with increasing distance from the stagnation point (cf. Eq. (2b)). This table is a summary of various detachment experiments. We observed that in the absence of polymer in the jet and at moderately low Reynolds number (Re $\doteq$ 54), no particles detached from the surface within a one day period. We found that by increasing the Reynolds number from 54 to 907, depending on the wall shear rate, between 0 and 10 percent of the coated particles were removed within two hours. By comparing these results of polymer coated latex particles with bare ones under the same conditions [6], one notices a larger fraction of

Fig. 3 Schematic representation of the detachment of deposited particles under unstable flow for various systems, using polystyrene particles of radius 1.5 μm, polyethylene oxide as polymer and glass as collector. (a) Coated particles (for circulating solution) and clean cover slide. (b) Cover slide coated with polymer and bare latex particles circulating in the flow. (c) Cover slide and latex particles both coated with PEO.

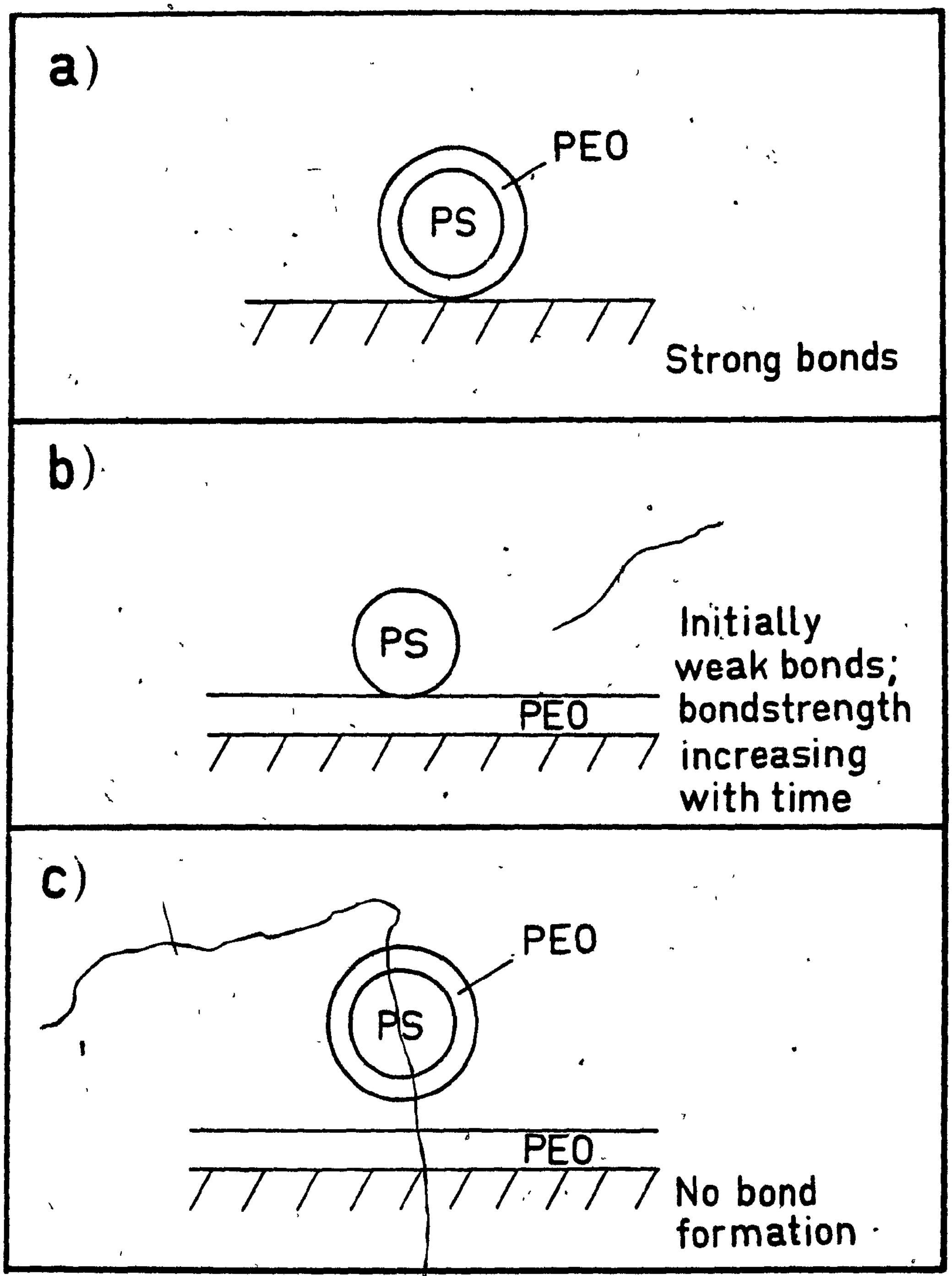
a)
PEO
PS
Strong bonds
b)
PS
PEO
Initially weak bonds; bondstrength increasing with time
c)
PEO
PS
PEO
No bond formation

TABLE I

Effects of [PEO] and Re on the fraction of remaining polymer coated particles deposited on a glass surface

[PEO] [a) (mg/l)	Re	G [b) (s^{-1})	Time (hr)	Fraction of remaining particles [b)
0	54	3, 10, 16	24	1.0 ,1.0 ,1.0
0	380	52,146,233	2	1.0 ,1.0 ,1.0
0	907	191,538,863	2	1.0 ,0.91,0.90
1	54	3, 10, 16	24	0.99,0.99,0.95
1	380	52,146,233	1	0.80,0.52,0.47
1	380	52,146,233	18,22	0.70,0.41,0.37
50	54	3, 10, 16	24	0.84,0.84,0.64

a) - Molecular weight of PEO was 5,000.

b) - The results are expressed for different distances from the stagnation point, corresponding, respectively, to $\bar{r}$ = 75,225, 375 μm.

escaped particles for bare latexes. For instance, by increasing the Reynolds number from 54 to 907, depending on the wall shear rate, between 0.3 to 0.6 of bare latex particles were removed within two hours. These results suggest that the adhesion force (estimated to be > 0.05 N) acting to keep polymer coated particles on the surface was too strong to permit escape from the surface. Thus the presence of polymer (PEO) greatly increases the strength of the bond between the particle and the glass.

By dissolving polymer in the jet (PEO of molecular mass 5000), the process of detachment is changed and the fraction of released particles is increased. It was found that with 1 ppm PEO and at moderately low Reynolds number (Re = 54), almost no particles detached from the surface. By increasing the Reynolds number to 380 (in the presence of 1 ppm PEO), depending on the wall shear rate, between 0.3 and 0.6 of the particles were removed within one day. By adding 50 ppm PEO to the jet and maintaining the Reynolds number at 54, between 0.15 and 0.35 of the particles were removed in one day. This example shows the importance of dissolved polymer. Hence, from the results given in Table I, it follows that under certain hydrodynamic conditions dissolved polymer is needed to detach polymer coated particles from glass surfaces. Next we determined how the molecular weight and the concentration of polymer affected the detachment rate. Also we performed experiments with a high concentration of polymer at high Reynolds number to see whether all the deposited particles detach or if some particles remain on the glass surface. Table II summarizes results of experiments performed at Re = 380 for three different molecular weights of PEO, 5×10^3, 7.9×10^4 and 5×10^6, for which rms end-to-

TABLE II

Effects of concentration and molecular weight of PEO dissolved in the jet on the fraction of remaining polymer coated particles deposited on a glass surface exposed to a flow with Re = 380 for one hour.

[PEO] (mg/1)	Molecular weight	Fraction of remaining particles a)
0	-	1.0 ,1.0 ,1.0
1	5 x 10^3	0.80,0.52,0.47
1	79 x 10^3	0.81,0.49,0.40
1	5 x 10^6	0.58,0.22,0.12
50	5 x 10^3	0.28,0.23,0.12
10	5 x 10^6	0.34,0.23,0.12

a) - The results are expressed for different distances from the stagnation point, corresponding, respectively, to $\bar{r}$ = 75, 225, 375 μm.

end distances are estimated as 7, 28 and 220 nm, respectively. In the absence of polymer in the jet, no detachment of polymer coated particles was observed for one hour. As can be seen from Table II, the detachment of deposited particles increases with increasing radial distance from the stagnation point and with increasing molecular weight. We also observed that the process of detachment is accelerated by increasing the polymer concentration.

Fig. 4 shows the curves obtained for the detachment of polymer coated particles from a collector when we dissolved 1 ppm PEO of molecular weight 5 x 10^6 in the jet at Re = 380. The three curves correspond to three regions from the stagnation point corresponding to $\bar{r}$ = 75,225, 375 μm. It can be seen that initially (< 1 min), the detachment rate (related to the slope of these three curves) increases with time but subsequently decreases at large times, as evidenced by the absence of further particle detachment. Hence by dissolving polymer in the jet we initially decrease the strength of the bond formed between PEO coated particles and glass. At large times the bondstrength increases because we observe no particle detachment.

We can determine the strength of the bond (F_{bond}) between PEO coated latex particles and glass by determining the slopes at various times of a plot of the fraction of remaining particles versus time (cf. Eq. (7)). Results are presented in Fig. 5 where the logarithm of $(-\frac{1}{n}\frac{dn}{dt})$ is shown as a function of time. The two curves refer to two different distances from the stagnation point. As one can see, F_{bond} increases during most of the process. The initial decrease must be extremely fast (< 1 min).

Fig. 4 Effect of dissolved polymer on the fraction of remaining particles as a function of time for the detachment of polymer coated particles from glass at Re = 380. The curves 1, 2, 3 are for $\bar{r}$ = 75, 225 and 375 μm, respectively.

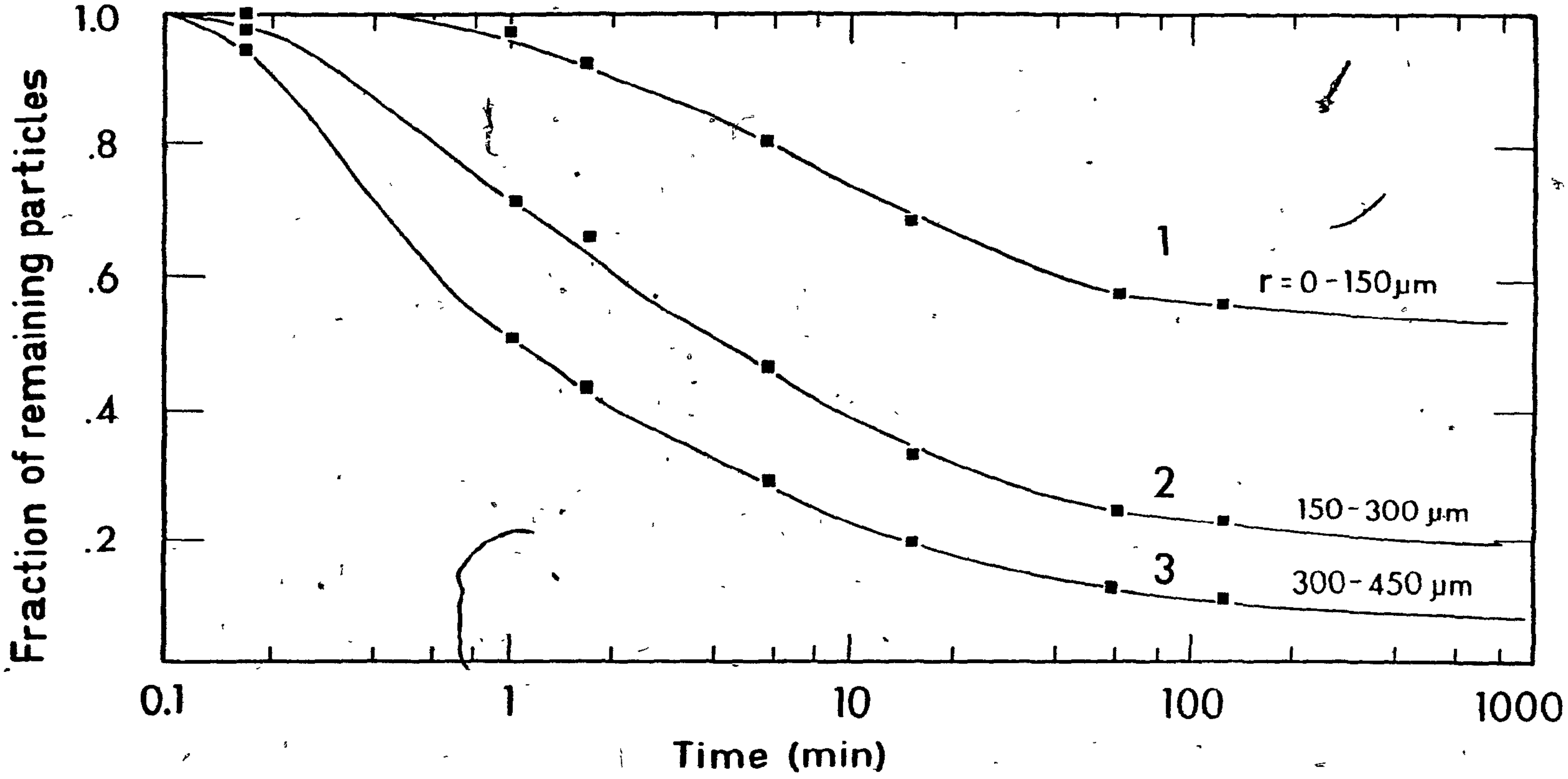
Fraction of remaining particles
1.0
.8
.6
.4
.2
0.1
1
10
100
1000
Time (min)
1
r = 0 - 150µm
2
150 - 300 µm
3
300 - 450 µm

Fig. 5 Logarithm of $\left(-\frac{1}{n}\frac{dn}{dt}\right)$ as a function of time (min) for the detachment of latex particles-PEO-glass in the presence of 1 ppm PEO with molecular mass of 5 x 10^6 dissolved in the jet.

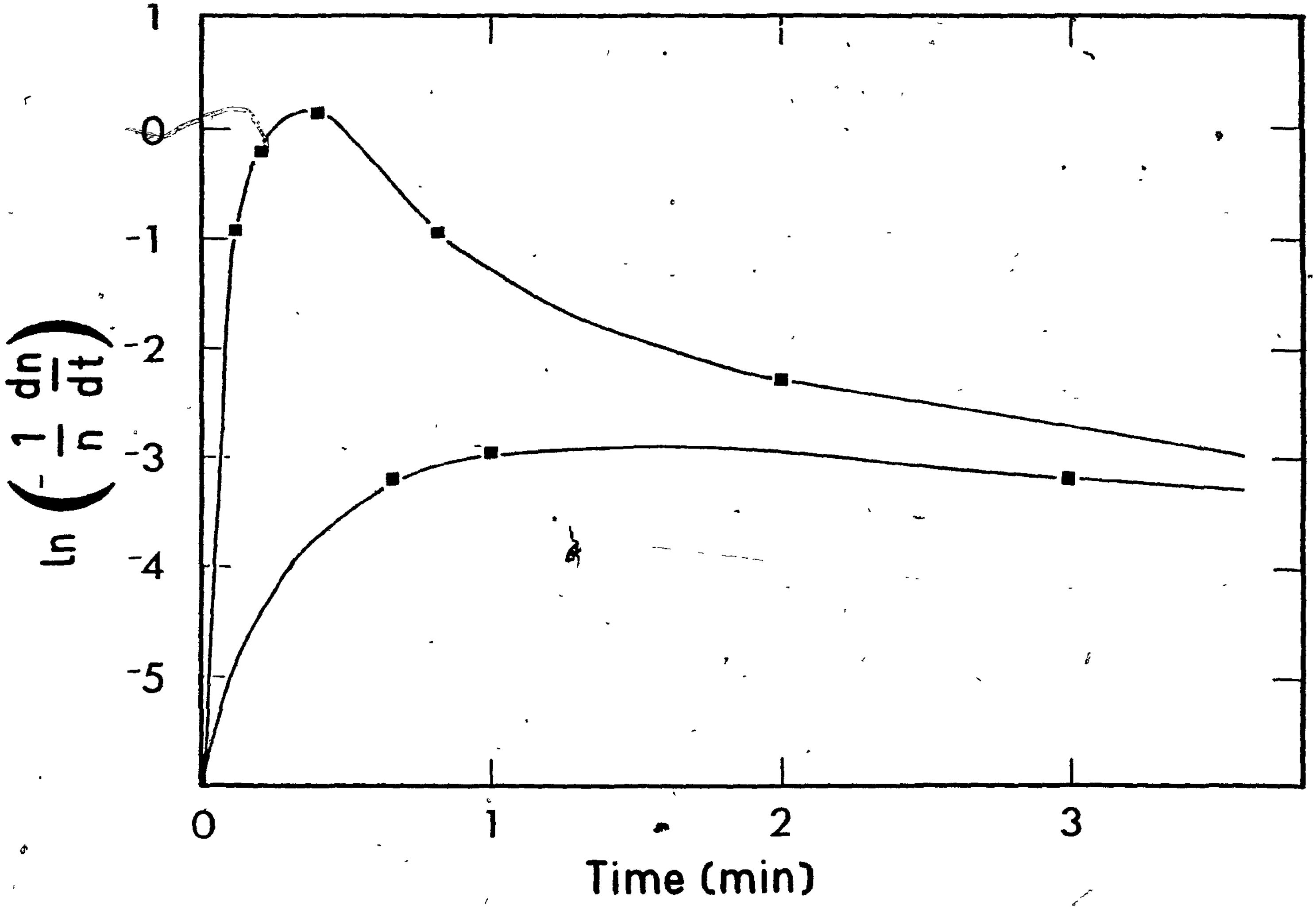
1
0
-1
-2
-3
-4
-5
$\ln\left(\frac{1}{n}\frac{dn}{dt}\right)$
0
1
2
3
Time (min)

Fig. 6 shows schematically the strength of bond F_{bond} between PEO coated latex particles and glass as a function of time. Also included is the critical hydrodynamic force F_c required to detach deposited particles from the surface within the time scale of an experiment. F°_{bond} is the initial bond strength, i.e. before the start of the detachment process. When we add dissolved polymer (t = 0) and start a release experiment, F_{bond} initially decreases steeply with time but subsequently increases again. As can be seen from this figure, initially when $F_{bond} > F_c$ no particles are detached (or at a very slow rate only). Hence for a certain initial period the fraction of remaining particles remains at 1. This interval is defined as the induction time, i.e. the time needed for the bond strength to drop from F°_{bond} to F_c. Different induction times t_{ind} were observed for different average distances from the stagnation point $\bar{r}$. As $\bar{r}$ increases, the induction time decreases. It is possible to observe the induction time for different detachment experiments, and to determine if the molecular weight and the concentration of polymer dissolved in the jet affect the induction time. Examples are shown in Fig. 7, where the fraction of remaining particles is plotted versus time. The four curves correspond to various release experiments using different concentrations and molecular weights of PEO. Results are expressed for distance from the stagnation point corresponding to $\bar{r}$ = 75 μm.

Values of induction times are given in Table III. As can be seen, the induction time decreases with increasing radial distance from the stagnation point.

The presence of dissolved polymer in the jet renders the detachment rate a function of time. After the induction period the detachment

Fig. 6 The strength of a bond, F_{bond}, between latex particle-PEO-glass as a function of time (schematic).

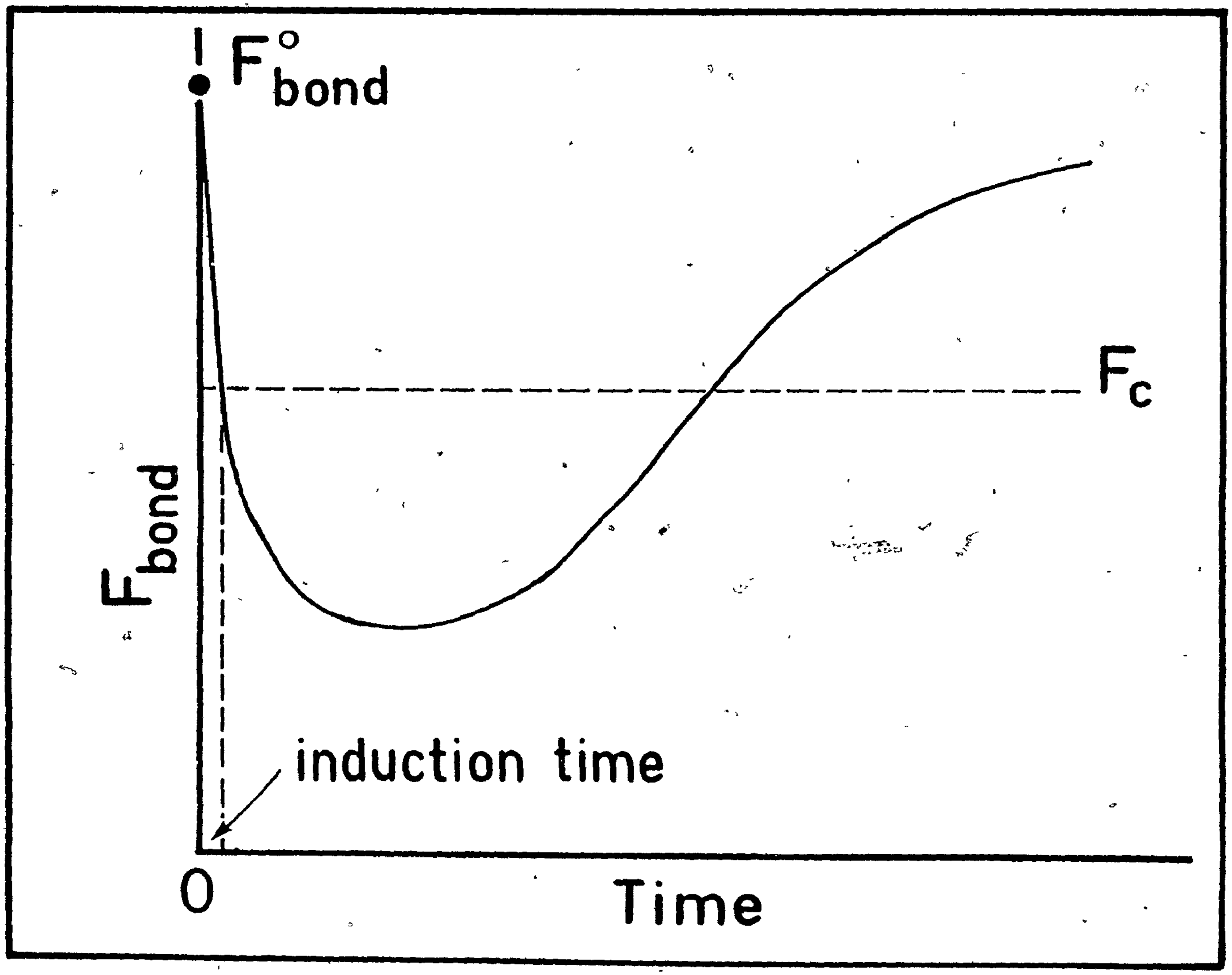F°_{bond}
F_c
F_{bond}
induction time
0
Time

Fig. 7. Fraction of remaining polymer coated particles as a function of time in the presence of dissolved PEO in the jet at various concentrations and molecular weights. The time for which no detachment occurs corresponds to the induction time. The curves are for $0 < r < 150$ μm. The molecular weights are ●: 5×10^3 and ▲: 5×10^6.

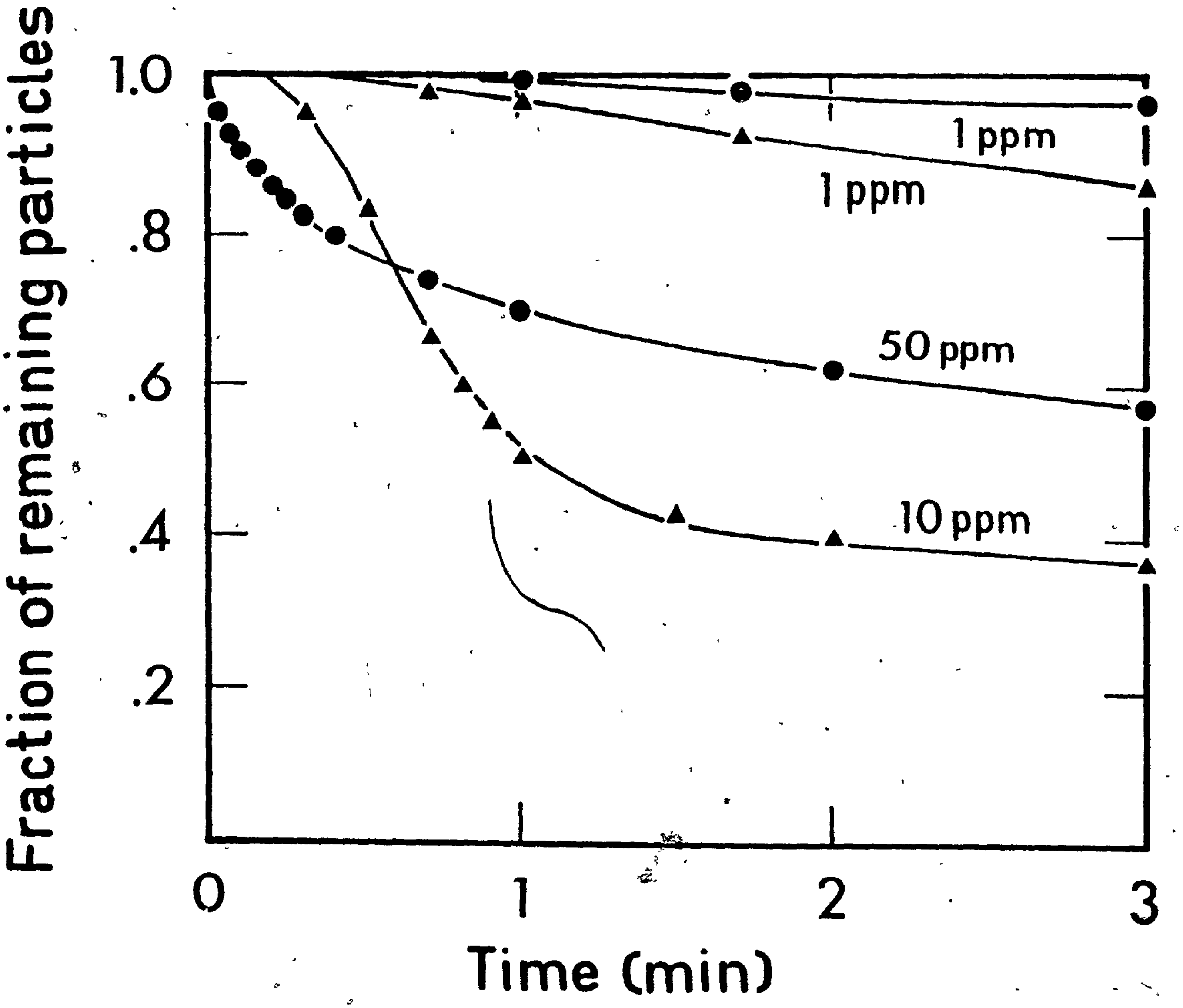
Fraction of remaining particles
1.0
.8
.6
.4
.2
0
1
2
3
Time (min)
1 ppm
1 ppm
50 ppm
10 ppm

TABLE III

Values of induction time as a function of molecular weight and concentration of polymer dissolved in the jet.

[PEO] (mg/l)	Molecular weight	Induction[a)] time (s)
1	5×10^3	54,10,9
1	5×10^6	24, 7,6
50	5×10^3	2, 2,1
10	5×10^6	12, 9,7

a) - The results are expressed for different distances from the stagnation point, corresponding, respectively, to $\bar{r}$ = 75, 225, 375 µm.

rate increases rather fast, while it decreases at larger times. We can propose a possible mechanism to explain these observations. Fig. 8 shows a schematic representation of a latex polystyrene particle coated with PEO deposited on a glass surface, in the presence of free polymer. An exchange occurs between free polymer segments and binding segments on the surface of the sphere or the glass. This exchange weakens the bonds and increases the probability of particle escape. At the same time, free polymer adsorbs on the surface around the particle, restricting access to the binding segments and thus preventing the exchange mechanism. The newly attached macromolecules can eventually become bridging molecules themselves. This increases the number of bonds and decreases the probability of escape.

The presence of dissolved polymers in the neighborhood of a deposited polymer-coated particle increases its probability of escape. We can explain the detachment rate by a possible mechanism which consists of two steps:

(1) Free polymer segments replace binding segments (on the surface of a sphere or on glass). We can estimate the rate of the segment replacement as

$$\frac{dm}{dt} = -k\phi m^{p} \tag{8}$$

where m is the number of binding segments, k is the rate constant, ϕ is the concentration of free polymer and p is an exponent allowing for the unaccessibility of the central segments. Because this process stops, we assume that k is a function of time. Polymer adsorbs on the solid sur-

Fig. 8. Schematic representation of a possible mechanism to explain the detachment of latex particles-PEO-glass in the presence of free polymer at Re = 380. The free polymer segments replace binding segments on the surface of sphere or glass. Free polymer adsorbs on the surface around the particle and newly attached molecules can also become bridging molecules.

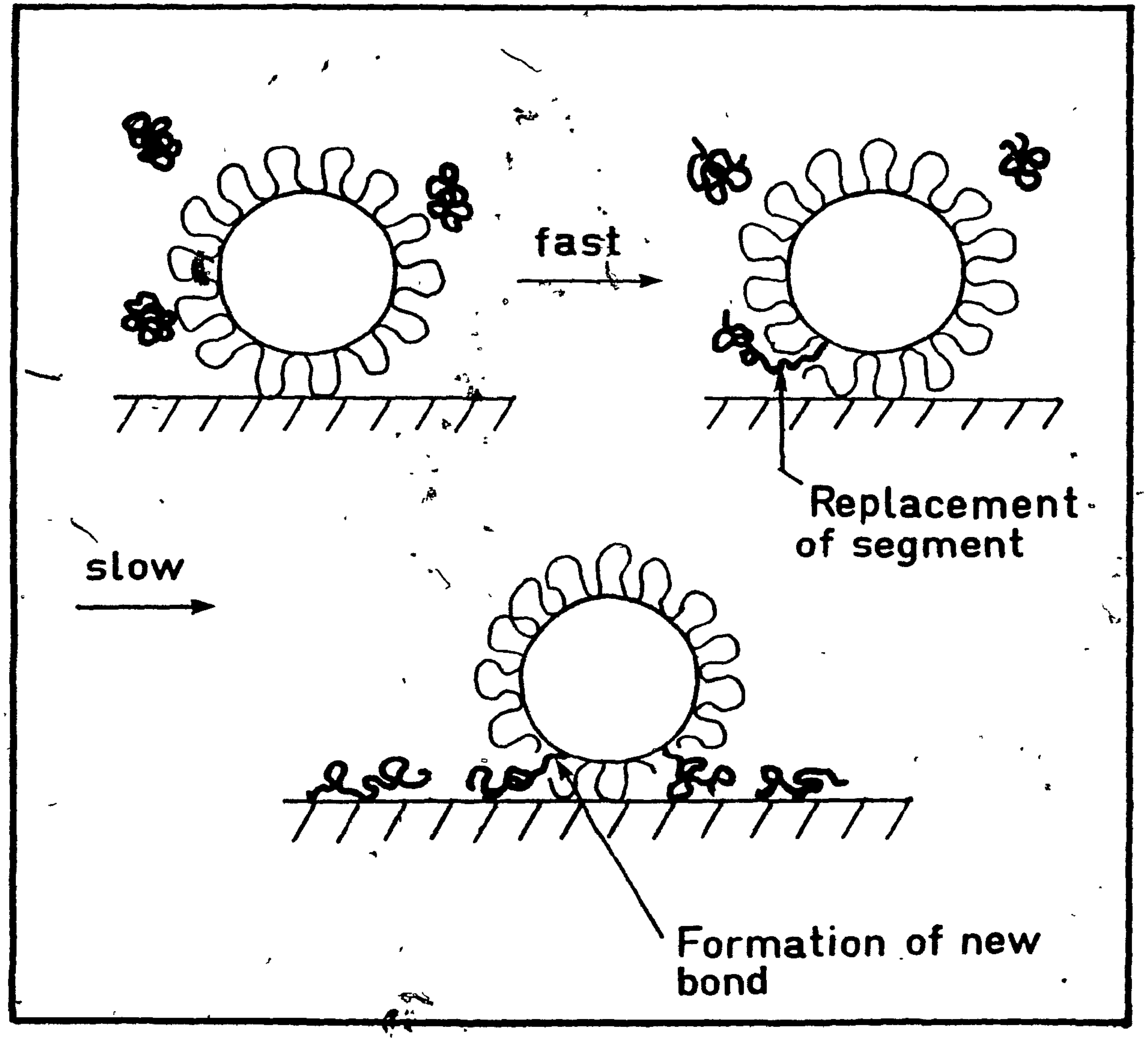
fast
slow
Replacement of segment
Formation of new bond

face around a deposited particle, preventing the exchange mechanism. Analogous to the deposition of solid particle, the surface gets coated with polymer at a rate

$$\phi_s = \phi_\infty \left(1 - e^{-\beta t}\right) \qquad (9)$$

ϕ_s is the concentration of polymer on the glass surface at time t and ϕ_∞ at time $t = \infty$. Here β is a masking coefficient defined as a product of the initial flux j (proportional to ϕ) and the surface blocked per polymer molecule;

$$\beta = \alpha\phi \qquad (10)$$

α being a proportionality constant. Assuming that the rate at which segments exchange slows down because polymer adsorption makes segments inaccessible, we can replace the rate constant k by

$$k = k_1 e^{-\alpha\phi t} . \qquad (11)$$

(2) Newly attached molecules can also become bridging molecules. This increases the number of bonds and by including this effect the variation in concentration of binding segments can be expressed as

$$\frac{dm}{dt} = - k_1 e^{-\alpha\phi t} \phi m^p + k_2(m_{eq} - m) . \qquad (12)$$

Here m_{eq} is the equilibrium number of binding segments for a given amount of polymer. Eq. (12) can explain qualitatively the behavior as indicated in Fig. 6.

Fig. 9 shows the fraction of remaining particles as a function of the product of time t and the volume fraction of dissolved polymer ϕ. The figure presents the detachment of polymer coated particles from a glass surface exposed to Re = 380 for various release experiments using different concentrations and molecular weights of PEO. Results are expressed for the distance from the stagnation point corresponding to $\bar{r}$ = 75 μm. We observe from Fig. 9 that the fraction of the remaining particles is almost constant up to $\phi t \simeq 2$. For short times, Eq. (12) predicts that $n \propto \phi t$. For $\phi t > 2$ the fraction becomes a function of the concentration and molecular weight of PEO dissolved in the jet. From Fig. 9 one can deduce two interesting observations: (i) at the same ϕ, more particles escape at high molecular weight M; (ii) at the same M, more particles escape at large ϕ. To explain the first observation, we can express the deposition time τ_{dep} (inversely proportional to the deposition probability)

$$\tau_{dep}^{-1} = \pi a^2 \gamma j , \qquad (13)$$

where γ is the area blocked per particle [9].

Because $j \propto n_o$ and

$$n_o \propto \frac{\phi}{M} , \qquad (14)$$

it follows that

Fig. 9 The fraction of remaining particles as a function of the product of the time (min) and the volume fraction ϕ of dissolved polymer present in the detachment of polymer coated particles from a glass surface exposed to Re = 380. The curves 1, 2, 3, 4 are for 1 ppm [PEO] molecular weight $M = 5 \times 10^3$, 50 ppm [PEO] $M = 5 \times 10^3$, 1 ppm [PEO] $M = 5 \times 10^6$ and 10 ppm [PEO] $M = 5 \times 10^6$, respectively. $0 < r < 150$ μm.

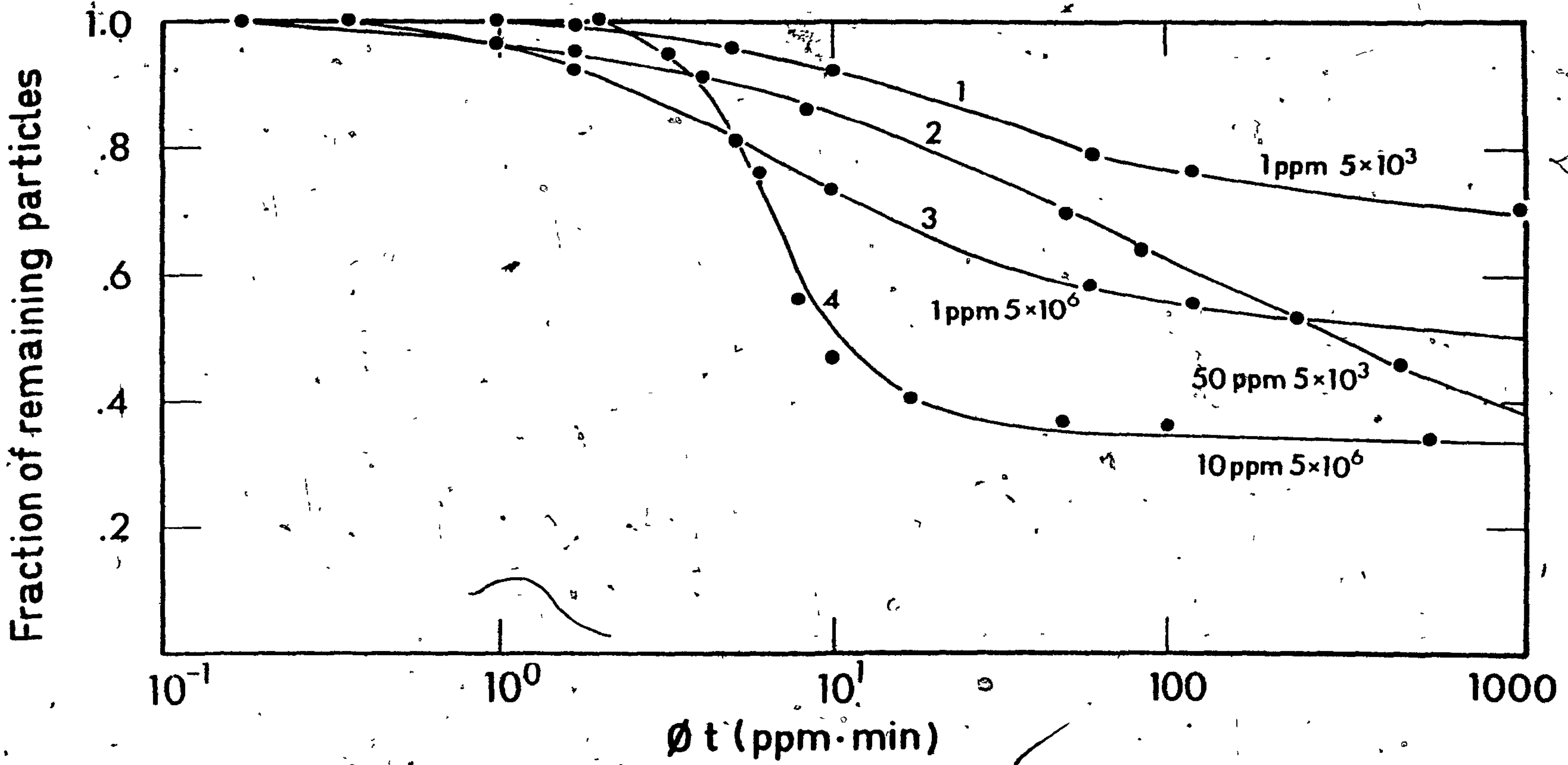
1.0
.8
.6
.4
.2
Fraction of remaining particles
10^{-1}
10^{0}
10^{1}
100
1000
Ø t (ppm·min)
1
2
3
4
1 ppm 5×10^3
1 ppm 5×10^6
50 ppm 5×10^3
10 ppm 5×10^6

$$\tau_{dep} \propto \frac{M}{\phi} \tag{15}$$

Polymers with large M take longer to coat the surface and therefore there is more time for particle escape. For the second observation we have two opposing effects: (i) at large ϕ the induction time is shorter and hence weaker bonds are formed earlier resulting in a higher probability of escape; (ii) τ_{dep} is shorter at large ϕ and hence there is less time for a particle to escape. It is possible that effect (i) is dominant and that the combined effects result in more escape.

It is interesting to note that by adding polymer after bond formation we can form a strong bond when both the latex and the glass are coated with polymer despite the presence of steric energy barriers. Fig. 10 shows schematically the expected total potential energies of interaction as a function of separation distance between polymer coated polystyrene particles and glass surfaces. The total interaction potential between the two solids in an aqueous medium is the sum of London-van der Waals attraction and steric (plus electrostatic) repulsion. Once the particles are on the surface, the probability of escape depends on the height of the energy barrier (V_{max}) the particles have to surmount. Particles were brought to the surface initially in the absence of the energy barrier and approached the surface to a distance $d < d_{max}$. When both the latex and the surface are coated with PEO, the height of the energy barrier prevents particles from approaching the surface closer than d_{max} (c.f. Fig. (3c)).

Fig. 10 The potential energy as a function of separation distance between the polymer coated particles and glass (schematic).

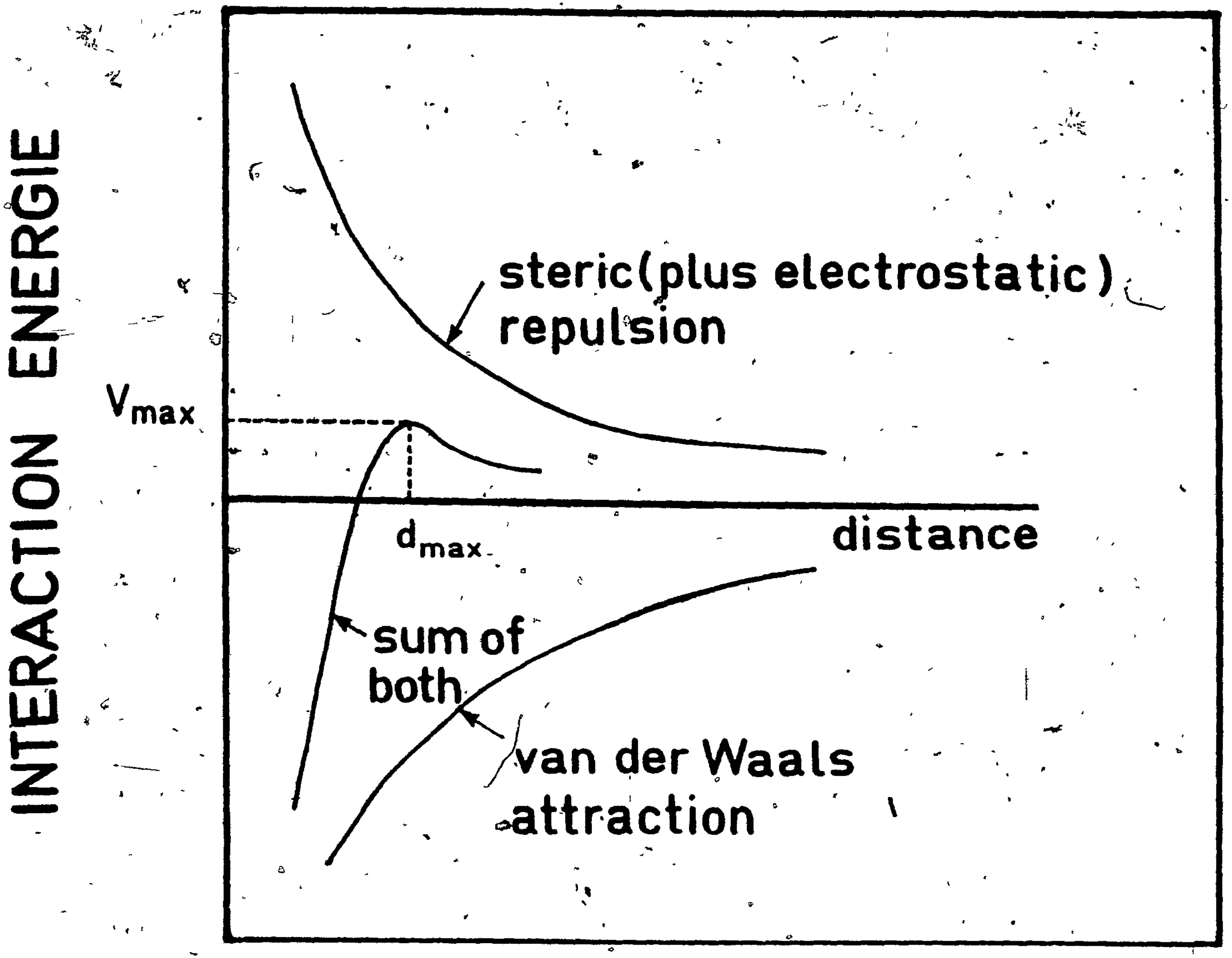
INTERACTION ENERGIE
V max
d max
distance
steric(plus electrostatic) repulsion
sum of both
van der Waals attraction

We also studied the effect of dissolved polymer in the jet on the detachment process of bare latex particles from glass surfaces. Experiments were performed to determine the rate of escape of previously deposited latex particles by changing the original suspension (latex, salt) after twenty minutes of deposition, for a solution containing PEO of various molecular weights and concentrations. Before starting a release measurement, we circulated a polymer solution in the impinging jet for one hour at the same flow rate as used during deposition (Re = 54). This step allows for the polymer to adsorb on the surface.

Fig. 11 shows the effect of molecular weight of PEO on the fraction of previously deposited bare latex particles remaining on the glass surface after one hour of release at a Reynolds number of 380. The three curves correspond to three average distances from the stagnation point $\bar{r}$ or shear rates G. Compared to the results for the detachment of bare latex particles presented in ref. 6, the fraction of the remaining particles becomes lower by adding only 1 ppm of the lower and intermediate molecular weight PEO and slightly higher for high molecular weight PEO.

Fig. 12 shows the fraction of the remaining particles as a function of concentration of PEO. The fraction of the remaining particles tends to reach a plateau by increasing the concentration of PEO. Depending on the molecular weight, the initial fraction increases or decreases until the concentration reaches 1 ppm and afterwards remains unchanged.

An explanation of why a significant release of particles occurred with the lower and intermediate molecular mass of PEO could be that a competition takes place for binding sites between "hairs" on the polystyrene latex and PEO.

Fig. 11 The fraction of the remaining bare latex particles as a function of molecular weight of PEO dissolved in the jet. [PEO] = 1 ppm Re = 380. (o) $\bar{r}$ = 75 μm; (Δ) $\bar{r}$ = 225 μm; (□) $\bar{r}$ = 375 μm. At time t = 1 hr.

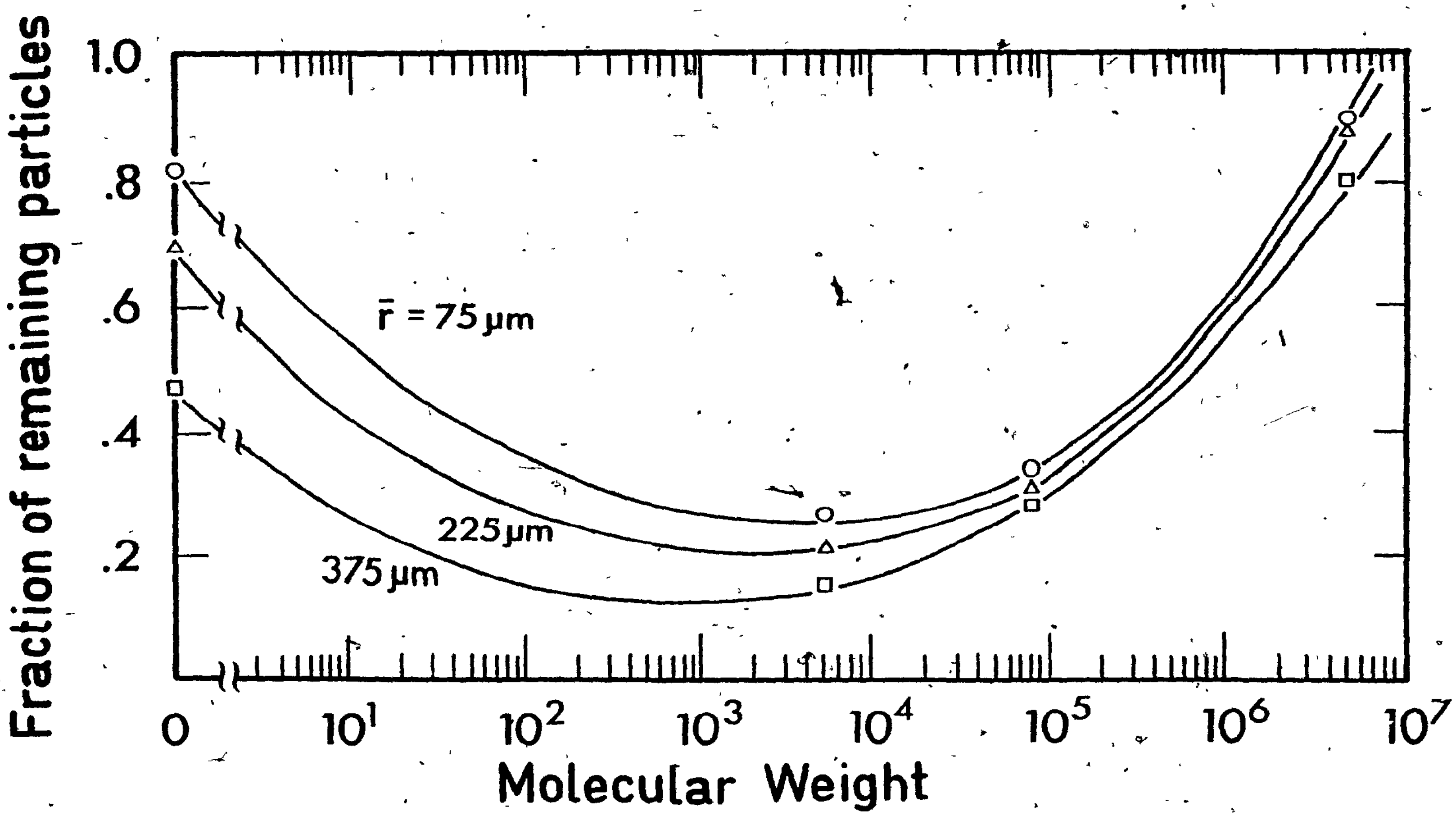

Fraction of remaining particles
1.0
.8
.6
.4
.2
0
10^1
10^2
10^3
10^4
10^5
10^6
10^7
Molecular Weight
r̄ = 75 μm
225 μm
375 μm

Fig. 12 The fraction of the remaining bare latex particles as a function of PEO concentration for two molecular weights. Re = 380. At time t = .1 hr.

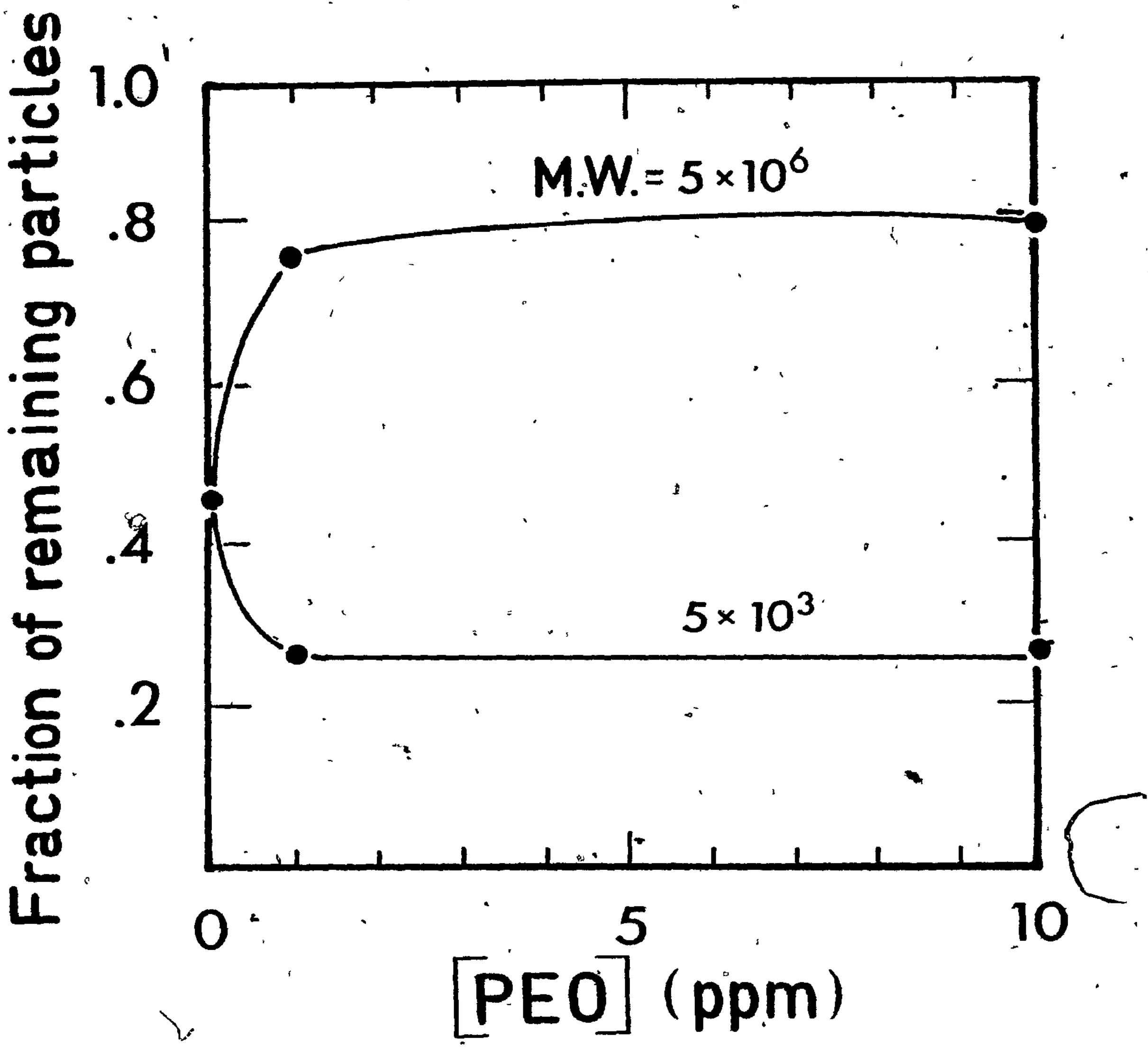
Fraction of remaining particles
1.0
.8
.6
.4
.2
M.W. = 5×10^6
5×10^3
0
5
10
[PEO] (ppm)

V. CONCLUSIONS

The adhesion on glass surfaces of polystyrene latex particles is increased by coating the particles with polyethylene oxide of molecular weight 5000. Detachment of polymer coated particles from glass is, at moderatly low Reynolds numbers, only observed in the presence of dissolved polymer in the jet. The detachment of deposited particles coated with polymer increases with increasing radial distance from the stagnation point, molecular weight and concentration of dissolved polymer. In the presence of dissolved polymer in the jet, the strength of the bond between PEO coated latex particles and glass initially decreases steeply with time, but subsequently increases again. To explain the time dependence of the detachment, we propose a mechanism that qualitatively accounts for the observations. The initial detachment rate is caused by the replacement of adsorbed segments of bridging molecules by segments of dissolved polymer. This replacement becomes more and more infrequent when the dissolved polymer adsorbs on the surface around the particles. Finally the newly attached molecules can become bridging molecules themselves, thus increasing the number of bonds and decreasing the probability of escape.

REFERENCES

1. Visser, J., J. Colloid Interface Sci., 34, 26 (1970).
2. Visser, J., J. Colloid Interface Sci., 55, 664 (1976).
3. Hubbe, A., Colloids & Surfaces, 16, 249 (1985).
4. Kuo, R.J., and Matijevic, E., J. Colloid Interface Sci., 78, 407 (1980).
5. Hubbe, A., private communication.
6. Varennes, S., and van de Ven, T.G.M., Chapter 2.
7. Goldman, A.J., Cox, R.G., and Brenner, H., Chem. Eng. Sci., 22, 653 (1967).
8. Varennes, S., and van de Ven, T.G.M., Chapter 3.
9. Dabros, T., and van de Ven, TG.M., Colloid Polym. Sci., 261, 694 (1983).

CHAPTER 5

EFFECTS OF POLYELECTROLYTE ON THE DEPOSITION AND DETACHMENT OF COLLOIDAL PARTICLES SUBJECTED TO FLOW

ABSTRACT

The kinetics of deposition and detachment of spherical latex particles onto and from glass surfaces in the presence of cationic polyelectrolytes and subjected to a stagnation point flow has been studied with the impinging jet technique. Conditions of barrierless deposition were created by adding a cationic polyelectrolyte (cat-floc) to the surface of the collector or the particles to achieve surfaces of opposite charge. Some differences between theory and experiment were found which could be explained by considering the effects of polyelectrolytes. When both particles and the glass surface are coated with cat-floc, no deposition occurs until a critical salt concentration is reached. By coating the glass surface with cat-floc, the force needed to detach the polystyrene spheres was greatly increased. The force of adhesion exceeded 55 pN and was much higher than values obtained in the absence of polymer.

I. INTRODUCTION

During recent years there has been, for various reasons, a growing interest in surface-polymer interactions. Our interest is a result of the wider use of polymers as wet end additives in the papermaking process. These additives are commonly used to increase the retention of fines and fillers in papermaking. Many people have studied the effects of retention aids on deposition and detachment processes. Adhesion forces due to polyelectrolytes have been measured in a few cases [1-4]. According to Britt and Unbehend [5,6], one of the roles of polymeric retention aids is to increase the strength of adhesion between oxide particles and cellulose.

The deposition of colloidal particles from flowing suspensions onto solid surfaces in the absence or presence of energy barriers is of intrinsic interest to colloidal science, since important information concerning the interaction of small particles and a collector surface and hydrodynamic transport conditions can be extracted from deposition experiments. According to theoretical treatments and several experimental observations [7-10], the rate of deposition of colloidal particles on a solid surface in the absence of a potential barrier should be mainly controlled by convective diffusion. The experimental work of Adamczyk et al. [10] deals with observations of barrierless deposition rates with various particle dimensions and flow intensities, with good agreement with theoretical predictions. They used the same method as used here, namely the stagnation point flow technique. This technique has the great advantage that particle deposition can be observed directly.

In the present study we performed deposition-detachment experiments with polystyrene particles on glass surfaces in the presence of polyelectrolyte. The aim of this work is to check whether under such conditions experimental results are in agreement with mass-transfer theory and whether polyelectrolyte increases the bond strength between a particle and the collector surface.

II. THEORY

The rate of particle deposition on a collector surface depends on colloidal forces acting between the particle and the collector (dispersion forces F_d, electrical double layer forces F_e, and forces due to the presence of polymers F_p), as well as external forces (e.g. a gravitational force F_g). Assuming additivity of these forces [11],

$$F_z = F_e + F_d + F_p + F_g \tag{1}$$

where F_z is the component of these forces taken normal to the surface. The net effect of the colloidal forces is characterized by the free energy of interaction, $V_{int}(d)$, which depends on the separation d. In the DLVO-theory it is customary to represent the interactions by the free energy of interaction, rather than by the forces exerted on the particles. The energy of interaction is related to the force by

$$F_{col} = -\frac{\partial V_{int}}{\partial d}, \qquad (2)$$

The shape of this curve and the presence or absence of a maximum, in particular, determines the kinetic conditions for particle deposition.

When no energy barrier is present (surfaces uncharged or of opposite sign) the rate of deposition is controlled only by diffusion and convection to the surface. The rate of deposition, when energy barriers are absent and gravity is the only external force, neglecting the opposing effects of hydrodynamic resistance and van der Waals attraction [12] (Smoluchowski-Levich approximation), can be approximated as:

$$Sh_{fast} = \frac{\exp\left[-\frac{Pe}{6}(\delta + 1)^3 - Gr\delta\right]}{\int_{\delta}^{\infty} \exp\left[-\frac{Pe}{6}(H + 1)^3 - GrH\right] dH} . \qquad (3)$$

Here H is the dimensionless gap width between the particle and the wall and δ the distance where the particle is captured.

The Sherwood number, Sh, is a dimensionless transfer number and is related to the deposition rate of colloidal particles flowing through an impinging jet cell by:

$$Sh = \frac{ja}{D_o n_o} . \qquad (4)$$

where j is the number of particles deposited per unit area per unit time (the deposition rate), a the particle radius and D_o its diffusion coefficient; n_o is the concentration of particles in the suspension.

The relative magnitude of hydrodynamic and diffusion effects can be denoted by the Péclet number Pe

$$Pe = \frac{2\alpha a^3}{D_o} . \tag{5}$$

where α is the strength of the flow in an impinging jet near the stagnation point. Gr is the dimensionless gravity number accounting for sedimentation effects defined as

$$Gr = \frac{2}{9} \frac{\Delta\rho g a^3}{n D_o}$$

where Δρ is the apparent density of the particles and g the acceleration due to gravity.

In the presence of an energy barrier, we can define a deposition efficiency α_d by

$$Sh = \alpha_d \, Sh_{fast} . \tag{6}$$

III. EXPERIMENTAL

The deposition and detachment of latex particles on glass surfaces, in the presence of polyelectrolyte, has been observed in a specially designed flow cell, in combination with a microscope and video equipment. The apparatus was described in detail in Ref. [13]. The flow in the cell is a well-defined stagnation point flow and can vary from laminar to unstable flow. For laminar flow in the neighborhood of the stagnation point, the flow field can be approximated by [12]

$$V_r = \alpha rz; \quad V_z = - \alpha z^2. \qquad (7)$$

The strength of the stagnation point flow α can be found from the flow rate through the deposition cell and the cell geometry. r and z are the radial and normal directions from the stagnation point, V_r and V_z the fluid velocities in these directions (Chapter 2).

The experiments reported in this chapter were performed on polystyrene latex particles with a mean diameter of 3 μm, identical to those used in previous chapters.

Material

The cationic polyelectrolyte used in this study is cat-floc (poly-N,N-3,5-methylene-pyridinium chloride) with a molecular weight of 2 x 10^5. This polyelectrolyte was purified from a commerial sample (Calgon Corp., Plattsburgh, N.Y.) by several recrystallizations.

A stock solution of the cationic polyelectrolyte was prepared by gradually adding it to distilled water while the solution was being stirred magnetically for a few hours. The solution contained 0.1 g/l of cat-floc.

Microscope cover glass slides used as collectors were throughly washed using nitric and hydrochloric acid to obtain clean surfaces.

Adsorption procedure

In experiments with cat-floc coated particles, the polyelectrolyte was added to the diluted latex suspensions, 4 to 5 hours prior to flow through the impinging jet cell, in order to ensure equilibrium adsorption of the polymer on the spheres.

To coat glass surfaces with cat-floc, freshly cleaned cover glass slides were suspended in a 20 cm^3 rectangular container containing the cat-floc solution for 4 or 5 hours as well.

General procedures for deposition and detachment experiments are described in detail in Chapters 2 and 4.

Measurement of zeta-potentials

The electrophoretic mobilities of the latex spheres, with and without adsorbed polyelectrolyte, were measured in a Rank Bros. Mark II microelectrophoresis apparatus. The electrophoretic mobilities measurements were converted to zeta-potentials using the Helmholtz-Smoluchowski equation.

IV. RESULTS AND DISCUSSION

In Chapter 2 we studied the deposition of polystyrene latex particles on glass surfaces. Both surfaces were negatively charged and a large energy barrier existed between them. To create conditions for barrierless deposition the electrokinetic properties of the system have to be changed. This may be achieved by the adsorption of a cationic polyelectrolyte.

The electrophoretic mobilities of latex spheres in 4 mM NaCl as a function of cat-floc concentration were measured. The measured ζ- potentials are plotted against the polymer concenteration in Fig. 1. From this figure it can be seen that the potential of polystyrene latex spheres is neutralized and reversed by the adsorption of cat-floc. With increasing cat-floc concentration the initial ζ-potential of - 64 mV increased slowly, followed by a rapid rise with reversal of charge at a

Fig. 1 Zeta-potential of the polystyrene latex particles as a function of cat-floc concentration in solution.

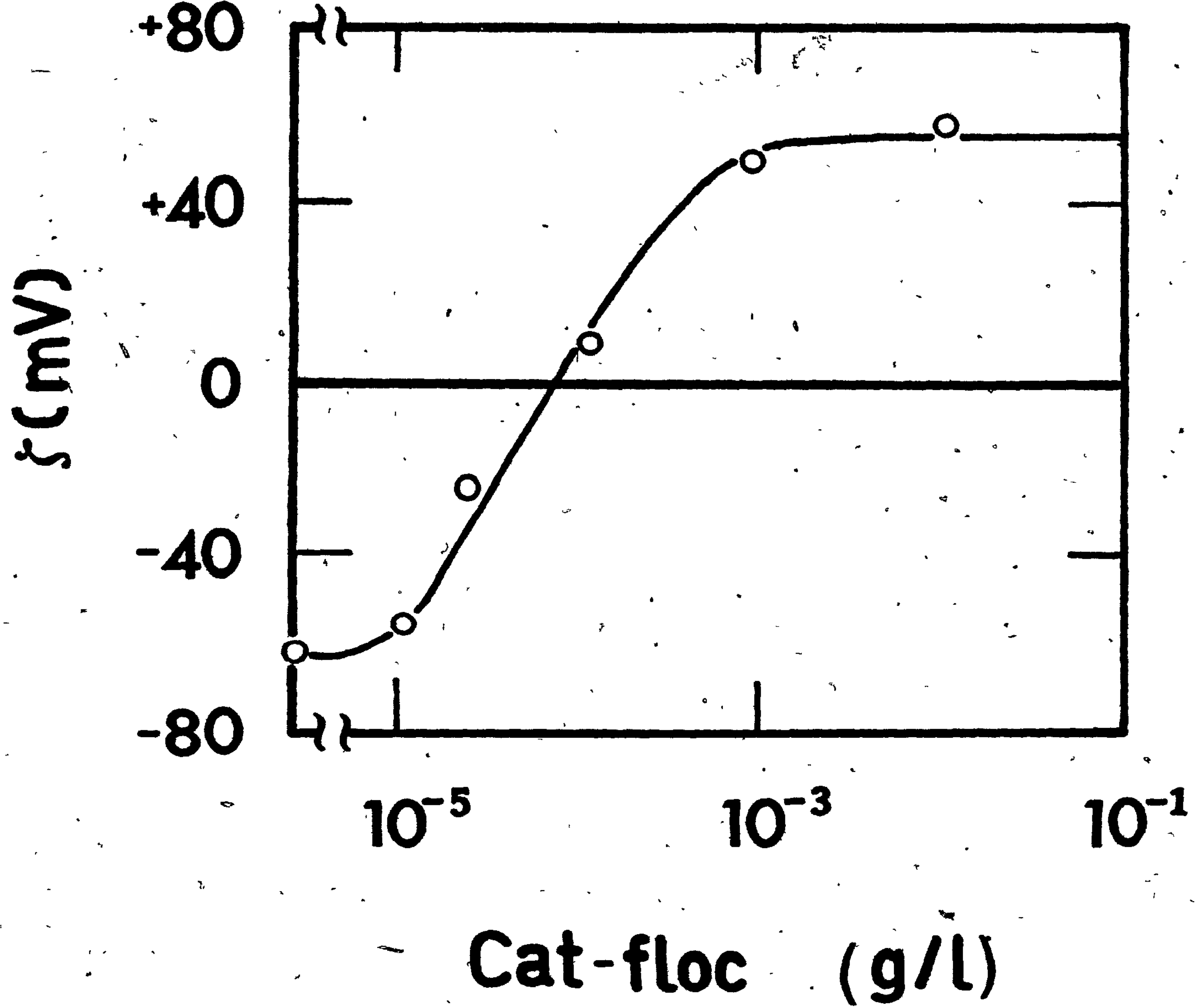

+80
+40
0
-40
-80
ζ (mV)
10^-5
10^-3
10^-1
Cat-floc (g/l)

polymer concentration of 0.08 mg/l, finally reaching a constant value of about 52 mV at concentrations larger than 1 mg/l. Furthermore, at polymer concentrations close to the charge inversion point, both negatively and positively charged particles were observed. These results suggest that there is a distribution in the amount of polymer adsorbed on the latex spheres.

Unfortunately no experimental data on the electrokinetic properties of the cover glass slides in the presence of cat-floc are available. We assumed that immersion of the cover glass slides in 0.1 g/l solution of cat-floc was sufficient to reverse the charge of the collector to a positive charge. Our deposition experiments bear out this assumption.

Deposition experiments of latex polystyrene particles on a glass surface in the presence of cationic polyelectrolyte (cat-floc) and subjected to laminar flow were performed in two ways. In the first case the polystyrene particles were separately coated with cationic polymer and then deposited onto a clean cover glass slide acting as the collector surface. In the second case, uncoated latex particles were deposited on a glass surface pretreated with cat-floc. In both cases, we create the conditions of barrierless deposition, i.e. the collector and particle surfaces are oppositely charged, and we expect that the deposition rates obtained for these experiments will conform to the prediction of mass-transfer controlled deposition.

Different deposition rates were observed depending on whether cat-floc adsorption occurred on the latex spheres or on the glass surface. For example, Figs. 2 and 3 show the variation of the coating

Fig. 2 Coating density on a glass surface of particles coated with cat-floc on a bare surface. The dashed line is the experimental initial slope, while the dashed line with dots is the theortical one. The three curves are for $\bar{r}$ = 75 (o), 225 (Δ) and 375 μm (□).

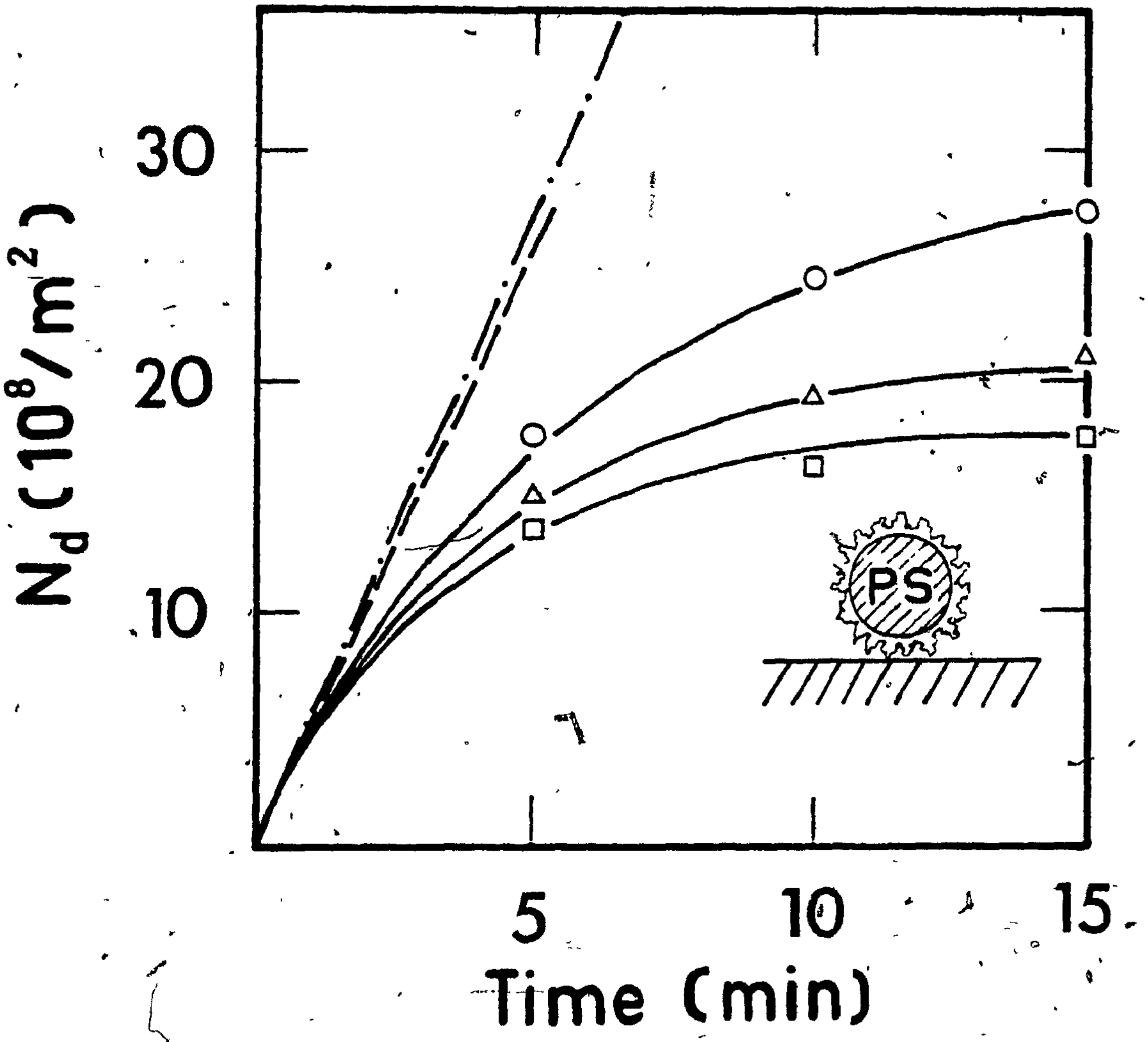
30
20
10
N_d ($10^8/m^2$)
5
10
15
Time (min)
PS

Fig. 3 Deposition of bare particles onto a positive surface (coated with cat-floc). The dashed line is the experimental initial slope, while the dashed line with dots is the theoretical one. The three different symbols are for different average distances from the stagnation point 0: 75 µm, Δ: 225 µm, □: 375 µm.

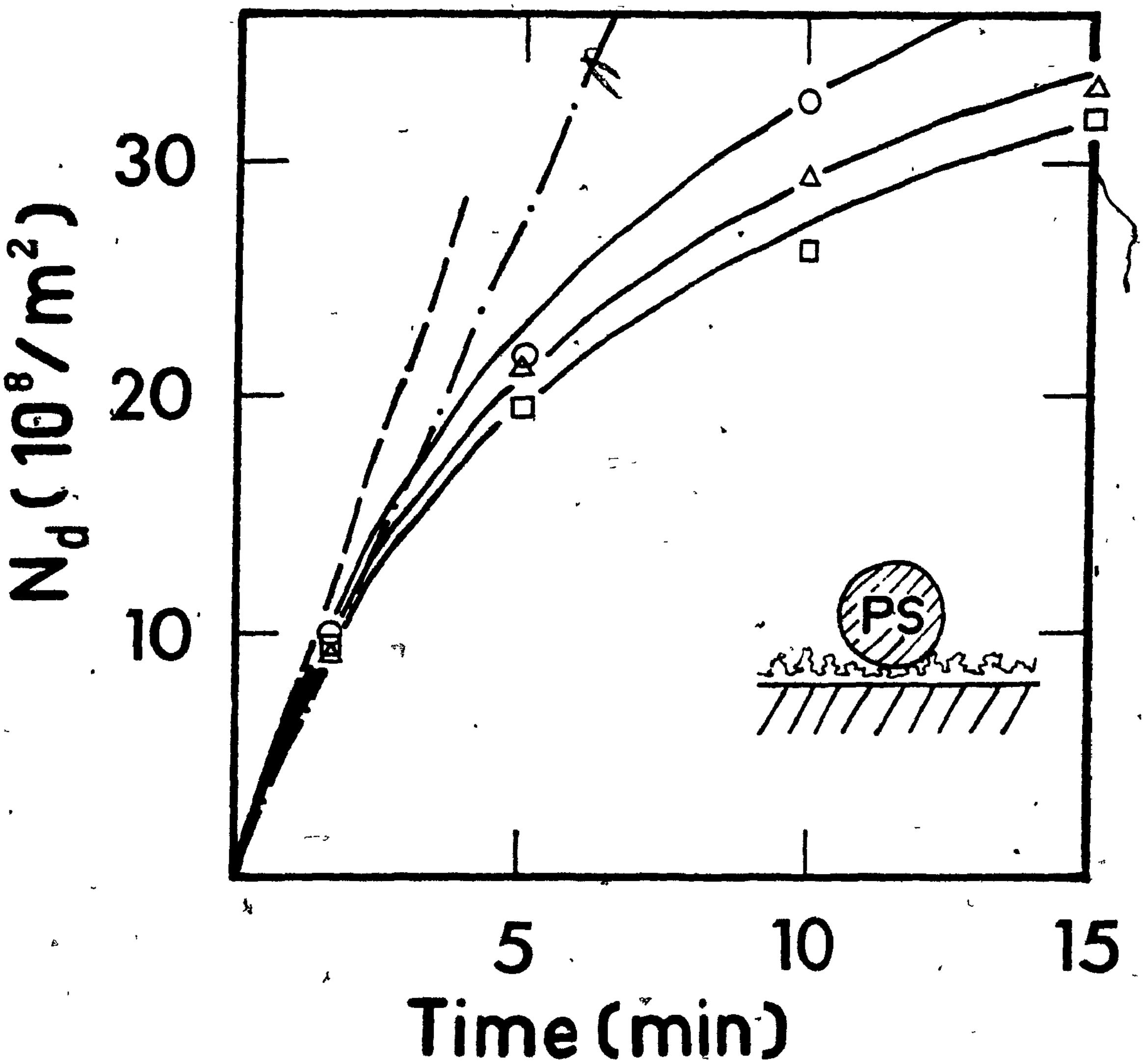

30
20
10
N_d ($10^8/m^2$)
5
10
15
Time (min)
PS

density (expressed as the number of deposited particles per unit area) as a function of time for Re = 54 measured for runs when the particles are or the glass surface is coated with polymer. The polymer concentration used in Fig. 2 was 1 mg/l. In these runs the suspending medium is an aqueous solution containing 4 mM NaCl. The three curves in Figs. 2 and 3 represent three different regions: one near the stagnation point (up to 150 μm), an intermediate region (150-300 μm), and one far from the stagnation point (300-450 μm). The experimental initial deposition rate j_{exp}, determined from the slope of the coating density vs. time curves (dashed lines), was found to be 8.5 x 10^6 particles $m^{-2}s^{-1}$ for $0 < r <$ 150 μm in Fig. 2 and 12.0 x 10^6 particles $m^{-2}s^{-1}$ for $0 < r < 150$ μm in Fig. 3. Under the conditions where the process is purely mass-transfer controlled, substitution of the relevant experimental parameters into Eq. (3) yields a theoretical initial deposition rate of 9.15 x 10^6 particles $m^{-2}s^{-1}$. Hence the deposition efficiencies in these cases are $\alpha_d = 0.93$ and 1.31, respectively.

Fig. 4 presents the dependence of the Sherwood number (dimensionless deposition rate) as a function of Péclet number for [NaCl] = 4 mM. The solid line in this figure was calculated from Eq. (3). In all cases we observed higher values of the Sherwood number when the collector was coated with cat-floc. A possible explanation is the following. In the theory we assume deposition occurs when a suspended particle comes within a distance δ of the collector surface (usually identified with the distance of the primary minimum). By coating the glass with polymer, loops and tails protruding from the glass increase the region where a suspended particle can be captured, thus increasing δ and hence Sh.

Fig. 4 Values of the Sherwood number Sh calculated from Eq. (3) (solid line) as a function of the Péclet number Pe for Gr = − 2.25, together with experimental data. [NaCl] = 4 mM; o $\bar{r}$ = 75 μm; Δ $\bar{r}$ = 225 μm; □ $\bar{r}$ = 375 μm. 1: For bare particles on coated glass; 2: For coated particles on bare glass.

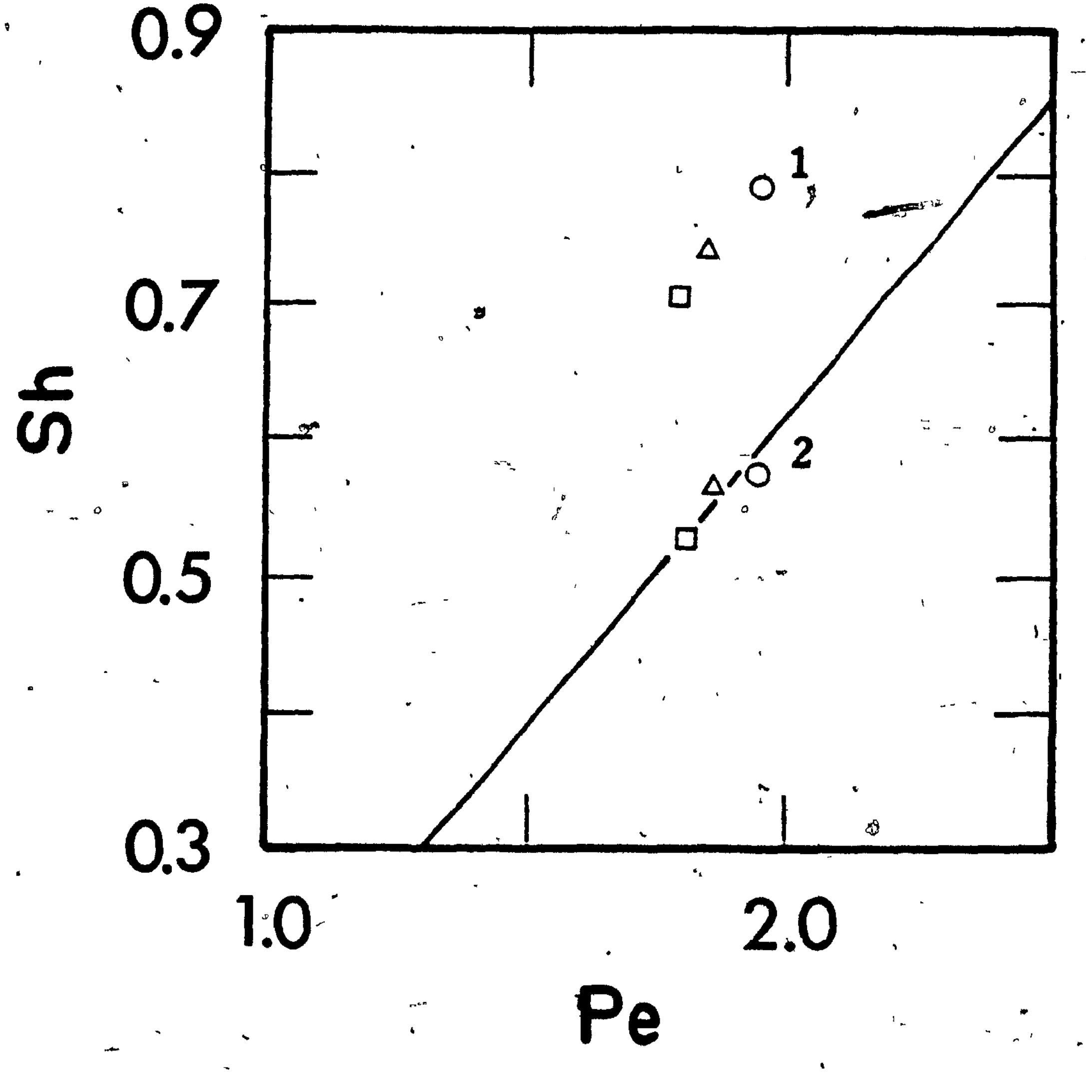
0.9
0.7
0.5
0.3
Sh
1.0
2.0
Pe
1
2

The declining rates of deposition with time observed in Figs. 2 and 3 can be explained by blocking effects of the already deposited particles [12]. Since the blocking arises from a repulsion between deposited and mobile particles [13], the higher asymptotic coverages obtained in Fig. 3 confirm the expected result that more repulsion occurs between coated particles than between bare ones.

We also observe from Figs. 2 and 3 that the coating density N_d decreases with increasing radial distance from the stagnation point flow.

The deposition rates were measured at various cat-floc concentrations for deposition experiments with coated spheres. The results are presented in Fig. 5. Curve 1 shows the data when no addition of cat-floc occurs and the particles and the collector surface have a negative ζ-potential. Under these conditions the highest deposition was observed. This anomalous deposition was discussed in detail in Chapter 2. It was deduced from the data that polystyrene latex particles possess "hairs" protruding from their surface. From Fig. 5 we see that the coating density is maximal within a narrow interval of cat-floc concentration ranging from 0.5 to 1 mg/l. For cat-floc concentration larger than 1 mg/l, we observed a large decrease in coating density and a constant value after 15 min. of deposition. The initial deposition rate for curve 4 (2 mg/l) is very close to the maximal rate with 1 mg/l. One can explain the saturation effect by the deposition of the excess polyelectrolyte onto the glass surface, thus preventing deposition, similar to the reduction of deposition rates caused by excess neutral polymer (Chapter 3).

When both the cover slide and the latex particles were coated with cat-floc, steric repulsion takes place between the particle and the

Fig. 5 Kinetics of latex particle deposition as a function of cat-floc concentration in a solution of 4 mM NaCl at Re = 54. 1. No polymer added. 2. 0.25 mg/l cat-floc. 3. 1 mg/l cat-floc. 4. 2 mg/l cat-floc.

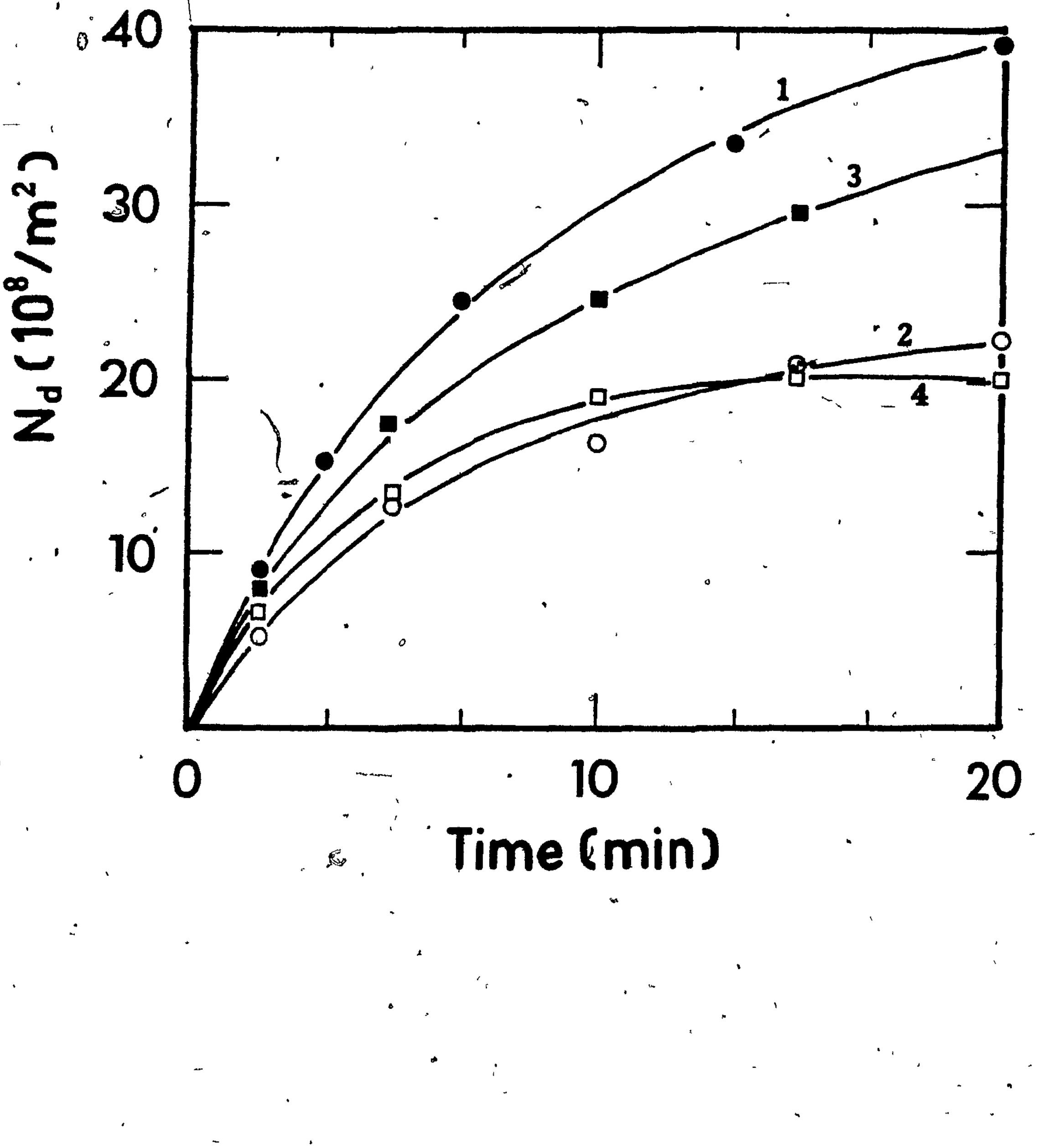

N_d (10^8/m^2)
40
30
20
10
0
10
20
Time (min)
1
3
2
4

surface. Fig. 6 shows the Sherwood number as a function of electrolyte concentration for average distances from the stagnation point equal to 75, 225 and 375 μm. In the range 0 < [NaCl] < 0.32 μM we observe no deposition. We observed deposition in the range 0.32 μM < [NaCl] < 8 mM. For [NaCl] > 0.48 μM, the value of Sherwood number is constant at 0.25, and for [NaCl] > 8 mM we observed coagulation and the deposition of flocs. At intermediate distances and far from the stagnation point, the value of Sherwood number is lower ($Sh = 0.17$). The deposition efficiency α_d is 0.42 and 0.28 for $\bar{r} = 75$, and 225, 375 μm, respectively. The fact that α_d is smaller than 1 may be due to the existence of an additional repulsion between the particle and the surface which is independent of salt concentration. Steric repulsion still exists, even after the addition of salt. By adding salt, we decrease the double layer thickness and, as a result, the height of the energy barrier is reduced, resulting in measurable deposition.

After 15 minutes of deposition, we stop the experiment and change the original suspension for a solution of 4 mM [NaCl]. Release experiments were performed for three different cases: (i) cat-floc was initially adsorbed onto the particles, (ii) cat-floc was initially adsorbed on the glass surface, and (iii) both the cover slide and the latex particles were coated with cat-floc. Fig. 7 shows the curves obtained for the detachment of cat-floc coated particles from a glass surface when the jet contains a solution of 4 mM [NaCl] at Re = 380. Curves 1,2,3 correspond to different concentrations of cat-floc; 1. no polymer, 2. 1 mg/l, 3. 2 mg/l. Curve 4 corresponds to the case when both the particles and the

Fig. 6 Experimental values of the Sherwood number Sh as a function of salt concentration at Re = 54 with [cat-floc] = 1 mg/l. The three symbols are for $\bar{r}$ = 75 (o), $\bar{r}$ = 225 (Δ), and $\bar{r}$ = 375 μm (□).

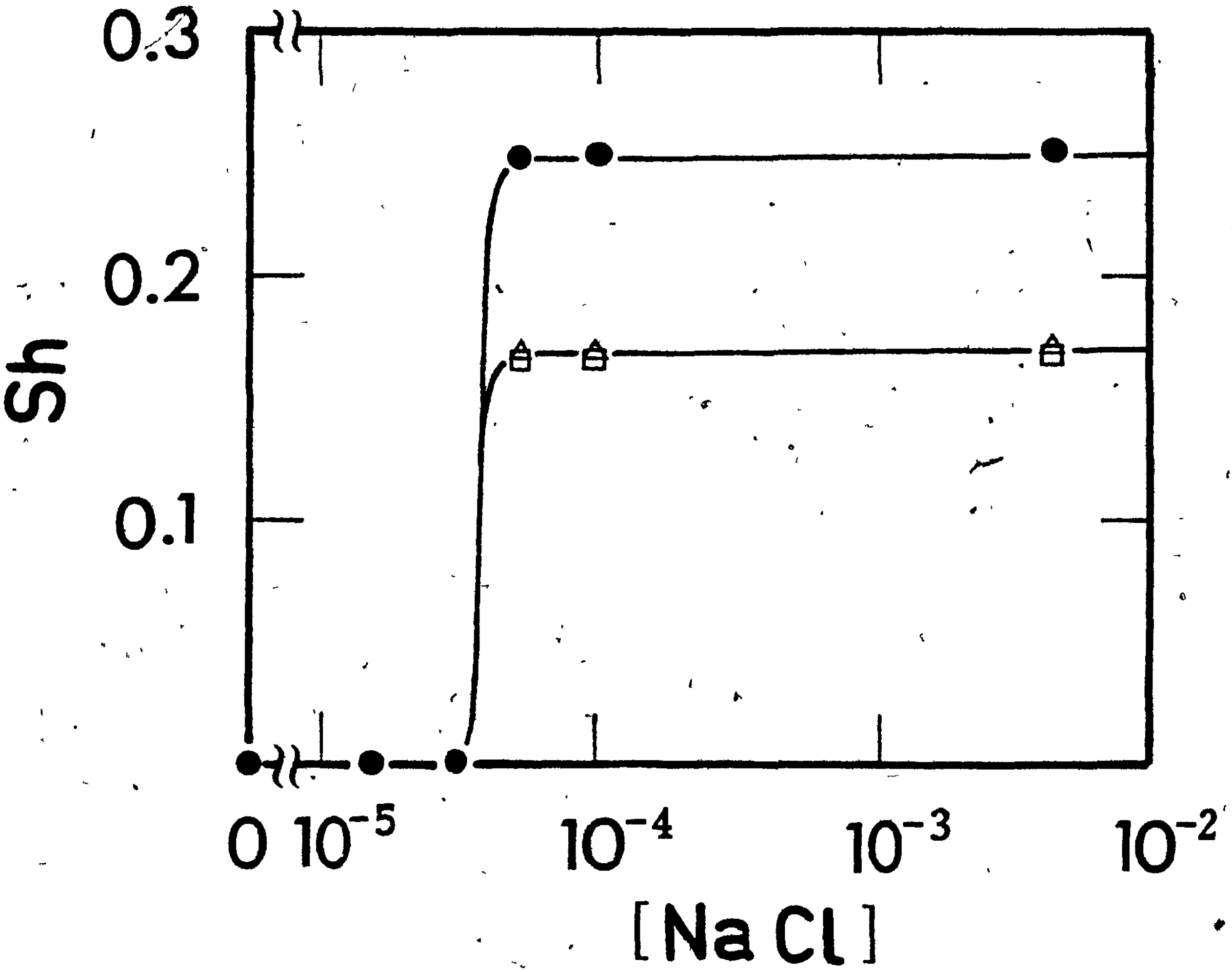
0.3
0.2
0.1
Sh
0
10^{-5}
10^{-4}
10^{-3}
10^{-2}
[NaCl]

Fig. 7. Fraction of remaining particles as a function of time in the presence or absence of cat-floc adsorbed on the particles. Release measurement in the presence of a solution of salt at Re = 380. The curves are for 0 < r < 150 µm. The curves 1,2,3 are for no polymer, 1 mg/l cat-floc and 2 mg/l cat-floc, respectively. Curve 4 is for coated particles (1 mg/l) on a coated surface.

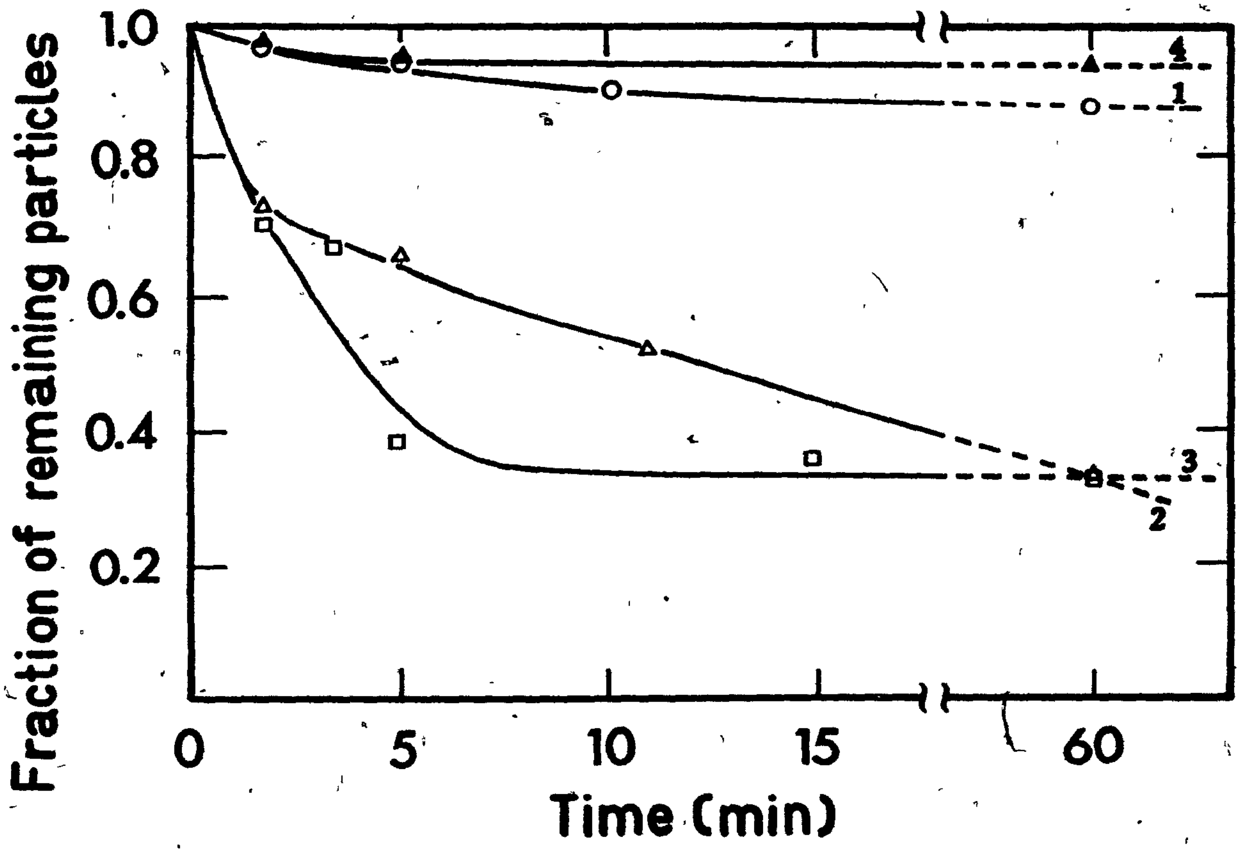
Fraction of remaining particles
1.0
0.8
0.6
0.4
0.2
0
5
10
15
60
Time (min)
4
1
3
2

glass surface are coated with cat-floc. The results are expressed in terms of the fraction of remaining particles as a function of time. The curves are for $0 < r < 150$ μm. Except for curve 4, at all times the fraction of remaining particles is higher for bare particles on bare glass than when either particles or glass are coated. We can conclude that for polystyrene particles coated with cat-floc and subsequently deposited onto a clean cover glass slide, the resulting contacts were easily broken at Re = 380. For detachment of particles with or without excess polymer, corresponding to curves 3 and 2, the initial detachment rate is about the same. This suggests that with excess polymer we have two kinds of bonds (see Fig. 8). In case (a) we have coated particles deposited on a clean glass surface, and in case (b) we have coated particles deposited on excess polymer adsorbed on the glass surface. This excess polymer can form additional bonds with the coated particles bound to the glass surface, or prevent escape by entanglement of polymer segments connecting the particles and the surface. Particles deposited on bare glass detach with the same rate, independent of whether there is excess polymer. Particles deposited on coated patches of glass do not detach as evidenced by the constant number of particles at times larger than 7 min. This explanation is confirmed by curve 4, which shows that for coated particles and coated glass, only 5% of the particles escaped from the surface after 1 hour exposure of a flow with Re = 380. Hence when both particles and glass surface are coated with polymer, the formation of a strong bond occurs between the particle and surface. Furthermore, from curve 2 (1 mg/l) it can be concluded that the strength of the bond between coated particles and bare glass increases with time because

Fig. 8 Schematic representation of polystyrene particles coated with cat-floc deposited on a clean cover glass slide.

(a) [cat-floc] = 1 mg/l.

(b) [cat-floc] = 2 mg/l.

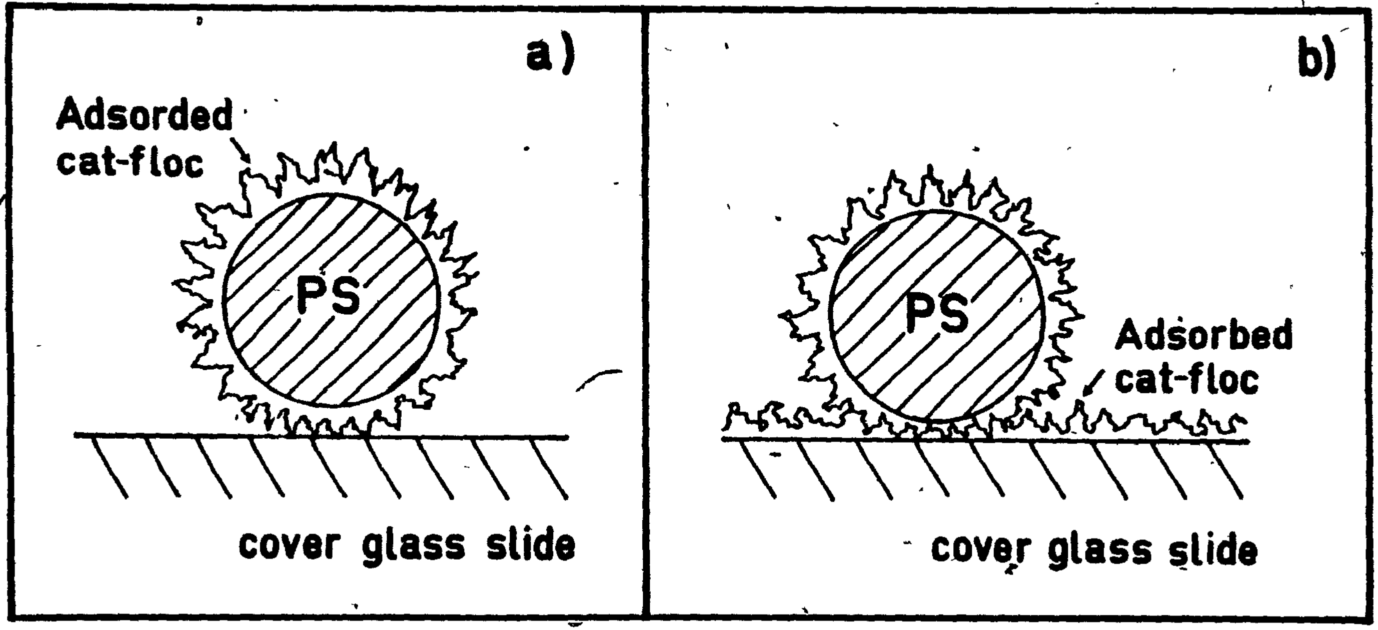
a)
Adsorded
cat-floc
PS
cover glass slide
b)
PS
Adsorbed
cat-floc
cover glass slide

we observed a change in the slope of the detachment rate after about 1 min. of detachment.

Table I contains additional data on particle detachment. The fraction of remaining particles is given for three different wall shear rates G (corresponding to the mean of the three regions near the stagnation point). G increases with increasing distance from the stagnation point. We observed that for particles coated with cat-floc and deposited on clean glass surfaces, the fraction of remaining particles remains almost constant, independent of the distance from the stagnation point. This could mean that the bond strength is non-uniform in the deposition area observed (increasing with increasing r), in contrast to what we found for bare particles. At higher Reynolds number, Re = 770, we found that for coated particles the fraction of remaining particles decreased with an increase in G. It appears that the wall shear rate must be larger than 400 s^{-1} to affect the dislodgement of particles after one hour.

Bonds formed by cat-floc for uncoated particles deposited on glass coated with cat-floc are definitely strong enough to prevent the release of deposited particles when the collector surface is subjected to unstable flow up to Re = 907. The strength of the polystyrene-cat-floc-glass bond is larger than 55 pN. It is clear from the data that the cationic polymer greatly increased the strength of the bonds between the particles and the glass surface. From the fact that the bond strength between bare particles and coated glass is much larger than between coated particles and bare glass, one can conclude that cat-floc has a higher affinity for latex than for glass.

TABLE I

Effect of the wall shear rate G on the fraction of remaining particles, either coated with polyelectrolyte or bare ones, on a glass surface. Duration of release experiment was 1 hour.

[cat-floc] (mg/l)	Re	G [b] (s^{-1})	Fraction of remaining particles
1[a]	380	52,146,233	0.95,0.89,0.81
0	380	52,146,233	0.89,0.74,0.62
1	380	52,146,233	0.33,0.35,0.34
2	380	52,146,233	0.34,0.36,0.31
1	770	145,414,618	0.35,0.27,0.20

a)– Coated glass; all other data are for bare glass surfaces.

b)– The results are expressed for different distances from the stagnation point, corresponding respectively to $\bar{r}$ = 75, 225, 375 μm.

The polymer tends to remain adsorbed even when there is free polymer in the solution. Experiments were performed for the detachment of bare particles from a glass surface coated with cat-floc when we dissolved 1 ppm cat-floc in the jet at Re = 907. We observed no detachment after 4 hours. Thus the replacement of adsorbed segments of bridging molecules by segments of dissolved polymer did not occur to the degree that the bond strength was reduced significantly, as happens with low molecular weight neutral polymers (Chapter 4).

It can be concluded that cationic polyelectrolyte promotes deposition of colloidal particles onto glass surfaces and prevents the release of these particles once contact has been established.

V. CONCLUSIONS

We studied the effects of polyelectrolyte on the deposition and detachment of colloidal particles subjected to flow. From these experiments we can conclude that by coating glass surfaces, or both the particles and glass surfaces, with cationic polyelectrolyte the shear rate required to detach polystyrene particles from glass surfaces is greatly increased. Bonds formed by cat-floc, when the cat-floc is adsorbed by the glass surface, are strong enough to prevent the release of deposited particles when the collector surface is subjected to a force equal to 55 pN. For polystyrene particles coated with cat-floc and subsequently deposited onto a glass surface, the resulting bonds were easily broken at

Re = 380, corresponding to a force of about 15 pN. Some differences between theory and experiment were observed with deposition of polystyrene particles onto a glass surface in the presence of cat-floc, by assuming that the process was mass-transfer controlled. The deposition efficiency varied from 0.42, 0.93 to 1.31, corresponding to the experiments in which (i) both particles and surface are coated with polymer and sufficient salt is added to eliminate double layer repulsion, (ii) coated particles are deposited on a clean cover slide, and (iii) uncoated particles are deposited on a glass surface coated with polymer. We can explain these differences with the theoretical prediction ($\alpha_d = 1$) tentatively as follows. For $\alpha_d = 0.42$ a residual steric repulsion may still exist, independently of salt concentration. The value of $\alpha_d = 0.93$ is in fair agreement with theory. For $\alpha_d = 1.31$, the higher value for the deposition rate can be explained by assuming that particles are captured at larger distances away from the surface, due to the presence of polymer loops or tails protruding from the surface.

In connection with papermaking, these results suggest that better retention of fillers (small colloidal particles) can be achieved by adding cationic polyelectrolyte to the papermaking suspension prior to adding the fillers. This allows time for the adsorption of polyelectrolyte on the fibers with subsequent deposition of negative fillers on positive fibers. Also, because the surface area of the fibers is usually less than that of fillers, less polyelectrolyte will be required.

REFERENCES

1. Pelton, R.H., Nugent, H., and Allen, L.H., Colloids Surf., 464, 397 (1982).
2. Smith, D.K.W., and Kitchener, J.A., Chem. Eng. Sci., 33(12), 1631 (1978).
3. Pelton, R.H., and Allen, L.H., J. Colloid Int. Sci., 99, 387 (1984).
4. Hubbe, M., private communication.
5. Britt, K.W., Tappi, 56,(10), 46 (1973).
6. Britt, K.W., and Unbehend, J.E., Tappi, 59(2), 67 (1976).
7. Hull, M.G., and Kitchener, J.A., Trans. Faraday Soc., 65, 3093 (1969).
8. Marshall, J.K., and Kitchener, J.A., J. Colloid Interface Sci., 23, 342 (1966).
9. Bowen, B.D., and Epstein, N., J. Colloid Interface Sci., 72, 81 (1979).
10. Adamczyk, Z., Zombala, M., Siwek, B., and Czarnecki, J., J. Colloid Interface Sci., 110, 188 (1986).
11. Dabros, T., and Adamczyk, Z., Chem. Eng. Sci., 34, 1041 (1979).
12. Dabros, T., and van de Ven, T.G.M., Colloid Polym. Sci., 261, 694 (1983).
13. Malysa, K., Dabros, T., and van de Ven, T.G.M., J. Fluid Mech., 162, 157 (1986).

CHAPTER 6

GENERAL CONCLUSIONS

I. GENERAL SUMMARY

With the impinging jet technique we were able to study the deposition and detachment of colloidal polystyrene particles of 1.5 µm radius on or from cover glass slides. Our experimental data provide information which can be used to improve and extend existing theories.

From the observations reported on bare latex particle deposition experiments, it is very probable that anomalous deposition rates and surface motions are caused by surface protrusions on the latex surface. It seems clear that not all monodisperse emulsion polymerization latices can be uncritically considered model colloidal systems. The nature of interactions at small particle collector separations are not governed by the DLVO-theory alone. We have outlined some of the problems associated with the prediction of deposition rates. Progress has been made in incorporating blocking effects in the theory.

Prediction of particle detachment rates is still difficult because no adequate theory exists to predict the depth of local energy minima. Progress has been made in incorporating hydrodynamic forces and surface collisions, which have a dramatic effect on escape times. Experimental data on detachment of bare latex particles indicate that the bondstrength does not vary much with hydrodynamic conditions. By assuming that Eq. (54) of Chapter 2 holds, we can calculate the values of the energy minima V_m. We found large values of Δh for reasonable values of V_m. This could be due to large elastic connections or, alternatively, the shape of the energy minimum is different from the one assumed (Eq. (47), Chapter 2).

Several factors that influence the detachment process, such as roughness, surface heterogeneity and dynamic effects, are poorly understood. As a result of all these complicating factors, no close agreement between experimental and theoretical data is found. However, even if the surfaces were sufficiently characterized and if the hydrodynamic (Navier-Stokes) equations could be solved exactly near surfaces partially coated by particles, and if all mentioned effects could be incorporated in the convective diffusion equation, solving the convective diffusion equation could present insurmountable difficulties. In such a case, dynamic simulation and Monte Carlo methods might provide useful alternatives.

We also looked at the effects of neutral or charged polymers on the impingement of polystyrene particles onto glass surfaces. The deposition on solid surfaces of polystyrene latex particles is decreased by coating them with polyethylene oxide (PEO) of molecular weight 5 x 10^3. The dependence of the deposition rate on polymer concentration and adsorption time shows that the presence of excess free polymer decreases the deposition rate.

We also studied the detachment of polymer coated latex particles from glass surfaces. With bare latex particles we had established the importance of surface collisions in the detachment process. Coating particles with neutral polymer changes the detachment behavior. The force of adhesion for particles coated with polymer was much greater than that obtained in the absence of polymer. The nature of interactions of small particle collector separations are not governed by the DLVO-theory alone, but also by macromolecular bridging. It was shown that the presence of polymers dissolved in the jet significantly affects the particle detachment process and was needed to detach polymer coated particles from glass surfaces. It was found that the detachment rate was a strong function of time, being initially zero for a certain induction period, subsequently increasing then decreasing and, finally, becoming zero again at long time. The rate increases with increasing molecular weight and polymer concentration in the jet.

We also studied the effects of polyelectrolyte on the deposition and detachment of colloidal particles subjected to flow. Conditions of barrierless deposition were created by adding a cationic polyelectrolyte to the surface of the collector or the particles to achieve surfaces of opposite charge. We studied three different systems: polymer coated on particles, on a glass surface, or on both surfaces. For polymer coated particles deposited on a clean cover glass, we obtained good agreement between experiment and theory by assuming that the process was mass-transfer controlled. The resulting polymer bond between the particle and glass surface was very weak and could easily be broken at Re = 380. The bond strength was much weaker than for bare latex particles. When uncoated particles are deposited on a glass surface coated with polymer, we observe a higher deposition rate than that predicted by theory. This higher value for deposition rate can be explained if one assumes that the particles are captured at larger distances away from the surface.

When both surfaces are coated with polymer, we observed deposition when a critical salt concentration is reached, but the deposition rate was lower than predicted by theory. We can explain this behavior by the existence of a residual steric repulsion, independent of salt concentration.

Bonds formed by polyelectrolyte for coated or uncoated spheres on coated glass are stronger than those of bare latex particles, especially when we coated only the glass surface. The bonds formed between the particle and glass surface are definitely strong enough to prevent the release of deposited particles when particles on the collector surface are subjected to a tangential hydrodynamic force equal to 55 pN. Coating glass surfaces with cationic polymer greatly increases the shear rate required to detach polystyrene particles from such surfaces.

II. CLAIMS FOR ORIGINAL RESEARCH

These are listed as follows:

1. Testing of transport theories with model latex particles using a recently developed experimental technique. The results indicate that latex is not a model system and that the latex surface is more complex than envisaged.
2. Modification of theories of escape of particles from surfaces, taking into account surface collisions. Hydrodynamic forces and collisions of deposited particles by suspended particles are responsible for the detachment of the particles.
3. The use of the impinging jet technique for studying the deposition

of latex particles coated with neutral polymer. The adsorption time and polymer concentration are found to be important factors in the deposition process. Excess free polymer prevents high deposition rates.

4. Measurements of escape rates using the impinging jet technique. We studied the detachment of polymer coated particles from glass surfaces subjected to a stagnation point flow by adding dissolved polymer to the jet. The results show an exchange of polymer segments between dissolved and adsorbed polymer segments, resulting in the weakening and breaking of bonds.

5. Systematic investigation of the effect of polyelectrolyte on the deposition and detachment of latex particles subjected to flow, showing that cationic polyelectrolyte promotes deposition and prevents the release of particles once contact has been established.

III. SUGGESTIONS FOR FURTHER RESEARCH

Further investigations which follow as a logical continuation of the present work can be outlined as follows:

1. Measuring the effects of high-molecular weight, non-ionic polyethylene oxide on the deposition and detachment of colloidal particles onto or from flat surfaces. Braun and Ehms [1] found that high-molecular weight, non-ionic polyethylene oxide is a more effective retention aid in papermaking furnishes than cationic polyelectrolyte, because the effectiveness of cationic polyelectrolytes is reduced by the presence of rela-

tively high concentrations of dissolved anionic species. We can measure the dependence of the deposition rate on polymer concentration, adsorption time, ionic strength and concentration of the colloidal particles. It would be desirable to measure the adhesive strength of polystyrene latex particles bonded to glass with high-molecular weight neutral polymer and to compare the deposition-detachment results with experiments using low molecular weight neutral polymer and cationic polyelectrolyte described in this thesis.

2. Implications to papermaking technology. As a step in this direction, future work should involve different particles, polymers and surfaces more closely resembling those present in a papermaking suspension. For example, using titanium dioxide particles (TiO_2) bonded to cellulose with cationic flocculant. We can vary the strength of bonds formed with a cationic flocculant by changing the solution chemistry, especially those parameters which influence the electrostatic interactions between the polymer and the surface and which appear to influence the stability of the particle-flocculant-polymer bond in flow. Thus it appears that with sufficient information it should be possible to optimize chemical variables during papermaking to achieve maximum flocculant effectiveness.

3. Natural polymers also play important roles in many biological processes. We can study some biological systems, such as the reaction between antibody and antigen, cell adhesion, bacteria, and other types of cell aggregates. With the impinging jet technique, we can observe the deposition of cells on surfaces and the dependence of shear on the

attachment or detachment of cells onto or from surfaces. It would be interesting to look at the interaction at small separations between flowing cells and surfaces and to look at polymeric materials at cell surfaces promoting or preventing cell adhesion.

4. To look at the effect of surfactants on dispersion stability by measuring the change in coating density with time. From these observations we can derive quantitative information concerning the influence of the surfactant on the forces acting between the particles.

5. Practical cases where polymers are added to stabilize dispersions occur in pharmaceutical products, cosmetics, paints, printing inks, etc. Direct observation with the impinging jet can provide direct measurement of the force between particles as a function of separation.

REFERENCE

1. Braun, D.B., and Ehms, D.A., Tappi Journal, 67, 110 (1984).

APPENDIX I

DETAILS OF IMPINGING JET TECHNIQUE

In this appendix, the apparatus used in the experiments performed in Chapters, 2, 3, 4 and 5 is described in detail.

Fig. 1 shows a close-up of the deposition cell. The frame of the cell is made of glass. The diameter of the outer and inner glass tubes are 25 mm and 14 mm, respectively. The separation between the top part of the outer and inner tube is 2.3 mm. At the upper end of the inner tube a thin stainless steel plate is fused of thickness 0.7 mm with a 2 mm orifice in its center. The cell contains two valves. One, when open, allows the liquid to enter the inner tube and then to leave it through the orifice; the second one allows the liquid to leave the deposition cell. The height of the cell measures 9.5 cm and it holds about 20 ml dispersions of latex.

The deposition cell is placed under an optical microscope (see Fig. 2). The latex suspension used in the deposition experiments was obtained by ultrasonically dispersing 0.2 cm^3 of concentrated latex in 197.8 cm^3 of distilled water. Before each experiment, 2 cm^3 of sodium chloride solution of various molarity was added to the latex dispersion. The suspension was prepared immediately before each experiment and was used for only one experimental run. The deposition cell and plastic tube, connecting the cell and a precision valve, are filled with the suspension. During the filling operation, care was taken to avoid any formation of bubbles. The intensity of the flow can be controlled by using a precision valve to provide a wide range of different flow rates. The volumetric flow rate Q is measured at this step, before starting a deposition experiment. We collected the fluid passing through the

Fig. 1 . Close-up of the deposition cell used in observing the deposition-detachment process.


INTERFLON

Fig. 2 Circulation of the colloidal suspension around a closed system.

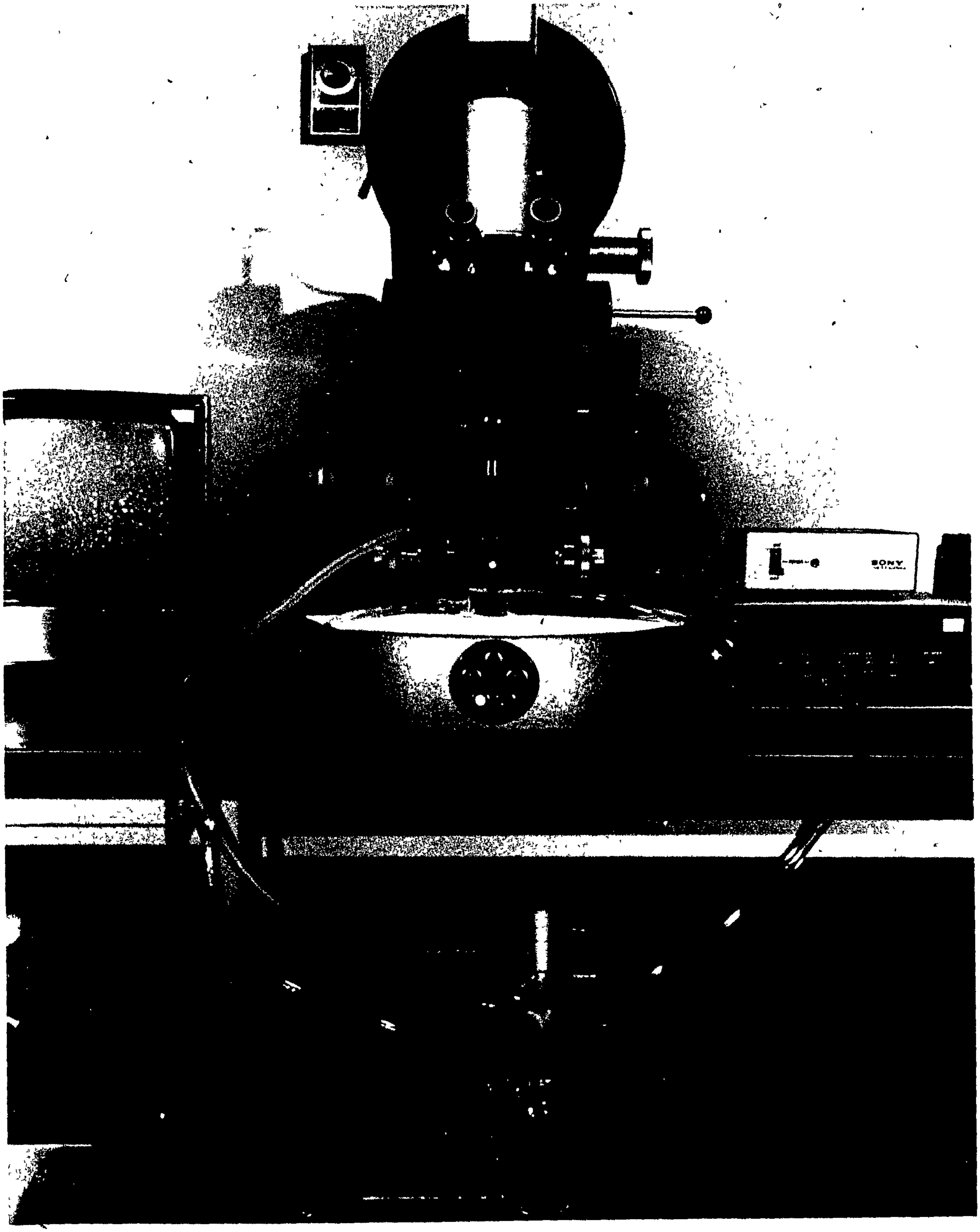
SONY

precision valve for a known amount of time and weighed it. Knowing the density of the suspending medium (water), we obtained Q (volume of liquid per second). From the volumetric flow rate we can calculate the mean velocity of the jet and then the Reynolds number Re. To perform deposition experiments at a specific Re, we made a calibration table where the number of suspension drops for a given time corresponds to a specific Re. A peristaltic pump was used to circulate the suspension around the system from a 100 ml vessel to a 50 ml beaker. We can control the speed of the circulating liquid and obtain a constant level of liquid in the beaker. The excess fluid in the beaker exits through a plastic tube and falls into the 100 ml vessel. This experimental set-up was designed to allow the fluid to flow in a closed system. This system assures, to a high extent, smooth flow conditions.

Fig. 3 shows a closer view of the deposition apparatus. Observations of the deposition process were performed with dark field illumination from above, using a Zeiss-Ultraphot II microscope. In the experiments, an objective EPIPLAN HD 8/0.2 was used. To fill the inner tube with the suspension, we put a microscopic cover glass slide at the top of the deposition cell. To allow the liquid to flow into the inner tube, we opened both valves simultaneously. The liquid rises and leaves the inner tube through the orifice. We then, first, close the valve between the cell and plastic tube and, subsequently, the second one. We removed the cover slide and filled the cell with the suspension and replaced the cover slide. We open the valves again, and the same operations are repeated until no more bubbles appeared. We checked the volume flow rate and again closed the valves. We then replaced the cover slide with a new

Fig. 3 Close-up view of the deposition cell fixed under an optical microscope.

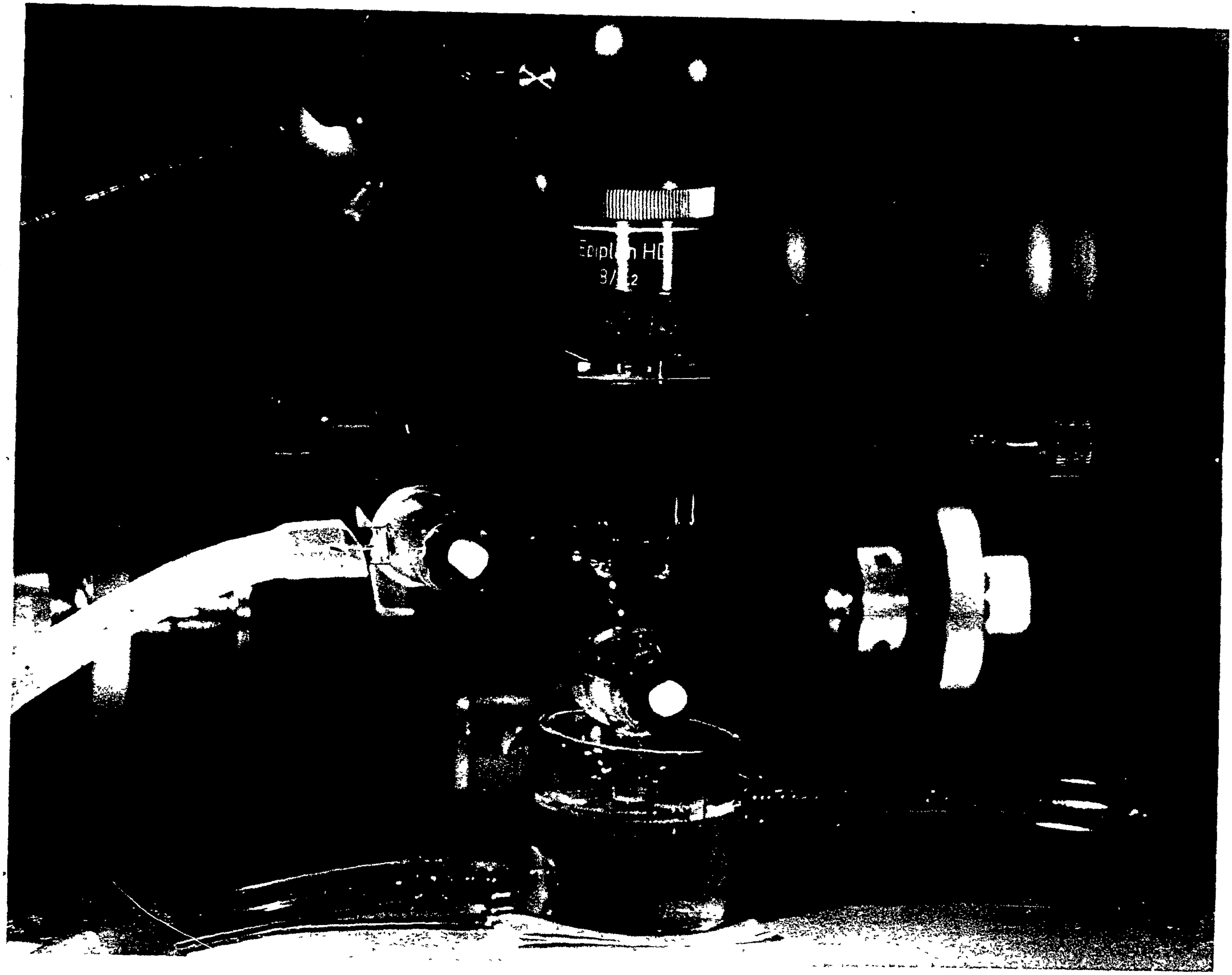
Epiplan HD

clean one. To start the deposition process we opened the two valves simultaneously.

For detachment experiments some procedural steps were added. After twenty minutes or less of deposition, we stopped the deposition process by closing the two valves. We pumped the suspension into a beaker and emptied the dispersion from the beaker and the 100 ml vessel, which were subsequently thoroughly rinsed with distilled water. Next we filled the 100 ml vessel and the beaker with a solution of polymer and salt or salt only, depending on the type of release experiment. We placed another recipient under the cell to collect the original suspension remaining in the deposition cell at the beginning of the removal experiment. To start the detachment process we again opened both values simultaneously.

A top view of the deposition cell is shown in Fig. 4. The deposition cell is fixed with 3 screws on the stage of the optical microscope. A microscopic cover glass slide is held in place on the top of the outer tube by the underpressure existing inside the cell. Fisher brand microscope cover glass slides were used, which have a uniform thickness and size of 25 x 25 mm. They are uniformly flat and corrosion resistant. The suspension flowing out of the orifice in the center impinges on the microscopic cover glass slide used as a collector.

Fig. 5 shows the complete experimental set-up for studying the deposition-detachment of colloidal particles onto or from glass surfaces subjected to flow. Observations of the deposition-detachment process were carried out under an optical microscope equipped with a TV camera. The microscopic image was recorded on video (Panasonic VHF) and simultan-

Fig. 4 Top view of the deposition cell covered with a microscope cover glass slide used as collector.

Fig. 5 Complete experimental set-up for studying the impingement of colloidal particles onto glass surfaces. From right to left; video VHF Panasonic, control for timing, microscope with the TV camera, TV monitor, control for the speed of the pumped liquid.

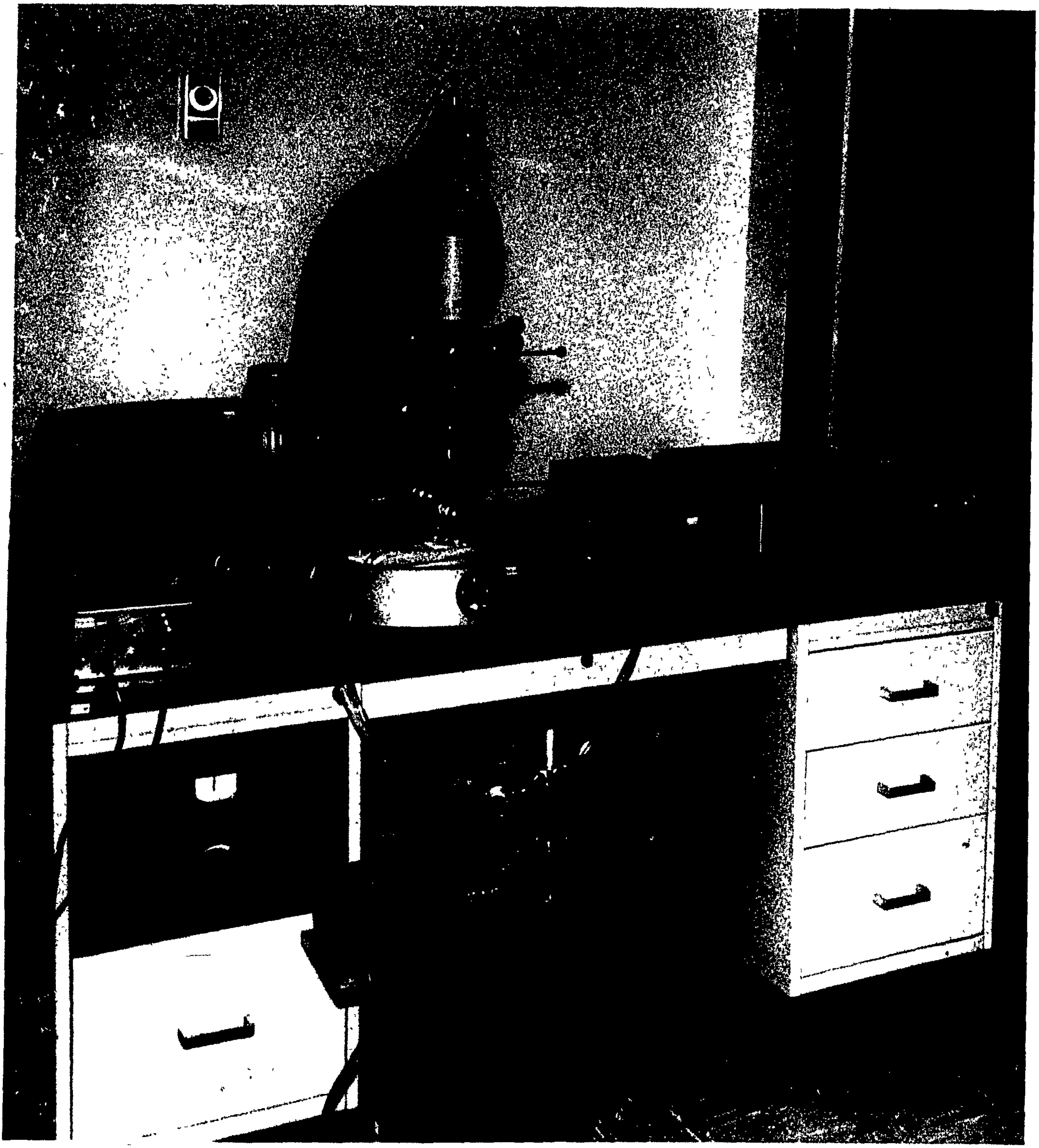

eously transmitted to a TV monitor. With this technique it is possible to observe directly the deposition-detachment process. The time in seconds appeared on the TV screen during the experiments.

Fig. 6 shows a typical example of what we see on the TV screen during a deposition experiment. The white spots are the polystyrene latex particles with a mean diameter of 3 μm flowing out of the orifice and impinging on a cover glass slide. With a fixed image we cannot distinguish between suspended and deposited particles, but by looking at subsequent frames we can separate them. The stagnation point for laminar flow was stationary and was set at the center of the area under observation. The coating density was determined by counting the particles deposited per unit area for various times. The area of observation has a radius of 450 μm. For non-uniform coating, the total observation region was divided into 3 regions; one near the stagnation point up to 150 μm, an intermediate region 150 to 300 μm, and one far from the stagnation point 300 to 450 μm. The number of particles in each of the 3 regions was counted as a function of time.

Fig. 6 Microscopic image of the deposition process. White spots are 3 µm polystyrene latex particles, either suspended or deposited on the slide.